MASTER IN BIOCHEMISTRY AND MOLECULAR AND CELLULAR BIOLOGY

Study of chromosome replication in the pathogen brucella abortus

Servais, Caroline

Award date:
2018

Awarding institution:
University of Namur

UNIVERSITÉ
DE NAMUR

Faculté des Sciences

STUDY OF CHROMOSOME REPLICATION IN THE PATHOGEN BRUCELLA ABORTUS

Mémoire présenté pour l'obtention

du grade académique de master 120 en biochimie et biologie moléculaire et cellulaire

Caroline SERVAIS

Janvier 2018

Université de Namur
FACULTE DES SCIENCES
Secrétariat du Département de Biologie
Rue de Bruxelles 61 - 5000 NAMUR
Téléphone: + 32(0)81.72.44.18 - Téléfax: + 32(0)81.72.44.20
E-mail: joelle.jonet@unamur.be - http://www.unamur.be

Etude de la réplication des chromosomes chez le pathogène Brucella abortus

SERVAIS Caroline

Résumé

Les bactéries du genre *Brucella* sont des alpha-protéobactéries, intracellulaires et pathogènes responsables d'une zoonose répandue mondialement, la brucellose. Actuellement, notre équipe étudie le cycle cellulaire et plus particulièrement les mécanismes de réplication des chromosomes chez *Brucella abortus*. DnaA, une protéine hautement conservée chez les bactéries, agit comme l'initiateur de la réplication des chromosomes et doit être régulée finement pour que la réplication n'ait lieu qu'une fois par cycle cellulaire. Ici, nous étudions le rôle de 3 protéines potentiellement impliquées dans cette régulation : HdaA, ClpA et Lon. En effet, ces protéines sont impliquées dans la régulation de DnaA chez *Caulobacter crescentus,* une autre alpha-protéobactérie qui est un modèle pour étudier le cycle cellulaire. Le but de ce travail est de générer des mutants pour ces trois gènes (*hdaA, clpA, lon*), afin d'investiguer leurs rôles dans la réplication des chromosomes de *B. abortus* en culture *in vitro* mais également en infection, étant donné qu'il a été montré que le cycle cellulaire de *B. abortus* est coordonné avec certaines infections cellulaires. Cependant, même si *lon* est considéré comme non essentiel d'après une étude Tn-seq, aucun mutant pour ce gène n'a pu être obtenu. Le gène *clpA* est en opéron avec la séquence codante de sa protéine adaptatrice, ClpS, et aucun des deux gènes n'a été démontré comme étant essentiel. Afin d'initier la caractérisation de ClpA, une souche de délétion a donc été créée pour les deux gènes (Δ*clpSA*). Cette souche présente un léger retard de croissance en phase exponentielle et des problèmes de morphologie. De plus, lors d'une infection de macrophages, une légère diminution du nombre de CFUs est observée à 24h post infection pour Δ*clpSA*, comparé à la souche WT. Concernant HdaA, ce travail a permis de mettre en évidence la présence éventuelle d'un domaine transmembranaire additionnel chez *B. abortus*. Cependant, la délétion de ce domaine n'impacte pas le fitness des bactéries. Enfin, nous avons créé une souche de *B. abortus* permettant de localiser HdaA par microscopie à fluorescence, en fusion avec la YFP. HdaA-YFP forme des *foci* dans une fraction des bactéries examinées. Des études plus approfondies sont nécessaires afin de mieux comprendre le rôle de ces protéines dans la réplication des chromosomes chez *B. abortus*.

Mémoire de master 120 en biochimie et biologie moléculaire et cellulaire

Janvier 2018

Promoteur: X. De Bolle

Université de Namur
FACULTE DES SCIENCES
Secrétariat du Département de Biologie
Rue de Bruxelles 61 - 5000 NAMUR
Téléphone: + 32(0)81.72.44.18 - Téléfax: + 32(0)81.72.44.20
E-mail: joelle.jonet@unamur.be - http://www.unamur.be

Study of chromosome replication in the pathogen Brucella abortus

SERVAIS Caroline

Abstract

Brucella spp. are alpha-proteobacteria, intracellular pathogens responsible for a worldwide zoonosis called brucellosis. Our team is currently investigating the regulation of the bacterial cell cycle and particularly the chromosomal replication mechanisms of *Brucella abortus*. DnaA, a highly conserved protein among bacteria, acts as the initiator of chromosome replication and must be tightly regulated to ensure that replication only happens once per cell cycle. Here, we investigate the role of three proteins potentially involved in this regulation: HdaA, ClpA and Lon. Indeed, those proteins were shown to be involved in DnaA regulation in *Caulobacter crescentus,* another alpha-proteobacterium being a model for cell cycle studies. The aim of this work is to generate mutants for these three genes (*hdaA*, *clpA* and *lon*) in order to characterize their roles in the replication control of *B. abortus* in culture but also in infection, since the cell cycle of *B. abortus* has been shown to be coordinated with cellular infections. However, even though *lon* is not considered as an essential gene according to a Tn-seq analysis, no mutant was obtained for that gene. The *clpA* gene is found in operon with the coding sequence of its adaptor protein ClpS and neither of those genes were shown to be essential. In order to initiate the characterization of ClpA, a strain carrying a deletion of both genes *(ΔclpSA)* was created. This strain displays a slight growth delay in exponential phase and morphological defects. Moreover, when infecting macrophages, a slight decrease in CFU is observed at 24h post infection for *ΔclpSA,* compared to the WT. This work also highlights the fact that HdaA in *B. abortus* could be found with an additional transmembrane domain. However, the deletion of this domain does not impact the bacterial fitness. Eventually, we created a *B. abortus* strain enabling us to localize HdaA with fluorescent microscopy, by fusing it the yellow fluorescent protein (YFP). HdaA-YFP formed *foci* in a fraction of the bacteria. Further investigations are needed in order to better understand the role of these proteins in chromosomal replication in *B. abortus.*

Mémoire de master 120 en biochimie et biologie moléculaire et cellulaire

Janvier 2018

Promoteur: X. De Bolle

REMERCIEMENTS

Le mémoire est un travail de longue haleine, qui nous fait vivre de véritables montagnes russes émotionnelles. Il représente non seulement l'apprentissage du travail en laboratoire au sein d'une équipe, de la rigueur et de la réflexion scientifique, mais il marque aussi la fin de cinq années d'études.

J'aimerais tout d'abord remercier mon promoteur, le professeur Xavier De Bolle, de m'avoir permis de réaliser mon mémoire dans son équipe. Merci pour son grand intérêt envers le projet et le temps qu'il y a consacré, que ce soit pour nos discussions ou pour la relecture de ce travail ; pour sa grande disponibilité malgré son planning chargé et pour sa bonne humeur au quotidien.

Je voudrais aussi remercier tous les membres de l'URBM pour leur accueil chaleureux ! Un merci plus particulier aux membres de la « Xa Team », Katy, Vicky, Phuong, J-F, Kevin, Angy, Pierre et Agnès, pour toutes nos discussions, votre aide et vos conseils. Katy, merci pour toutes tes petites anecdotes au bureau des mémos. Vicky, merci d'avoir pris du temps pour m'expliquer imageJ alors que tu étais toi-même overbookée. Pierre, merci pour ton aide lors de mes western blot (tiens, la voilà ta gommette :🟢). Merci à tous de faire régner une si bonne ambiance au sein du labo.

Je tiens également à te dire un énorme merci à toi, Mathilde. Merci pour tous tes conseils, ta patience et ta grande disponibilité en tout temps, que ce soit en weekend, malade ou même en vacances (!), tu étais toujours là. Tu avais peur de ne pas être au top comme tu n'avais jamais encadré personne avant, mais j'aurais pas pu espérer mieux comme doctorante :) Merci de m'avoir formée comme tu l'as fait ! Bonne continuation, surtout maintenant que tu n'as plus une petite mémo dans les pattes qui vient te poser des questions toutes les 5 minutes haha

Mais aussi merci aux mémos : Bea, Audrey, Pauline, Sarah, Thomas et Elie ! Cette année n'aurait pas été pareille sans vous. Bea, merci pour ta bonne humeur en toutes circonstances, même quand les f****** diagnostic PCR d'omp2b ne fonctionnaient pas, tu as été un vrai petit rayon de soleil au labo. Merci de m'avoir aidé à croire en moi. Audrey, merci pour tous tes encouragements, ton soutien jusqu'au bout (on peut le dire !), et pour les bonnes tranches de rire au bureau (« hopela ») ! Sarah, merci pour tout ton soutien et pour tes histoires plus folles les unes que les autres, qui avait le don de nous changer les idées quand la science ne fonctionnait pas. Pauline, merci d'avoir toujours été là pour nous expliquer les petits trucs qu'on ne comprend pas, tu feras une assistante au top, j'en suis sure. Mais surtout, merci à vous pour le soutien qu'on se donnait, on formait une super équipe !

Je voulais aussi remercier ma famille, papa et maman de m'avoir permis de faire ces études, pour le soutien qu'ils m'ont apporté pendant ces années, même par les plus petites attentions. Merci à mes frères et sœurs qui étaient toujours là pour me faire rire dans les moments les plus intenses de rédaction.

Merci à toi aussi Do, pour toutes les fois où je t'ai parlé de sciences et où tu m'as écouté avec intérêt alors que ce n'est pas ton domaine. Merci pour tout le soutien que tu m'apportes depuis plus de 5 ans maintenant.

Enfin, merci aussi aux membres de mon jury, M. Pierre Bogaerts M. Sébastien Gillet, M. Jean-Yves Matroule, M. Carlo Yague-Sanz, pour le temps que vous accorderez à ce travail. Je vous souhaite une bonne lecture!

"Success is stumbling from failure to failure with no loss of enthusiasm."

Winston S. Churchill

TABLE OF CONTENTS

LIST OF ABBREVIATIONS

AAA+	ATPase associated with diverse cellular activities
aBCV	Autophagic *Brucella*-containing vacuole
ADP	Adenosis diphosphate
ATP	Adenosine triphosphate
ATPase	Adenosine triphosphatase
B.	*Brucella*
BCV	*Brucella*-containing vacuole
bp	Base pair
CFU	Colony Forming Unit
ChrI	Chromosome I
ChrII	Chromosome II
DNA	Deoxyribonucleic Acid
DUE	DNA Unwinding Element
eBCV	Endosomal *Brucella*-containing vacuole
EE	Early endosomes
EEA1	Early Endosome Antigen 1
ER	Endoplasmic reticulum
ERES	Endoplasmic reticulum exit site
kb	Kilobase
kDa	kilos-Daltons
LAMP1	Lysosomal Associated-Membrane Protein 1
LB	Luria-Bertani
LE	Late Endosome
Lys	Lysosomes
MOI	Multiplicity Of Infection
OD	Optical density
ori	Origin of chromosomal replication
P	p-value
PBS	Phosphate Buffer Sodium
PCR	Polymerase Chain Reaction
PI	Post-infection
PFA	Paraformaldehyde
pH	Hydrogen Potential
rBCV	replicative *Brucella*-containing vacuole
RIDA	Regulated inactivation of DnaA
RNA	Ribonucleic Acid
RPM	Rotation per minutes
RT	Room Temperature
spp.	Species pluralis
ST	Stalked cells
SW	Swarmer cells
T4SS	Type 4 Secretion System
TRSE	Texas Red Succinimidyl Ester
WT	Wild type
YT	Yeast extract Tryptone
YFP	Yellow Fluorescent Protein

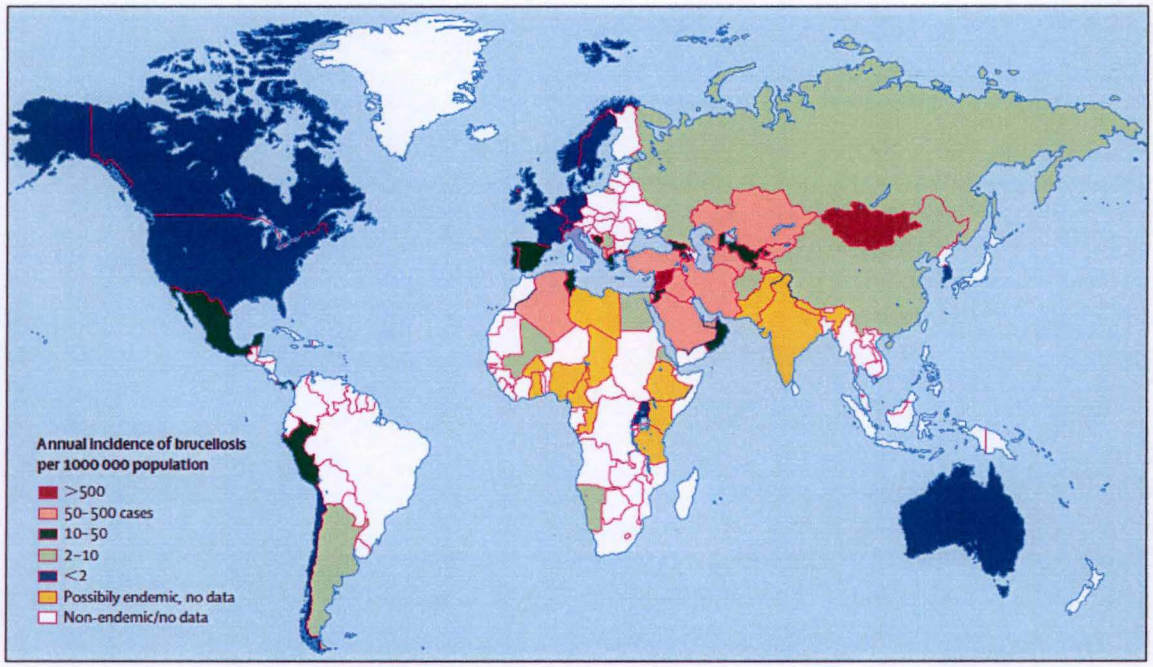

Figure 1 | Worldwide distribution of human brucellosis in 2006 (Pappas *et al.*, 2006).

INTRODUCTION

1. Brucellosis

1.1. History of brucellosis

The discovery of the agent responsible for brucellosis dates back to the end of the 19th century. Back then, many British soldiers standing in the Malta island appeared to be affected by a new type of fever. They were afflicted by an undulant fever that confined them to bed, and sometimes led them to death (National Academy of Sciences (U.S.) 1980). In 1887, the British physician David Bruce, his wife and a Maltese microbiologist managed to isolate the responsible microorganism from spleens and livers of deceased soldiers (Moreno 2014). They found out that this microorganism was a small Gram-negative coccobacillus. The bacterium was named "*Micrococcus melitensis*" because of its small size and because the disease was first found in Malta - "*melita*" meaning Malta in latin (Vassallo 1996). The name of *Brucella melitensis* was given later, in honor of Sir David Bruce. However, at the time, the disease's origin of transmission remained unknown. A few year after the isolation of the bacterium, Themistocles Zammit demonstrated that the infection of British soldiers was due to contaminated goat's milk consumption (Wyatt 2005). Over the following decades, other *Brucella* species were found in other hosts. *Brucella abortus* was isolated from bovine aborted fetuses, placenta and uterine wall secretions (Ficht 2010; Moreno 2014). *Brucella suis* was isolated from aborted swines, *B. canis* from dogs, and *B. ovis* from sheeps, just to name a few (Ficht 2010). The relation with all these bacteria belonging to the same genus was made in 1918 by an American microbiologist, Alice Catherine Evans (Moreno 2014). Since that relation has been made, many eradication campaigns were done, allowing the eradication of brucellosis from Malta island in 2005, for example (Moreno 2014). However, at the end of the 20th century, other *Brucella* species have been isolated from dolphin, porpoises (*B. ceti*), from pinnipeds (*B. pinnipedialis*) and other marine mammals (Foster *et al.*, 2007).

Even though the discovery of the bacteria took place in the 19th century, the disease itself has an older history. Indeed, studies have shown that brucellosis responsible agents, more precisely *Brucella abortus* and *Brucella melitensis*, were present about twenty million years ago (Moreno *et al.*, 2002). The precise moment of brucellosis apparition is still unknown, but it is now sure that the disease occurs since the first contacts of humans with animals (Moreno *et al.*, 2002).

1.2. Epidemiology

Although brucellosis has been eradicated from many countries since its discovery, it remains one of the most important bacterial zoonic disease worldwide, with about half million new cases reported per year **(Figure 1)** (Pappas *et al.*, 2006). Indeed, even if many countries have been characterized "brucellosis-free[1]" in Europe, Spain and Greece are still considered as endemic area, with one of the highest annual incidence in Europe (Pappas *et al.*, 2006). Moreover, Mexico, together with Peru and Argentina in south America, is considered as one of the most important endemic zone for human brucellosis. Asia and Africa are also part of the area with the highest incidence of human brucellosis worldwide, showing that the disease remains an important burden mostly in developing countries nowadays (Pappas *et al.*, 2006). However, few cases of human brucellosis have been reported in non-endemic countries, suggesting that these sporadic events may be due to food importation and traveling from endemic to

[1] meaning that they show a low incidence of human brucellosis annually (Pappas *et al.*, 2006)

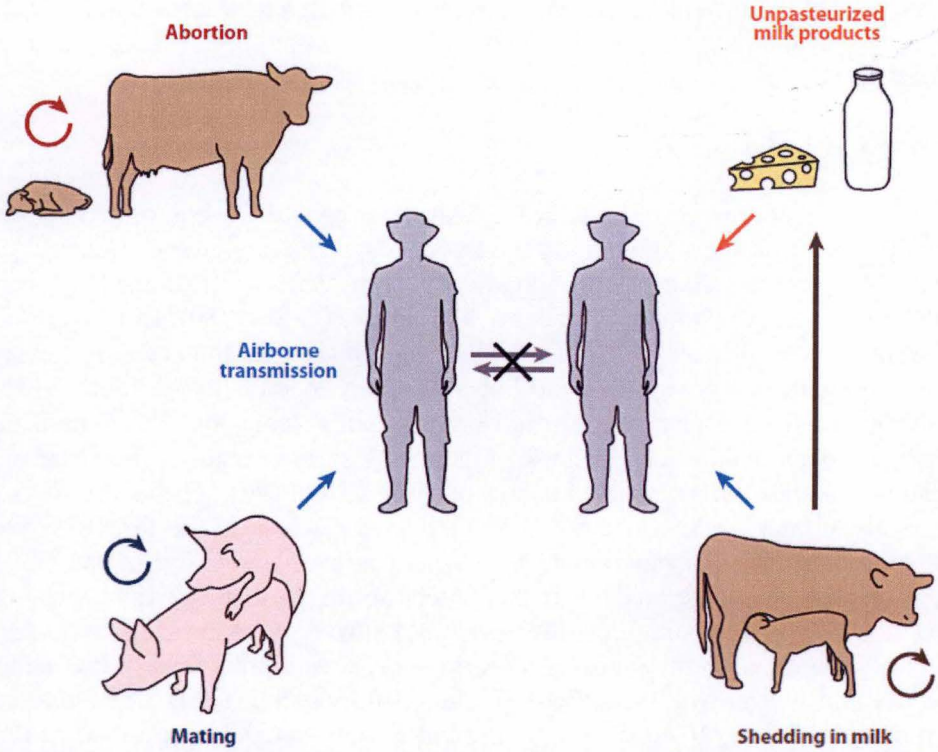

Figure 2 | Different transmission modes of brucellosis between its hosts (Atluri *et al.*, 2011). Brucellosis can be transmitted between animals through the licking of aborted fetuses, through genital secretions during mating or through suckling. The disease can also infect humans mainly via aerosolization and through consumption of unpasteurized milk products. Transmission of the disease between human beings is rare.

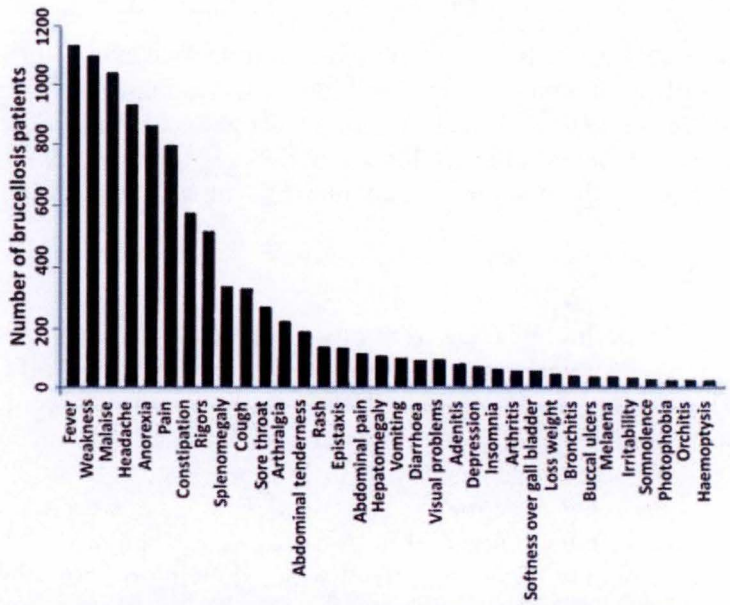

Figure 3 | Bar graph representing the most common symptoms shown for human brucellosis for 1500 patients infected (Moreno 2014). Fever, weakness and malaise are the three most frequent signs of a *Brucella* infection.

non-endemic area. These data further confirm the importance to manage the disease in developing countries in order to have a better global control on the disease (Pappas *et al.*, 2006; Moreno 2014).

1.3. The disease

Brucellosis is a worldwide anthropo-zoonosis caused by bacteria of the *Brucella* genus (Moreno & Moriyón 2006). It affects many different mammals including domesticated, wild and see animals, but also humans (Moreno *et al.*, 2002). In animals, the disease is mostly characterized by late term abortion in females and sterility or epididymitis in males, and therefore results in huge economical losses (Neta *et al.*, 2010). The disease can be vertically transmitted from the mother to the fetus, or horizontally through close contacts with infected secretions, sexually intercourse, or through the licking of aborted fetuses **(Figure 2)** (Moreno 2014). In the presence of enough carbon sources and if protected from the sun's rays, bacteria of the *Brucella* genus may also survive in the external environment for weeks. However, this is considered as a dead end for the bacteria (Moreno 2014).

Although the natural hosts of brucellosis are animals, this infectious disease may affect humans leading to the so-called "Malta Fever". They can be infected by direct contact with tissues or blood from infected animals through skin abrasions or conjunctiva, by consumption of contaminated milk or milk-derived products (Moreno & Moriyón 2006). *Brucellae* are also highly virulent bacteria through aerosolization, with an estimated dose of only 10 to 100 microorganisms being sufficient to infect humans (Bossi *et al.*, 2004). Therefore, farmers, veterinarians, slaughterhouse workers but also scientists working with this bacterium are more at risk to contract the disease (Corbel 2006; Fiori *et al.*, 2000). However, few transmissions between humans have been reported (Meltzer *et al.*, 2010; Wyatt 2010), making these cases irrelevant from an epidemiological point of view. Humans are considered as end hosts for *Brucella* (Moreno 2014). Nevertheless, brucellosis in human is often severe, with a lot of different symptoms varying from an asymptomatic disease to a debilitating undulant fever **(Figure 3)** (Moreno 2014). If left untreated, brucellosis becomes chronic, leading to a granulomatous disease that may affect many organs of the host. For example, the chronic disease often generates arthritis, hepatitis or endocarditis, and may sometimes have a fatal outcome (de Figueiredo *et al.*, 2015).

1.4. Diagnosis and treatment

Considering the wide range of symptoms and the lack of pathognomonic signs for the disease in animals as well as in humans, brucellosis is quite difficult to diagnose. In humans, it might even be mistaken with other diseases such as syphilis, malaria or tuberculosis (Moreno 2014). Therefore, the disease is underdiagnosed. Several diagnostic tests have been developed in order to strengthen the detection of the pathogen. Among these, the most common methods include bacterial cultures in the Farrell medium, biotyping analysis, DNA detection using the polymerase chain reaction (PCR), but also serological analysis and skin tests. Serological tests are often characterized by a good specificity but lower sensitivity, often confusing *Brucella* with *Yersinia enterolitica* O:9 strain because of serum cross reactivity, making these tests not highly reliable. To date, only the PCR enables a correct diagnostic, even allowing the distinction between the different *Brucella* strains (Godfroid *et al.*, 2010).

The current treatment for human brucellosis is an antibiotic bitherapy composed of doxycycline and rifampicin for 6 weeks. However, patients treated with that cure may experiment relapses

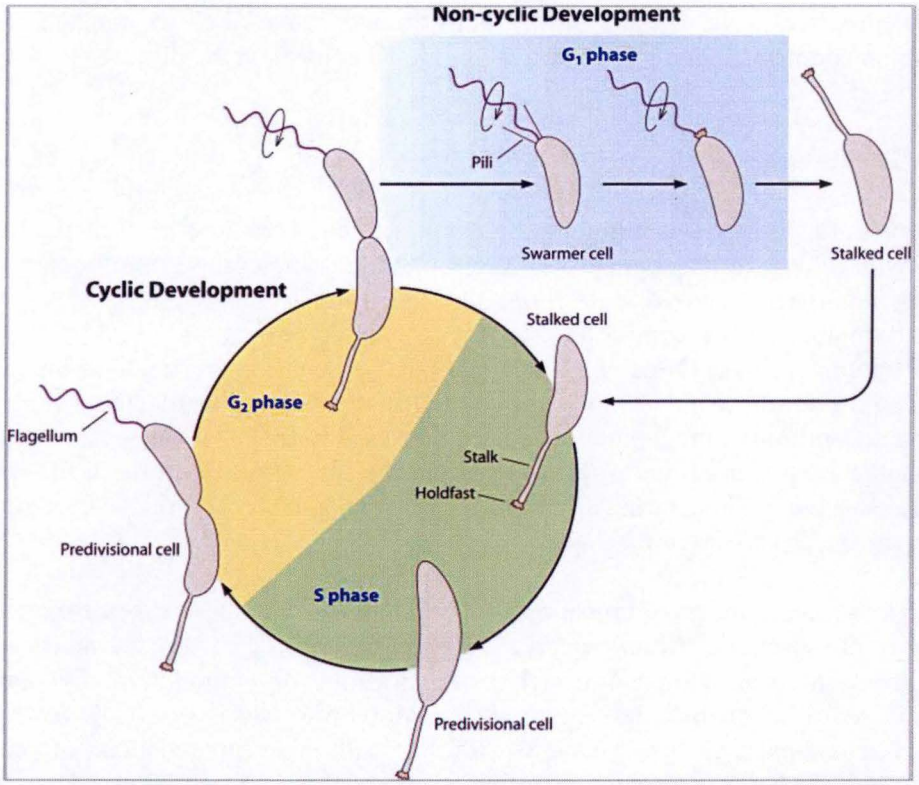

Figure 4 | Schematic representation of the *Caulobacter crescentus* life cycle. *Caulobacter* cell cycle is divided in two major steps, the cyclic development and the non-cyclic development. In the first kind of development, the bacteria possess a stalk and are therefore named stalked cells. The stalked cells are anchored to a surface and are able to initiate chromosomal replication, enter the S phase and eventually become predivisional cells. At this stage, the bacteria divide in two different daughter cells, one stalked cell able to resume another cell cycle, and one swarmer cell that cannot replicate its DNA. The swarmer cell needs to differentiate into stalked cell in order to be able to initiate DNA replication.

(Al-Tawfiq *et al.*, 2013). Therefore, the *Brucella* species are currently classified as class 3 risk micro-organisms[2] (Moreno *et al.*, 2002). Vaccines could help to control and, to some extents, completely eradicate the disease. Up to now, several vaccines have been developed but only few of them were proven to be efficient in animals. For cattle for example, two main vaccines are now approved, the S19 and the RB51 (Dorneles *et al.*, 2015). The S19 vaccine, whose name comes from "Strain 19", was the first to be massively used. This vaccine is a smooth live attenuated vaccine while the RB51 is a rough rifampicin resistant strain, which has lost its virulent phenotype for animals (Dorneles *et al.*, 2015; Schurig *et al.*, 1991). Nevertheless, both of them have shown side effects, and both can cause infections in humans. Therefore, none of them can be used for humans (Dorneles *et al.*, 2015). Other studies are now focusing on new vaccines development to help prevent the disease apparition (Barbosa *et al.*, 2017).

2. The *Brucella* genus

2.1. *Brucella* species and phylogeny

Bacteria of the *Brucella* genus are facultative intracellular-extracellular pathogens, Gram-negative coccobacilli from 0.5 to 1.5 µm long (Moreno & Moriyón 2006). Several species have been identified and differentiated from one another based on metabolic and antigenic characteristics, on their preferential hosts, but also based on their 16S RNA sequences (Michaux-Charachon *et al.*, 1997; Moreno & Moriyón 2006). They have been classified in two groups, the "classical" species and the "non-classical" species. The first class include *B. abortus* (primarily infecting cows), *B. suis* (suidae), *B. melitensis* (goats), *B. canis* (dogs), *B. ovis* (sheeps), and *B. neotomae* (desert wood rat). These species were the first to be described (Moreno *et al.*, 2002). Among them, only the four first are known to infect humans, with different severity degrees (Moreno & Moriyón 2006). The non-classical species include the marine strains (*B. ceti* and *B. pinnipedialis*) (Foster *et al.*, 2007), *B. microti* that was isolated from the common vole (Scholz *et al.*, 2008), *B. inopinata* from the breast implant of a woman (Scholz *et al.*, 2010), *B. papionis* from baboon (Whatmore *et al.*, 2014) and *B. vulpis* from foxes (Hofer *et al.*, 2016). The reason for such a tropism is unknown but a research suggests that it may be related to alterations of the genome (Wattam *et al.*, 2009).

These bacteria belong to the Rhizobiales order in the group of the alpha-proteobacteria. This group contains highly diversified Gram-negative bacteria (Batut *et al.*, 2004). It includes plant symbionts and pathogens such as *Sinorhizobium meliloti* and *Agrobacterium tumefaciens* respectively, intracellular animal pathogens such as *Bartonella*, *Rickettsia* and *Brucella*, but also non-pathogenic free-living bacteria such as *Caulobacter crescentus* (Moreno *et al.*, 2002). They live in different ecological niches varying from soil to water, and can interact with eukaryotes through an extra or intracellular manner. Moreover, they also show a great variability in metabolic capacity, in morphology but also in life cycle (Batut *et al.*, 2004). Despite these different lifestyles, some of the alpha-proteobacteria display common features such as asymmetric division (Hallez *et al.*, 2004). This feature is shared by *B. abortus* and *C. crescentus,* another alpha-proteobacterium used as model to study the cell cycle regulation. Indeed, *C. crescentus* generates two different cells after the division and these cells differ in morphology, in size as well as in replication fate. The smaller cells named swarmer cells are motile and display a flagellum whereas the larger cells display a stalk at the tip of which an adhesive holdfast allows the binding of the bacteria to surfaces **(Figure 4)**(Curtis & Brun 2010).

[2] Class 3 micro-organism corresponds to a group of pathogens that can cause a severe disease in humans and/or may easily be spread in the environment. For this class, treatment or prophylaxis measures exist (Belgium Society Server)

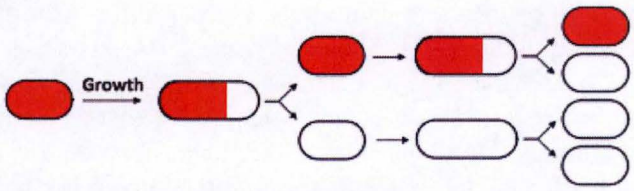

Figure 5 | Representation of unipolar growth in bacteria labeled with TRSE. Bacteria are first incubated with the dye and are therefore completely labeled. The bacteria are then washed. When the growth starts, the newly incorporated material can be easily detected since it will not be labeled. The red cells therefore represent the mother cells that have been labeled, whereas the white cells represent the new daughter cells that have never been in contact with the dye (Van der Henst *et al.*, 2013).

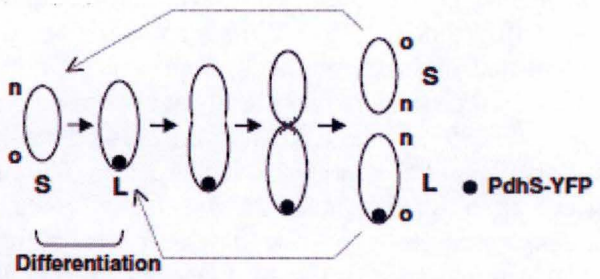

Figure 6 | Model of PdhS localization in *B. abortus* cell cycle. Each cell is characterized by an old (o) and a new (n) pole in the asymmetrically dividing *B. abortus*. PdhS is an old pole marker and was shown to be localized at the old pole of the large cells (L) while no PdhS is found in the small cells (S) that must undergo a differentiation event to acquire the old pole marker and thereby become large cells. PdhS-YFP is represented by the dark spot (Hallez *et al.*, 2007).

In *B. abortus*, cell division gives two daughter cells that only present a slight difference in size (Hallez *et al.*, 2004; Van der Henst *et al.*, 2013).

2.2.Unipolar growth and polar markers

Another particularity in *Brucella* spp. is that they display an atypical growth mode, called the unipolar growth. This type of growth is widespread among bacteria of the Rhizobiales order and is defined by the addition of new material at only one pole of the bacterium, before cell division (Brown *et al.*, 2012). The daughter cells always emerge with a new cell envelope, while the mother cells keep the old one (Van der Henst *et al.*, 2013). Thus, the bacteria are always characterized by an old and a new pole. The new poles are generated by the division whereas they become old when a new division cycle is complete (Van der Henst *et al.*, 2013). Using the fact that *B. abortus* grows unipolarly, the growth can be highlighted using a dye labeling the cell envelope. For example, the Texas Red conjugated to Succinimidyl Ester (TRSE) binds to the amine groups on the bacterial surface. By doing so, it enables the distinction of previously labeled mother cells from the unlabeled growing bacteria (**Figure 5**) (Brown *et al.*, 2012).

The old and the new pole can be highlighted as well, using fusion proteins that are localized at one pole or another. PdhS, an essential cytoplasmic protein conserved in the Rhizobiales order, is found at the old pole of the large cells of *B. abortus*. Once they have achieved a division, the small cells maturate into large cells and eventually acquire PdhS (**Figure 6**). It has been shown that a fusion protein PdhS-YFP accumulates at the old pole in *B. abortus* but also in other alpha-proteobacteria. Therefore, PdhS fused to a fluorescent protein can be used as a marker of the old pole, further allowing to discriminate the small from the large cells directly after division in *Brucella* species (Hallez *et al.*, 2007). Moreover, another protein, PopZ, can be used as a new pole marker in *B. abortus* (Deghelt *et al.*, 2014)

2.3. *Brucella* infection and intracellular trafficking

Brucellae are intracellular pathogens facultatively extracellular, meaning that they are able to proliferate inside a host cell as well as in a rich culture medium *in vitro* (Moreno 2014). Depending on the infection way, *Brucella* may enter a host through skin abrasions or through mucosal surfaces that could either be the respiratory or the digestive tract (Atluri *et al.*, 2011). At the beginning of the infection, *Brucella* preferentially replicates inside phagocytic cells such as macrophages or dendritic cells (Archambaud *et al.*, 2010), but it is important to note that this bacterium may also enter epithelial cells (Gorvel and Moreno, 2002). The infected phagocytic cells migrate to the regional lymph nodes, causing the systemic spreading of the bacteria. From there, *Brucella* subsequently reaches myeloid lineage cells such as macrophages found in the spleen and the liver, leading to the chronicity of the disease and to granulomatous lesions (Atluri *et al.*, 2011). Furthermore, the bacteria can also invade the trophoblastic cells in pregnant animals, which is responsible for abortion in females (Atluri *et al.*, 2011).

As one can imagine, survival and multiplication of bacteria in host cells are crucial for *Brucella* infection establishment (Liautard *et al.*, 1996; Porte *et al.*, 1999). Therefore, like the intracellular pathogens, those bacteria have developed several strategies to survive inside their host cells (Pizzaro-Cerdà *et al.*, 1998). Directly after internalization in macrophages or in epithelial cells, the bacteria are found in a membrane-derived compartment, called the *Brucella* containing vacuole (BCV). This compartment enables the survival of the bacteria and will be maturated progressively (Celli *et al.*, 2015). The BCV primarily interacts with the early endosome network, therefore becoming an endosomal BCV (eBCV), and acquires markers of

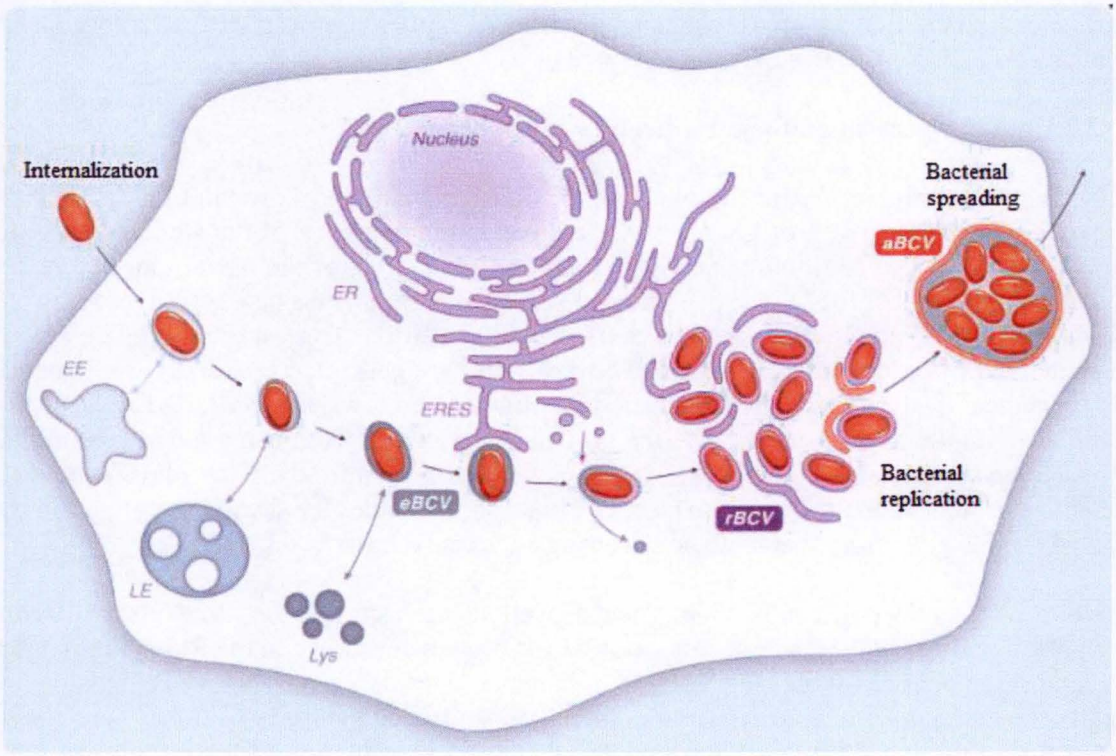

Figure 7 | Intracellular trafficking of *Brucella* inside a mammalian host cell. Following their internalization, the bacteria first reside within a BCV, that is progressively maturated into an eBCV by interacting with the endosomal pathway. Afterwards, the eBCV turns into to rBCV by interacting with the ER. Once they have reached the ER, the bacteria replicate. The rBCV undergoes a last maturation step and evolves into an autophagocytic vacuole that further allows the spreading of the bacteria to other cells (Modified from Celli *et al.*, 2015).

this network, namely EEA1 (early endosomal antigen 1) (Pizzaro-Cerdà *et al.*, 1998). However, this interaction is transient and the eBCV rapidly loose its early endosome markers to make the acquisition of the lysosomal associated-membrane protein 1 (LAMP1) and other makers of late endosomes (Pizzaro-Cerdà *et al.*, 1998, Starr *et al.*, 2008). The vacuole subsequently undergoes an acidification, lowering the intravacuolar pH to 4-4.5 (Porte *et al.*, 1999; Starr *et al.*, 2008). This step is crucial for the maturation of the vacuole because it acts as an activating signal for one of the major virulence factor in *Brucella*, the Type IV Secretion System (T4SS), VirB (Boschiroli *et al.*, 2002). The T4SS is essential to exit the endocytic pathway since it was shown to secrete effector proteins controlling the interaction of the vacuole with the endoplasmic reticulum exit sites (ERES) (Celli *et al.*, 2003). The eBCV will eventually fuse with the endoplasmic reticulum, generating a ER derived-vacuole constituting the replicative BCV (rBCV), in which the bacterial proliferation occurs (Celli *et al.*, 2005). The intracellular cycle is not completely understood but is thought to be completed when the vacuoles become autophagic (aBCV). Those aBCV are thought to be responsible for the cell-to-cell spreading of the bacteria (**Figure 7**) (Starr *et al.*, 2012; Celli, 2015).

2.4. Structure of *Brucella* genome

As compared to most intracellular bacteria, members of the *Brucella* genus are characterized by a large genome (Sällström & Anderson, 2005). Apart from *B. suis* biovar 3 which only shows one large chromosome, all *Brucella* species have two circular chromosomes. More precisely, the genome of *Brucella* species is composed of a large chromosome (ChrI) and a small chromosome (ChrII) with a size of 2.1 Mb and 1.2 Mb respectively (Jumas-Bilak *et al.*, 1998). These two replicons display different partitioning systems. The first chromosome encodes a ParAB segregation system, where ParB is a centromere-binding protein that binds to *parS* sites located close to the replication origin (*oriI)* and promotes its segregation (Livny *et al.*, 2007). The second chromosome is classified as a chromid, i.e. a replicon sharing plasmidic and chromosomic features (Harrison *et al.*, 2010). This chromid shares a similar GC content as the first chromosome (57%) and also contains essential genes such as housekeeping genes essential for growth (Wattam *et al.*, 2009; Harrison *et al.*, 2010). The ChrII encodes a *repABC* cassette in which RepB acts as a centromere-binding protein, recognizing *repS*, which is localized near the replication origin II (*oriII*), thereby driving the segregation. This chromid family carrying a *repABC* cassette similar to plasmidic one is exclusively found in alpha-proteobacteria (Pinto *et al.*, 2012).

3. *Brucella* infection and cell cycle

3.1. Cell cycle monitoring

Taking advantage of the fact that the two chromosomes of *Brucella* display different partitioning systems, two reporter strains have been constructed (Deghelt *et al.*, 2014). The *oriI* can be highlighted using a mCherry-ParB fusion protein. In that purpose, a strain *mCherry-parB* was constructed by allelic replacement in the *parB* locus by *mcherry-parB*, to express the fusion protein directly from its chromosomal locus. Since the creation of a fusion protein for ParB was too toxic for the bacteria, an additional copy of the intact gene was used to escape this detrimental phenotype. In order to visualize the *oriII*, RepB was fused to YFP (YFP-RepB) and the strain was constructed using the same method as *oriI*. Using other known partitioning systems, these strains were confirmed to be reliable to investigate the replication state of *B. abortus* (Deghelt *et al.*, 2014).

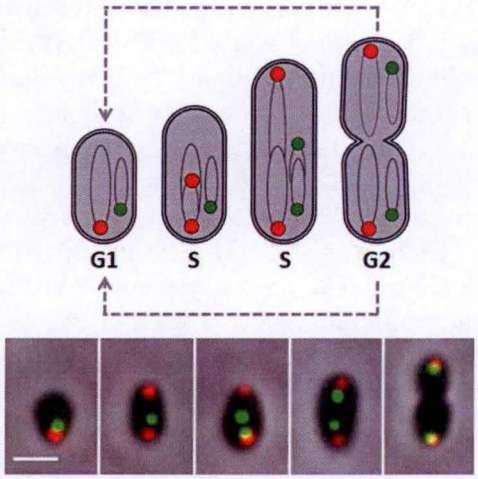

Figure 8 | Localization of the replication origins in *Brucella abortus*. The *oriI* and *oriII* were highlighted using fluorescent fusion proteins, mCherry-ParB for ChrI (red) and YFP-RepB for ChrII (green). These fusions allow to observe the replication status of the bacteria. When the replication has not been started, bacteria are in the G1 stage, which is characterized by only one *oriI* and one *oriII*. During the S stage, bacteria replicate their DNA. When the replication is initiated, the first chromosome always duplicates its *oriI* whereas the second shows a little delay (adapted from Deghelt *et al.*, 2014). The scale bare represents 2µm.

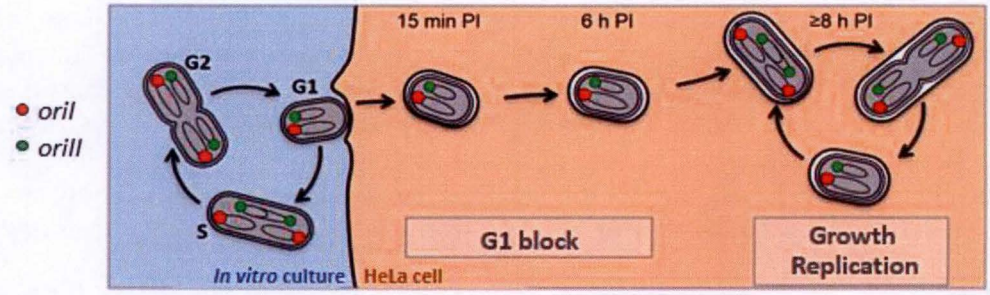

Figure 9 | *Brucella abortus* cell cycle in an *in vitro* culture and infection of HeLa cells. Upon growth on a rich medium, *Brucella* initiates the replication of ChrI first. When infecting mammalian cells (HeLa cell in this model), not only the bacteria in G1 stage were found to be to predominant infectious form but those bacteria stay blocked in G1 phase until they reach their proliferation niche. There, they eventually start DNA replication and resume growth. The *oriI* is represented in red and the *oriII* in green (Adapted from Deghelt *et al.*, 2013).

By counting the number of *oris,* it has been shown that the cell cycle of *Brucella* is composed of three main stages. As long as the replication has not been started, only one *oriI* and one *oriII* are seen as two distinct foci (mCherry-ParB and YFP-RepB). These bacteria are called "newborns" and they correspond to the G1 phase of the cell cycle. Once initiation of replication occurs, two fluorescent foci corresponding to *oriIs* (mCherry-ParB) are observed. This event corresponds to the entry into the DNA synthesis phase (S phase) followed by segregation of the duplicated replication origin. These data revealed that the chromosome I initiates its replication first, indicating a coordination between the replication of both chromosomes (Deghelt *et al.*, 2014). The molecular mechanism of this coordination is unknown. The bacteria found in this stage have initiated chromosomal replication, but no constriction site is not detectable. Then, two foci of *oriII* are detected indicating that the ChrII has initiated its replication in turn **(Figure 8)** (Deghelt *et al.*, 2014). When the bacteria have duplicated their termini, they are in G2 stage of the cell cycle. However, using the strain highlighting the *ori* only allows to discriminate bacteria in the G1 stage from those in the S/G2 phase.

Using these strains, it has also been shown that the *oriI* is localized either at the old pole for the G1 stage or at both poles during the S/G2 phase, whereas the *oriII* does not show any polar attachment. This is consistent with the fact that the two chromosomes show difference in terms of partitioning systems and evolutive origin (Deghelt *et al.*, 2014).

3.2. Cell cycle and infection are coordinated

The intracellular trafficking of *Brucella* infecting mammalian cells is defined by two main stages. The infection starts with a long non-proliferative stage characterized by a stable number of CFUs (colony forming units) where the bacteria transit within endocytic vacuoles, and is followed by a proliferative phase where bacteria have reached their proliferation niche and initiate their replication (Deghelt *et al.*, 2014).

Investigating the replication status of bacteria inside the host cells in culture using the reporter strain *mcherry-parB/yfp-repB*, it was observed that no chromosome replication occurred for 4 to 8 hours post-infection, depending on the type of cells infected. This observation suggests that bacteria stay blocked in G1 phase after internalization in host cells (**Figure 9**) (Deghelt *et al.*, 2014). Moreover, at fifteen minutes post-infection, about 80% of the engulfed bacteria are in G1 phase, while in a rich culture medium, this population only represents 18 to 26% of the bacterial population, suggesting that G1 bacteria preferentially invade the host cell. The second stage of the infection is characterized by an increased number of CFUs and a high number of bacteria in S/G2 phase indicating that the cell cycle has restarted. Using a marker of the endoplasmic reticulum (ER), it was observed that this proliferative phase corresponds to the stage where bacteria reside in this compartment, that constitutes the only replicative niche for *B. abortus*. However, the growth and replication have previously been started, when the bacteria were in Lamp1 positive compartment (Celli *et al.*, 2015). Taken together, these data indicate a coordination between the cell cycle and the infection process of *B. abortus* (Deghelt *et al.*, 2014). Therefore, studying the regulation of chromosomal replication in *Brucella* might be of particular interest to further understand the mechanism underlying this phenomenon.

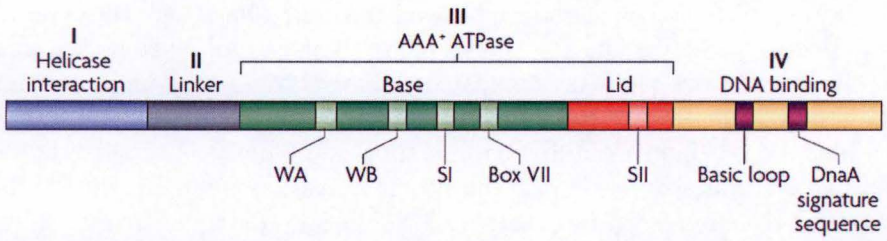

Figure 10 | Schematic representation of the 4 domains of DnaA. The domain IV recognizes DnaA binding boxes within the *ori*, through a helix turn helix motif. The domain III consists of an AAA+ motif binding ATP, and is able to change conformation in order to allow a proper oligomerization of the protein into a filament. Domain II is thought to be a linker joining the first with the third domain. Finally, the first domain enables the interaction of DnaA with the helicase (adapted from Mott & Berger 2007).

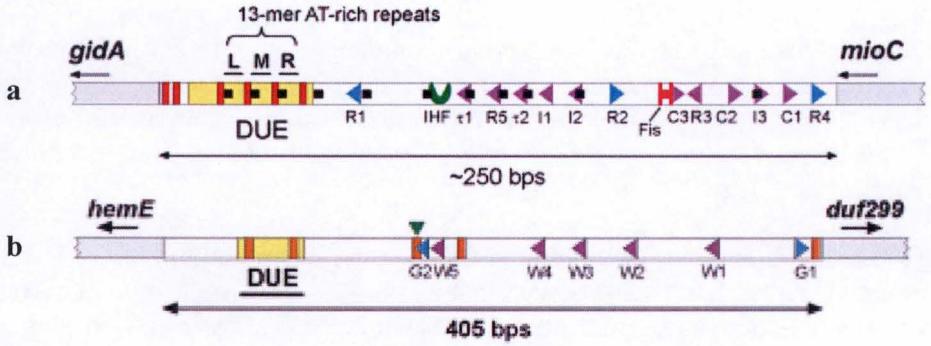

Figure 11 | Representation of the chromosomal origin of replication of *E. coli* (a) and *C. crescentus* (b). The arrow directions represent the orientation of the DnaA binding boxes. The blue arrows indicate high affinity binding sites for DnaA, allowing the binding of DnaA-ATP and ADP (R1, R2 and R4 for *E. coli*; G1 and G2 for *C. crescentus*). On the contrary, the purple arrows represent the low affinity binding sites, only allowing the binding of DnaA-ATP (R5, R3, tau and I sequences for *E. coli*; W sequences for *C. crescentus)*. The DNA unwinding element (DUE) is found in *E. coli* as well as *C. crescentus.* This sequence is composed of AT repeats. Other elements bind within the chromosomal origin of replication of both bacteria, such as IHF (represented in green) and Fis (red H) for *E. coli,* and IHF (green arrow) and CtrA (orange line) for *C. crescentus* (Wolanski *et al.*, 2015).

4. Chromosomal replication

4.1. Generalities

Chromosomal replication in bacteria is a highly complex and coordinated mechanism involving three main steps: initiation, elongation and termination (Baker & Bell 1998). In most bacteria, the replication starts at one single place in the chromosome, the origin of replication, also named *ori.* This *ori* can have different sizes depending on the bacteria and usually contains an AT rich region, called DNA unwinding element (DUE), and several binding sites for a specific initiator protein (Messer *et al.*, 2001; Leonard & Grimwade 2004). This specific initiator protein binds to the *ori,* allowing the denaturation of the double strand DNA and the assembly of factors involved in DNA replication, leading to the formation of the replisome. This complex contains several activities such as specialized polymerases that synthetize new strands of DNA, editing exonucleases, proteins controlling polymerases interactions with the DNA, and a replicative DNA helicase that unwinds the two strands of the DNA (Baker & Bell 1998). From there, two replication forks are generated and proceed in opposite directions until they reach the termination site, named *ter* (Mackiewicz *et al.*, 2004). This process leads to the duplication of the chromosome (O'Donnel *et al.*, 2013; Skarstad & Katayama, 2013).

4.2. Initiation of chromosomal replication

DnaA is the key protein for the initiation of chromosomal replication in bacteria, and also act as a transcription factor in some bacterial species, i.e. *Escherichia coli*, *Bacillus subtilis* and *Caulobacter crescentus* (Messer & Weigel 2003; Smith & Grossman 2015; Hottes *et al.*, 2005). This protein is composed of four domains **(Figure 10)**, including a central ATPase domain and is highly conserved among bacteria (Messer 2002; Zawilak-Pawlik *et al.*, 2017). DnaA is part of the ATPases associated with diverse cellular activities (AAA+) superfamily. Members of this superfamily are characterized by an ability to oligomerize, but also by a nucleotide binding domain and a conserved ATPase domain that constitutes the catalytic domain (Snider *et al.*, 2008). DnaA has an intrinsic ATPase activity and can therefore be found in two forms, either bound to ATP or to ADP (Speck *et al.*, 1999).

Using its C-terminal domain, DnaA binds to consensus sequences, named DnaA-binding boxes, which are repeated and organized in cluster in a short distance around the chromosomal replication origin (*ori*) (Bramhill & Kornberg 1988; Mackiewicz *et al.*, 2004). In *E. coli*, this protein is able to bind with a high and a low affinity to DnaA-binding boxes, in the *ori*. The high affinity boxes were shown to be 9 mers and are part of the so-called R-boxes (Schaper & Messer 1995). Two different affinity level are found within the R-boxes, the high affinity one are accessible for both forms of DnaA (R1, R2 and R4), whereas only the ATP bound form of DnaA is able to bind to the low affinity sites (R3 and 5) (McGarry *et al.*, 2004). Other low affinity boxes can be found within the *ori* of *E. coli*, and are 6 bases pair sequences (Speck *et al.*, 1999). Those sequences are named tau (τ) and I sites and only allow the binding of DnaA-ATP (Ryan *et al.*, 2002). However, *C. crescentus* does not contain I and tau boxes and only shows two apparent DnaA-binding boxes within the *ori*. They differ from the R-boxes of *E. coli* and are named G- and W-boxes (Taylor *et al.*, 2011; Shaheen *et al.*, 2009). The G-boxes are 9mers and the W-boxes are 6mers (**Figure 11**). They are respectively weak and very weak binding site for DnaA when compared to the R-boxes of *E. coli* (Taylor *et al.*, 2011).

Nevertheless, in *E. coli* as well as in *C. crescentus*, when enough DnaA-ATP has accumulated in the cell, the DnaA monomers oligomerize into a helical filament and/or a nucleosome-like

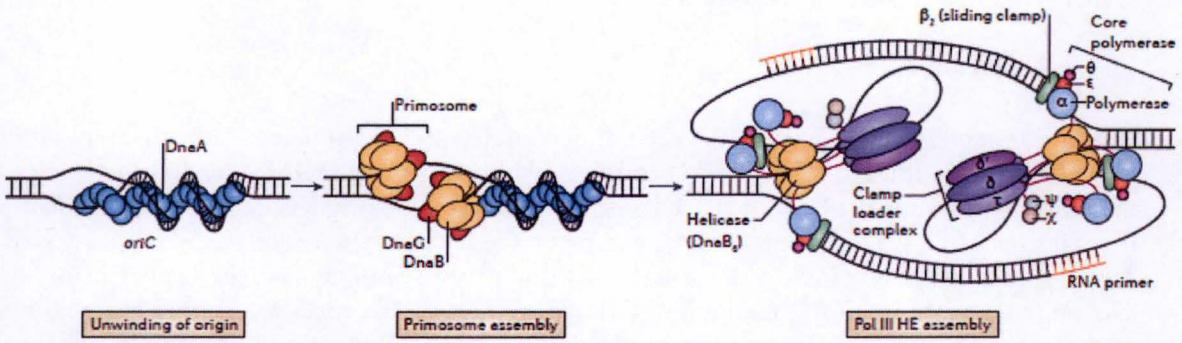

Figure 12 | Simplified model of replication initiation and elongation in *E. coli*. DnaA first binds to the DnaA binding boxes localized within the replication origin. By doing so it triggers the unwinding of the double strain DNA, further allowing the recruitment of the helicase DnaB and the primase DnaG, forming the so-called primosome. Then, the DNA polymerase-based replisome assembles. Replication forks are formed and proceed bidirectionnaly until they reach the termini (Robinson *et al.*, 2013).

structure (Zawilak-Pawlik *et al.*, 2017). This oligomerization process is in fact one major feature found in the AAA+ proteases (Snider *et al.*, 2008). This event induces a conformational change in the bound DNA, resulting in a local unwinding at the AT rich region of the *ori.* The unwinding of the double strand DNA generates simple strand DNA which allows the loading of the DNA helicase, DnaB, by DnaC (Erzberger *et al.*, 2006). DnaC is another AAA+ ATPase that not only acts as a loading factor for DnaB, but also inhibits the helicase activity and the adenosine triphosphatase (ATPase) activity of DnaB (Makowska-Grzyska & Kaguni 2010). DnaB becomes activated through the interaction of the complex DnaB-DnaC with the DnaG primase, which causes the dissociation of DnaC and thereby the activation of DnaB (Makowska-Grzyska & Kaguni 2010). From there, DnaB triggers the bidirectional unwinding of the double strand DNA and generates the two replication forks (Bramhill & Kornberg 1988). The DNA polymerase holoenzyme III-based replisome assembles at each replication fork and the elongation starts (**Figure 12**) (Bramhill & Kornberg 1988).

4.3. Elongation: role of the DNA polymerase III and its β sliding clamp

The elongation occurs through the action of two main kinds of polymerases: the primase which synthesize primers to start the replication and the replicative polymerase that allows the elongation (Kornberg & Baker 2006). The DNA polymerase III holoenzyme is a replicative polymerase composed of three parts: the core, the β sliding clamp also called DnaN, and the clamp loader complex (**Figure 12**) (O'Donnell 2006). The core of the DNA polymerase itself is divided in three subdomains: α, containing the DNA polymerase activity, ε, subunit responsible for the 3' to 5' proofreading exonuclease activity and θ, for which no essential activity has been shown (Bloom *et al.*, 1996). However, the binding of the core of the DNA polymerase on its own is a highly inefficient process. Therefore, it needs to be attached to the DNA during the elongation and this process is mediated by the β sliding clamp of the DNA polymerase. DnaN is a ring-shaped homodimer which is actively loaded by the clamp loader to the 3'-ends of the previously synthetized primers. When loaded, it anchors the core of the DNA polymerase III to the DNA during the DNA synthesis (Baker & Bell 1998). Moreover, since the replication forks move bidirectionally and the DNA polymerase only works in the 3' to the 5' direction, the parental strands of the DNA are copied in opposite directions generating two strands, the leading and the lagging strand (O'Donnell 2006). The leading strand is the one whose synthesis is made from the 3' end, this strand is called leading because it can be continuously replicated. On the contrary, the lagging strand is uncontinuously synthetized which generates several segments of DNA, called the Okazaki fragments. Each of those segments requires the loading of one β sliding clamp of the DNA polymerase, that remains on the DNA after the fragment synthesis, whereas the core and the clamp loader of the polymerase are recycled. In fact, the β clamp has additional roles, i.e. allowing the binding of other proteins, and was shown to act as a kind of toolbelt for the replisome (O'Donnell 2006).

4.4. Termination

The end of the elongation phase is completed when the replication forks reach the replication termini (*ter*) (Brussiere & Bastia, 1999). Following the replication forks arrest, the two daughter chromosomes achieve their replication and the replisome disassembles as soon as the DNA replication is over (Brussiere & Bastia, 1999). The termination is followed by the chromosome segregation and the creation of a constriction site through the polymerization of FtsZ into a ring-like structure (Jonas, 2014). The FtsK proteins, localized near the FtsZ ring, help the *ter* regions of the replicated chromosomes to move away from the constriction site, to avoid them to be cut during cell division (Stouf *et al.*, 2013).

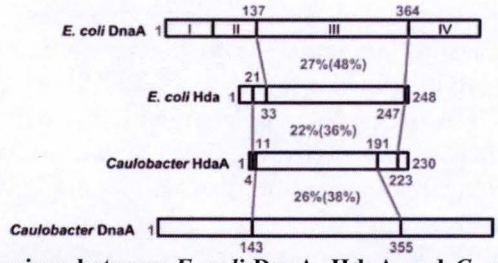

Figure 13 | Homology regions between *E. coli* DnaA, HdaA and *C. crescentus* HdaA and DnaA. HdaA is shown to be similar to both DnaA and Hda of *E. coli*. The 4 domains of DnaA are represented in *E. coli* DnaA, with the 3rd domain corresponding to the AAA+ domain which is found in Hda as well as DnaA. The numbers in grey are representing the amino acids positions on the protein; the percentages show the identities between the regions, the similarities between the regions being in brackets.

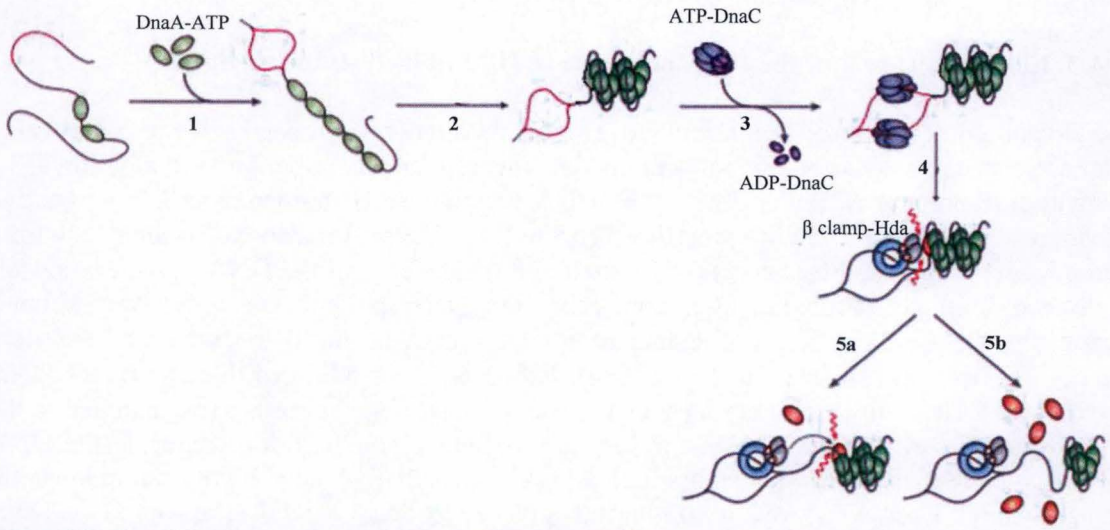

Figure 14 | Simplified model for the regulated inactivation of DnaA by Hda, based on the *E. coli* model (adapted from (Mott & Berger 2007)). DnaA binds to DnaA binding boxes within the chromosomal origin of replication, near an AT rich region (represented in red) (1). When enough DnaA-ATP (represented in green) has accumulated in the cell, the proteins oligomerize forming an homomultimer of DnaA. This homomultimer generates a remodeling of the chromosomal origin of replication that leads to the unwinding of the downstream AT rich region (2). The DnaB helicase is then loaded to the simple strand DNA molecule thanks to its loading protein, DnaC (3), and allows the unwinding of the double strand DNA, generating two replication forks. The β sliding clamp of the DNA polymerase is recruited and recruits in turns Hda (4). The complex formed by the β clamp and Hda enables Hda to interact with DnaA and to stimulate its intrinsic ATPase activity leading to the inactivation of the initiator of chromosomal replication. Two mechanisms have been proposed for its inactivation, it may either be sequential (5a), meaning that Hda inactivates one DnaA molecule at a time generating DnaA-ADP (represented in orange), or catastrophic (5b), inactivating several DnaA in the same time (Mott & Berger 2007).

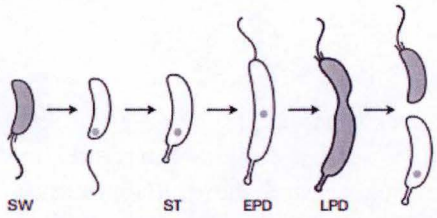

Figure 15 | Schematic representation of the subcellular localization of HdaA in C. crescentus. The grey color indicates the localization of HdaA while the grey dots represent foci. When the cells are fully colored, HdaA is homogeneously distributed within the bacteria. HdaA is first found homogeneously distributed in the non-replicating swarmer cells (SW), then a focus is formed in the replicative stalked cells. This focus evolved with the replisome within the ST and the the early predivisionnal cells (EPD). Then, the replisome disassembles and and HdaA is found distributed in the late predivisionnal cells (LPD) (Fernandez-Fernandez et al., 2011).

5. Regulation of chromosome I replication

Chromosomal replication can be regulated at several levels. The initiation of chromosome replication is a process that needs to be tightly regulated to have a specific coordination with the cell cycle, i.e. only one initiation of replication per cell cycle, depending on the bacterial species (O'Donnell *et al.*, 2013; Duderstadt *et al.*, 2011). Several mechanisms are involved in this regulation such as post-translational modifications, proteolysis, but also transcriptional control. Those mechanisms can be regulated by an alarmone, the ppGpp, which is known to induce a stringent response thereby blocking the replication in stressful conditions (Magnusson *et al.*, 2005), or by proteins displaying different activities. This work will focus on proteins exerting a role on chromosomal replication in *B. abortus*.

5.1. Control of replication by HdaA

The regulated inactivation of DnaA (RIDA) is one of the most important regulatory mechanism preventing the over-initiation of replication. In *E. coli*, this mechanism is essential and is mostly mediated by Hda, a protein homologous to the ATPase domain of DnaA (**Figure 13**) (Kato & Katayama 2001). Hda was first identified and described in *E. coli*, where it was shown to be a regulator of the chromosomal replication (Camara *et al.*, 2003; Kato & Katayama 2001). This protein can be found bound to ADP or in its « apo » state, meaning that Hda is not bound to any nucleotide. When bound to ADP the protein is active and is found in a monomeric state, whereas Apo-Hda is inactive and forms multimers (Su'etsugu *et al.*, 2008). More precisely, the binding of ADP enables the dissociation of the inactive Hda multimers (Su'etsugu *et al.*, 2008). Once DNA replication is started, Hda-ADP is recruited to the replisome by binding the β clamp (DnaN) of the replisome. The interaction between those two proteins is required for the RIDA process and this interaction is mediated through a β clamp binding motif localized at the N-terminus of Hda (Kurz *et al.*, 2004). Then, Hda-ADP stimulates the intrinsic ATPase activity of DnaA leading to DnaA-ADP. The exact mechanism of this inactivation is unclear but it may occur at the replisome or at the *ori*, directly after the recruitment of the sliding clamp **(Figure 14)** (Kim *et al.*, 2017). This process occurs through a putative arginine finger located in the AAA+ domain of Hda (Fernandez-Fernandez *et al.*, 2013; Kato & Katayama 2001; Nakamura & Katayama 2010). This motif was shown to be essential for the hydrolysis of ATP bound to DnaA because it enables the interaction between the AAA+ domains of Hda and DnaA (Nakamura & Katayama 2010). Moreover, since Hda is recruited by the β clamp, and since the complex β clamp-Hda is only active when bound to DNA, it provides a temporal control of the replication ensuring the requirement of Hda only when the replication has already been started (Su'etsugu *et al.*, 2004).

Hda is conserved in the group of alpha-proteobacteria, including in *Caulobacter crescentus* where its homolog is named HdaA **(Figure 13)** (Collier & Shapiro 2009). This protein was shown to dynamically colocalize with the replisome (**Figure 15**), which is consistent with the fact that it displays the same function as in *E. coli*, even though HdaA of *C. crescentus* also affects the stability of DnaA (Wargachuk & Marczynski 2015). Especially, HdaA enables the degradation of DnaA-ATP during exponential phase and the degradation of all the DnaA in stationary phase, therefore providing a better control of chromosome replication (Wargachuk & Marczynski 2015). Two major hypotheses have been proposed to explain how HdaA could lead to proteolysis. First, HdaA may indirectly expose DnaA to proteolysis by removing it from the DNA, by triggering a conformational change, or by forming DnaA-ADP which would lead to a less stable protein that would be easily degraded. The second hypothesis is that HdaA

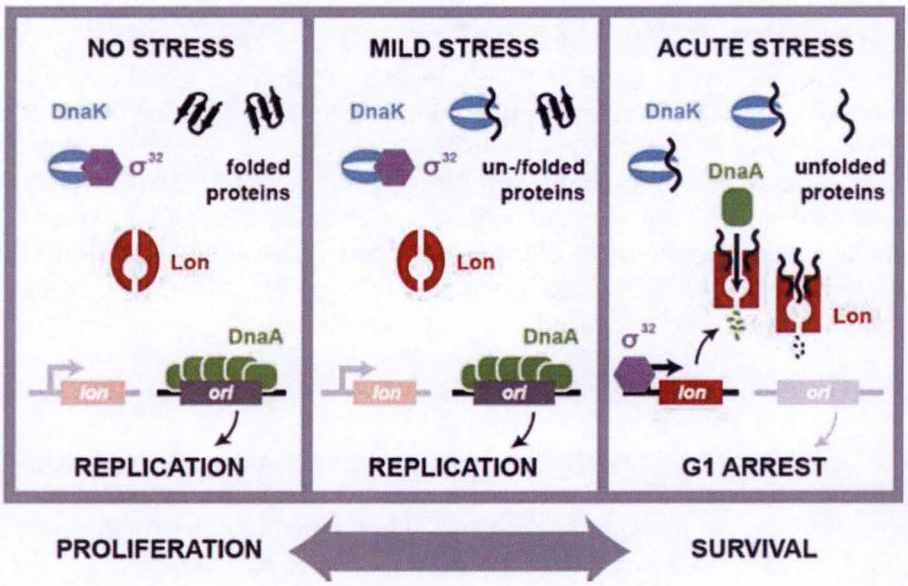

Figure 16 | Different stress conditions and their effect on DnaA degradation by the Lon protease. When the bacteria are not facing any stress, a basal expression of the Lon protease is present, but this will not trigger the degradation of DnaA. Therefore, the initiator protein will bind the chromosomal origin of replication and start the replication. If the bacteria have to cope with a mild stress, the few misfolded proteins will be folded by a chaperone (DnaK, for example), no degradation of DnaA will occur and there will be replication. However, if the stress is acute, a lot of unfolded proteins will accumulate in the bacterium and the chaperones will rapidly be saturated, releasing the sigma factor and thereby leading to the transcription of Lon. The Lon protease then degrades DnaA and by doing so, inhibits the chromosomal replication leading to a G1 arrest (Jonas *et al.*, 2013).

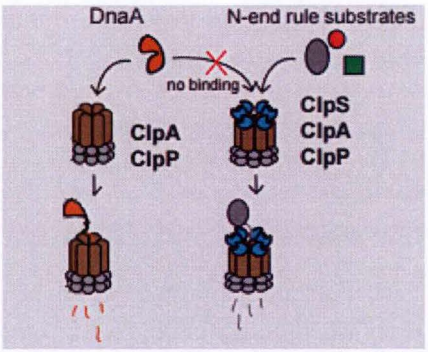

Figure 17 | Schematic representation of ClpAP roles. ClpAP shows two different ways for degrading proteins. The first mechanism involves ClpS (blue), which recognizes the N-end rule substrates and targets them into the proteolytic chamber, ClpP (grey) by passing through ClpA (brown). The second mechanism is the one used for the degradation of DnaA in *Caulobacter crescentus.* In this mode of action, ClpS is not involved in the recognition of the substrate but rather inhibits the recognition when it is not needed. ClpA is able to recognize DnaA on its own and then targets it toward the ClpP protease to degrade the proteins (Liu *et al.*, 2016).

acts as a chaperone when inactivating DnaA and guides the protein to the ClpAP protease or to the Lon protease for degradation (Wargachuk & Marczynski 2015).

5.2. DnaA proteolysis mediated by Lon and ClpAP

Regulated proteolysis during the cell cycle is one of the mechanisms driving its progression. The mechanism is also critical for bacterial growth by helping to maintain a correct level of proteins at the right time (Vass *et al.*, 2016). This could be crucial in the case of replication because an excess of DnaA leads to an overinitiation of replication, and is toxic in many bacteria (Jonas *et al.*, 2011; Liu *et al.*, 2016). In *C. crescentus*, Lon and ClpAP, two proteins from the AAA+ family of proteases, are involved in DnaA degradation (Liu *et al.*, 2016; Vass *et al.*, 2016). These proteases use the energy provided by ATP to recognize, unfold and degrade their targets and are both responsible for normal and stress related proteolysis. They are characterized by an ATPase domain and several protease domains (Joshi & Chien 2016; Vass *et al.*, 2016). Because they are involved in DnaA proteolysis in *C. crescentus*, they play an important role in the regulation of chromosome replication in this bacterium too (Jonas *et al.*, 2011; Liu *et al.*, 2016).

The conserved Lon protease is formed by a single polypeptide and is involved in misfolded/damaged proteins degradation (Gur 2013; Vass *et al.*, 2016). Despite its important role in protein quality control, this protease is also responsible for the degradation of different regulatory proteins when they are natively folded (Vass *et al.*, 2016; Van Melderen & Aertsen 2009). Lon regulates several physiological processes such as cell division, DNA replication, and stress adaptation (Gur, 2013). How the Lon protease recognizes its targets is still unclear, but it has been suggested that they might be recognized by a tag rich in non-polar amino acids (Shah & Wolf 2006). The AAA+ domain of Lon enables the unfolding of its substrates and their translocation to the proteolytic chamber (Van Melderen & Aertsen 2009). Among its activities, the degradation of DnaA is a process particularly important during proteotoxic stress or starvation in *C. crescentus* (Jonas *et al.*, 2013; Leslie *et al.*, 2015). Indeed, it has been shown that Lon can be allosterically activated by unfolded proteins and that in these given conditions, DnaA degradation by Lon was more efficient **(Figure 16)** (Jonas *et al.*, 2013). Lon is deficient for degrading DnaA-ATP whereas it is able to degrade ADP-bound form of DnaA, in exponential as well as in stationary phase (Gur 2013; Jonas *et al.*, 2013; Leslie *et al.*, 2015). Thus, Lon plays an important role for physiological processes such as the control of DNA replication, however, considering its numerous targets, it can be rapidly saturated. Therefore, other studies have suggested the importance to have other proteases presenting a similar function (Gur 2013; Liu *et al.*, 2016).

ClpAP is composed of two conserved polypeptides, ClpA and ClpP, forming a functional protease. ClpA is an ATPase with a chaperone activity that unfolds and translocates substrates through its central pore toward ClpP, which constitutes the proteolytic chamber (Liu *et al.*, 2016). In *C. crescentus* as well as is *E. coli*, the *clpA* gene is co-transcribed with a *clpS* gene coding for an adaptor (ClpS) which binds the N-terminal part of ClpA and has a dual role in ClpAP-mediated degradation (**Figure 17**). Since proteolysis is an irreversible process and since the recognition is the determinant step leading to degradation, the function of ClpS is crucial (Vass *et al.*, 2016). On one hand, ClpS can help ClpA to identify substrates by recognizing a specific amino acid residue on the N-terminal part of the target proteins. This signal is sufficient to trigger the binding of ClpS to its targets and to direct the substrates to the proteolytic chamber (Erbse *et al.*, 2006). This mode of degradation is the one used for the N-end rule degradation pathway (Dougan *et al.*, 2010). On the other hand, when ClpA is able to recognize its substrates

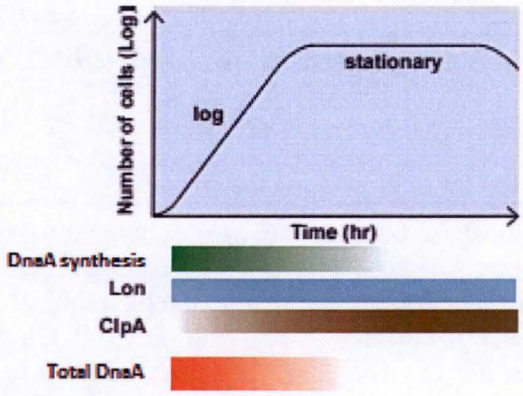

Figure 18 | Representation of the global amount of the Lon and ClpA in *Caulobacter crescentus* over culture time. When the bacteria are in logarithmic phase, they are synthetizing new DNA and therefore need DnaA to initiate chromosomal replication. However, when they reach the stationary phase, the total amont of DnaA progressively decrease leading at the end to the total degradation of all DnaA molecules in the late stationary phase. This degradation is mainly due to Lon that is present during exponential as well as stationary phases, but also to the ClpA chaperone that is progressively produced until the bacteria reach their stationary phase where the concentration of ClpA is higher. This indicates a role of ClpA during the stationary phase more than during the exponential phase. This role is directly linked to the degradation of DnaA, even though this protease was shown to be an auxiliary protease for DnaA degradation (Liu *et al.*, 2016).

on its own, ClpS can block the access of some substrates to ClpA and thereby indirectly inhibits ClpAP proteolytic activity on these substrates (De Donatis *et al.*, 2010; Liu *et al.*, 2016). For example, in *C. crescentus,* ClpA is involved in the recognition, followed by the degradation of FtsA and FtsZ by the ClpP protease, two major cell division proteins, and was shown to be required for the cell division (William *et al.*, 2014). Moreover, ClpAP was shown to be an auxiliary protease for DnaA degradation during exponential and stationary phases (Liu *et al.*, 2016). During entry into stationary phase, the levels of ClpAP rise whereas DnaA levels decrease in *C. crescentus*, suggesting that ClpAP has a role in DnaA degradation during this phase (Liu *et al.*, 2016).Therefore, it has been suggested that ClpAP could be of great interest during exponential phase as well as when the Lon protease is saturated (**Figure 18**) (Gur 2013; Liu *et al.*, 2016).

OBJECTIVES

The general objective of this is to understand the mechanisms underlying the regulation of initiation replication of the first chromosome in *Brucella abortus*. Therefore, we want to investigate the role of three proteins potentially involved in chromosomal replication: HdaA, Lon and ClpA. Those three proteins are more precisely thought to be involved in the control of the initiator protein, DnaA.

Regarding HdaA, we first want to create a *hdaA-yfp* strain in order to observe the localization of the protein in wild type (WT) bacteria and in a *mCherry-parB* strain highlighting the *oriI*. This mutant will be achieved by allelic replacement at the chromosomal locus. If the fluorescent signal of the YFP is stable after fixation of the bacteria, we also plan to study localization patterns of the strain in infection of eukaryotic cells. Since *hdaA* is an essential gene, as shown in a Tn-seq experiment, we want to create a depletion mutant (*hdaA*$^-$) by inserting the coding sequence of *hdaA* under the control of an inducible promoter on a replicative plasmid (pBBRi), and by deleting the chromosomal copy of *hdaA*, which will be achieved by allelic replacement. Using the same plasmid, we want to create an overexpression strain of *hdaA* in a WT background and in the *mCherry-parB* strain in order to further investigate the impact of HdaA on the initiation of ChrI replication in *B. abortus*.

Because *lon* is not essential according to the Tn-seq analysis, we plan to delete it by allelic replacement in a WT background as well as in the *mCherry-parB* strain, in order to investigate their impact on the initiation of ChrI replication (Δ*lon*). Concerning *clpA,* since the gene is organized in operon with *clpS* and since none of the genes are essential according to the Tn-seq, both will be deleted in a first time (Δ*clpSA*) in a WT and in a *mCherry-parB* backgrounds. Because the ClpAP and the Lon proteases were shown to degrade DnaA in *C. crescentus*, we want to do western blot analysis to investigate if ClpA and Lon may have a role in DnaA degradation in *Brucella abortus* as well. For each mutant, we want to characterize the growth in rich medium, and the status of chromosomal replication using fluorescence microscopy to highlight the *mCherry-parB* fusions. In order to test the ability of the *lon* and *clpSA* mutants to invade and replicate inside host cell, we plan to perform infection of eukaryotic cells and compared them to WT bacteria by counting the colony forming units (i. e. living bacteria) at different times post infection. If DnaA is degraded by Lon or ClpAP and if uncontrolled initiation of replication is toxic early in the intracellular trafficking, we could expect to see a decreased survival of the bacterial mutants in host cells.

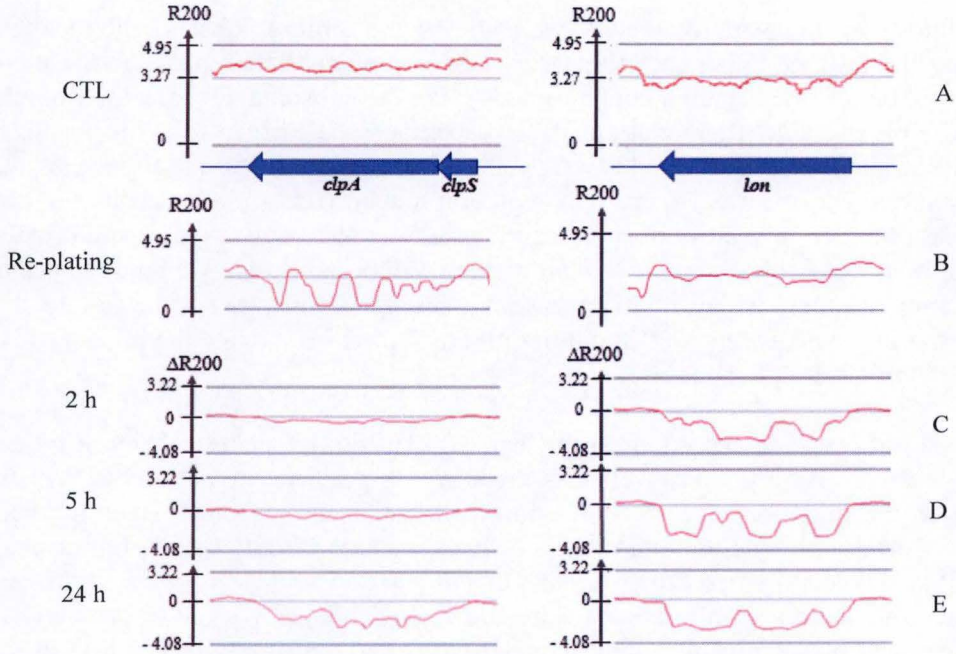

Figure 19 | Tn-seq analysis for *clpA*, *clpS* (2475 and 411 bp respectively, on the left) and *lon* (2439 bp, on the right). The experiment consists in creating a library of transpositionnal mutants and then investigating their global wellness in a 2YT rich medium (A, representing the control; CTL), when re-plated in 2YT rich medium (B, Re-plating), and in RAW 264.7 macrophages infection at different times post infection: 2 h, 5 h, and 24 h (C, D, E respectively). The red line represents the global insertion of the transposon in the genome (R200 representing the log10 of the number of mini-Tn5 insertion(s)+1 computed in a sliding window of 200 bp). If R200 is above the average value for the chromosome (thin grey line), it means that bacteria can grow with a Tn-insertion at this place. If the red line is below the average (grey line), it means that the mutant presents defect for growth and if the R200 is equal to 0, it indicates that the corresponding gene is essential. The three lower graphs represent the infection profile at 2, 5 and 24 h minus the control data, centering the average on zero (ΔR200). Therefore, the genes showing negative values are proposed to be important for infection.

As mentioned in the Objectives, we chose to investigate the role of three proteins potentially involved in chromosomal replication in *B. abortus.* We first investigated the roles of the Lon and the ClpAP proteases in *B. abortus.*

1. Lon and ClpA

1.1. Tn-seq analysis of the *lon* and *clpSA* loci

We first searched for homologs of those proteins and found *clpSA* (BAB1_1191 and BAB1_1192) and *lon* (BAB1_1130) in *B. abortus.* Indeed, like in *C. crescentus* and many other bacteria, the *clpA* coding sequence is in operon with *clpS* (**Figure 19**). Using a Tn-seq analysis, we investigated whether those genes are essential or not in *B. abortus*. The Tn-seq is a high throughput experiment highlighting essential genes for growth in rich medium as well as genes required for survival in RAW 264.7 macrophages at different times post infection. For this experiment, a library of transpositional mutants was first created by the random insertion of a transposon, the mini-Tn*5*, in the genome of *B. abortus.* The mutants were then tested for growth on rich medium, for replating on rich medium or for survival in RAW 264.7 macrophages. The genomic DNA of all mutants was extracted for each condition and the regions flanking the mini-Tn*5* were amplified, sequenced and mapped on the genome in order to highlight insertion sites. Since the insertion of the mini-Tn*5* is spread over all regions of the genome, the region where no sequence was mapped are highly likely to be essential in the given condition. In this case, the interpretation is that the insertion of a mini-Tn*5* would be detrimental for the bacterial survival and/or ability to form a colony.

The Tn-seq analysis suggests that mutants containing the transposon in *clpA* gene are attenuated at 24 hours in infection of RAW 264.7 macrophages and that the gene coding for its adaptor protein ClpS starts to be attenuated at 24 h post infection (**Figure 19E,** left). This effect could be due to the fact that insertion in *clpS* and *clpA* has a negative effect on the fitness of bacteria. Another hypothesis could involve polar effects, since it is possible that Tn-insertions in the *clpS* coding sequence could impair the expression of *clpA*. According to the Tn-seq, the *clpSA* mutant should not show a strong growth defect on plate, suggesting that this gene may be required for infection (**Figure 19A**, left). However, it is noticeable that when Tn-seq is performed by simply replating the library on rich medium plates, the transpositional mutants in *clpA* display a huge drop in the R200 values (**Figure 19B,** left), suggesting that they have a growth defect. This is difficult to interpret since at 2 h PI, there is also a second round on culture on rich medium plates, and not growth defect is detected in Tn-seq (**Figure 19C**, left). In summary, this result suggests that we must be cautious when we interpret Tn-seq data that have been performed in a single experiment, without biological replicates.

Regarding the Tn-seq profile of *lon* we can observe an attenuation immediately at 2 hours post infection, and this attenuation seems to be more important at 5 hours and 24 hours post-infection (**Figure 19C, D, E**, right). The *lon* mutants already show a growth defect for the control condition on rich medium (**Figure 19A** right), that was not worsening in the replating condition (**Figure 19B**, right), further suggesting that the profile obtained in infection is really due to the infection itself rather than to an aggravation of the previous phenotype. This result suggests that *lon* might be required for a successful infection in *B. abortus.*

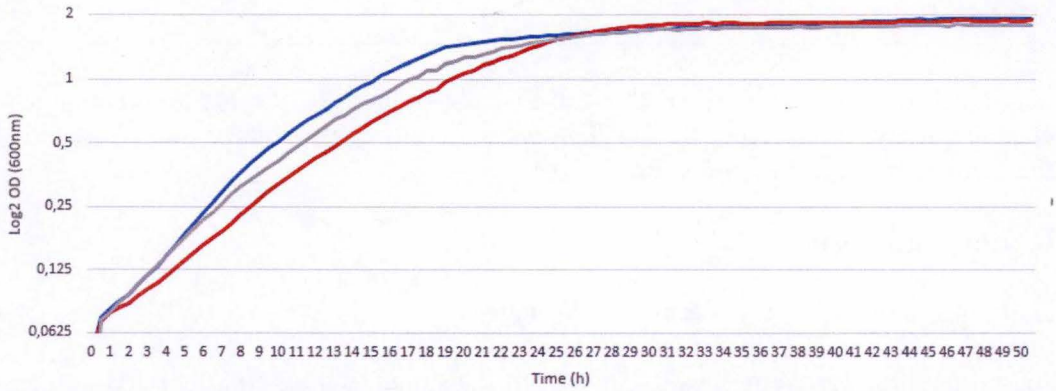

Figure 20 | Growth curve for the WT *B. abortus* (blue), the Δ*clpSA* (red) and the complemented strain Δ*clpSA*$^+$ (grey) for one representative experiment (logarithmic scale). For all conditions, bacteria were grown in 2YT rich medium and the bioscreen was performed for 50 hours. The OD of the WT, the Δ*clpSA* and the Δ*clpSA*$^+$ strains were taken every 30 minutes for 50 hours.

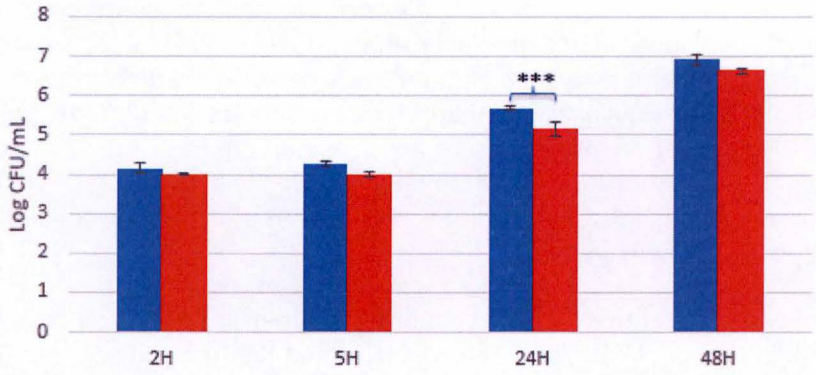

Figure 21 | Number of CFUs for the WT *B. abortus* (blue) and the *ΔclpSA* (red) at 2, 5, 24, 48 h and post infection of RAW 264.7 macrophages (logarithmic scale). The *** indicate a highly significant difference between the WT and the mutant (p-value<0.001) (n=3 technical replicates, error bars represent standard deviation (SD)).

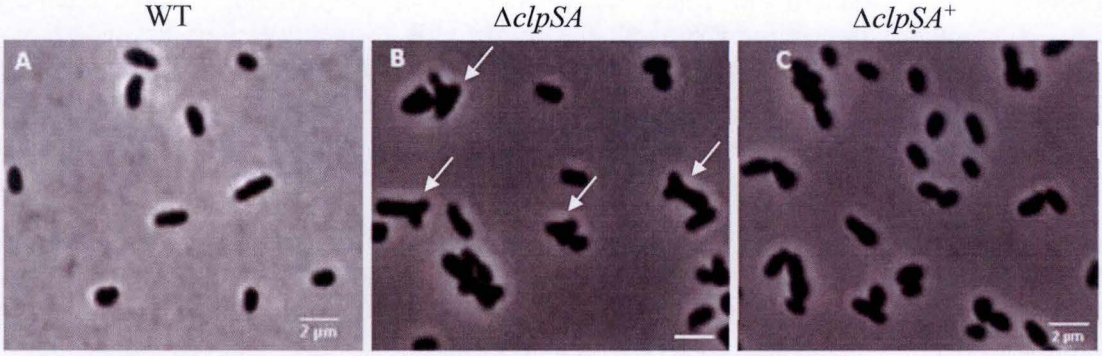

Figure 22 | Phase microscopy of WT *Brucella abortus* (A), Δ*clpSA* (B) and the complementation strain (C). The Δ*clpSA* strain shows morphological defects such as Y shapes, indicated by the white arrows. The complementation strain displays a morphology similar to the WT. The scale bar represents 2µm.

Since the results of the Tn-seq suggest that those genes do not seem to be essential, we decided to generate deletion mutants for both genes. Unfortunately, the *lon* deletion mutant (*Δlon)* was never obtained, suggesting that disturbing this locus could be deleterious for *B. abortus*. However, we obtained the deletion mutant for the *clpSA* operon (Δ*clpSA*) and performed several analyses on this mutant.

1.2. The growth of the Δ*clpSA* is impaired in culture

Concerning Δ*clpSA,* we first observed that the growth on plate as well as in a liquid culture medium was slowed down for the mutant compared to the WT. Therefore, the growth of the Δ*clpSA* strain was investigated by performing a bioscreen, i.e. an experiment consisting in measuring the optical density (OD) at 600 nm of a liquid culture over the time. This experiment was repeated three times, in order to have biological replicates. An exponential phase culture of the WT and *ΔclpSA* was diluted in rich medium at an initial OD of 0.1. The OD of both strains were then measured every 30 minutes for 50 hours. We observed that Δ*clpSA* presents a slight growth delay during the first 20 hours, corresponding to the exponential phase, but reaches the WT strain during stationary phase (**Figure 20**). In order to confirm that this phenotype was due to the *clpSA* deletion, a complementation strain (Δ*clpSA*$^{+}$) was also constructed by inserting a copy of the coding sequences under the control of their endogenous promoter (P*clpS)* in a pMR10 low copy replicative plasmid. The sequence was inserted in the opposite direction of the P*lac* promoter to further allow an expression level as close as possible to the WT situation. A bioscreen was performed for this strain, and we observed a slightly less important growth delay in exponential phase when compared to the Δ*clpSA* (**Figure 20**). However, the experiment was only performed once for the complementation strain and needs to be repeated twice in order to confirm these results.

1.3. The growth of the Δ*clpSA* is impaired in RAW 264.7 macrophages

Since the cell cycle and the infection are coordinated in *B. abortus* (De Bolle *et al.*, 2015), we wanted to investigate the infection profile of the Δ*clpSA* mutant. Indeed, it is possible that altering the proteolysis of DnaA or other substrates could disturb the ability of *B. abortus* to survive and proliferate inside macrophages. Therefore, we decided to infect RAW 264.7 macrophages with the WT and the Δ*clpSA* strains, to investigate a potential role of ClpSA during infection. The colony forming unit or CFUs (number of living bacteria estimated in 1 mL of cellular lysate, allowing to evaluate the number of intracellular bacteria still able to form a colony) were counted at different times post-infection (PI). At 2 hours PI no significant difference was observed between the WT and the mutant, meaning that there is no detectable difference for the entry in host cells between both strains. After 5 hours PI, a slight but not significant decrease in the number of CFUs was observed for the mutant strain. However, at 24 hours PI, a highly significant decrease was observed for the mutant compared to the WT. An interesting fact is that at 48 hours PI a slight but not significant decrease is observed for the mutant when compared to the WT (**Figure 21**).

1.4. The Δ*clpSA* mutant displays aberrant morphologies

Because we saw that the deletion of *clpSA* leads to an impaired growth in exponential phase, we wanted to further characterize the mutant by monitoring its morphology. To investigate this feature, bacteria were observed in exponential phase by phase contrast microscopy. The Δ*clpSA* clearly displays aberrant morphologies such as Y shapes, which are related to division defects in unipolarly growing bacteria, donut-shapes and other aberrant morphologies revealing fitness

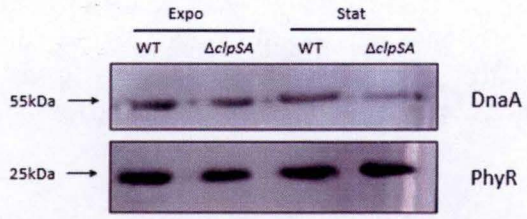

Figure 23 | Western blot analysis against DnaA in the WT and in the *ΔclpSA* strain in exponential and stationary phases. The strains were grown until a mid-exponential phase (DO 0.4) and until late stationary phase (DO 2.1) for the sampling. They were normalized to an optical density of 1 to perform the western blot analysis and 10µm of each were loaded on the SDS gel. The first antibody (anti-DnaA produced in rabbits) was used at a concentration of 1/3000 and incubated for one hour at RT. The secondary antibody was an anti-rabbit used at the same concentration (1/5000) for 1h at RT. The nitrocellulose membrane was exposed to chemiluminescence for 1 minute. PhyR represents the loading control.

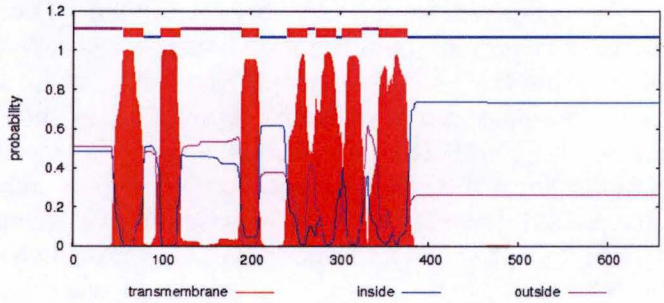

Figure 24 | Domain prediction on HdaA of *Brucella abortus* (658 aa). HdaA presents a transmembrane domain containing 7 predicted transmembrane segments in the N-terminal part. The C-terminal part (from aa 434 until 651) constitutes the conserved part which is homologous to HdaA of *C. crescentus*.

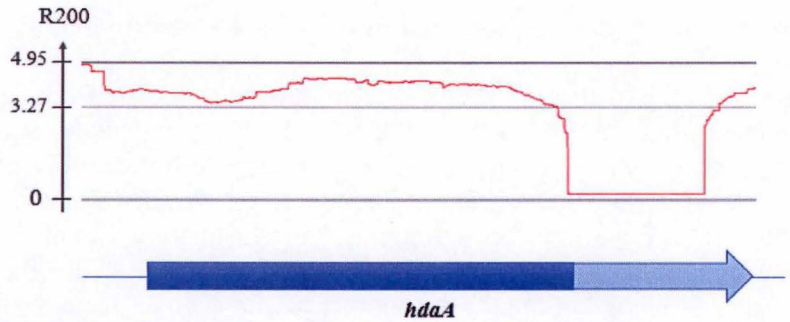

Figure 25 | Results of the Tn-seq analysis for *hdaA* in *Brucella abortus*. The N-terminal part of HdaA, corresponding to the transmembrane domain (dark blue), is not essential while the C-terminal, corresponding to the conserved part of HdaA, is essential (light blue).

```
HdaA B. abortus      434  QIPLNLSHQPGYNREDLIVTASNRAAVDLIDRWPNWLSPVTILAGPTGAGKTHLAEIWRS  493
                          Q  L L     + RED  V+ SN  AV  +D WP+W     +L GP G GK+HLA  W +
HdaA C. crescentus   4    QFKLPLASPLTHGREDFAVSPSNGEAVARLDAWPDWAEGRLVLVGPAGCGKSHLARAWAA  63

HdaA B. abortus      494  GTDALLVDPSNITEEAVNSAA--ERPVLIDNI-----GAEAFDETGLFHLINSVRQHAAQ  546
                            A++V+ +N    +V+ +A   R VL+++      GA   DE  LFH++N     A
HdaA C. crescentus   64   AAGAVVVEAANPDAASVDLSALRGRAVLVEDADRRAQGAAVSDEA-LFHILN-----MAG  117

HdaA B. abortus      547  GPGPSLLMTSRLWPANWNVKLPDLASRLKAATVVEIAEPDDMLLSGVIHKLFADRQVSVE  606
                            G ++L+T R  P  W+ ++ DL SRL A +V EIAEPDD +L  V+ + FA      E
HdaA C. crescentus   118  VDGGTVLLTGRTAPLTWSAEVADLRSRLNALSVAEIAEPDDAVLEAVLRRAFAAAWWKPE  177

HdaA B. abortus      607  PHVVSYLVSRMERSLLSAIQIVDRLDRAALEQKSRITRALAAQIL  651
                          P +  YL++R+ RS   A      L  AA + +  +T+ALA ++L
HdaA C. crescentus   178  PDLYPYLLARLPRSAAEAQAAAALLAEAAADGRRELTKALAREVL  222
```

Figure 26 | Blast analysis of HdaA in Brucella abortus against HdaA in Caulobacter crescentus. The red square shows the potential β binding clamp sequence of B. abortus as compared to the confirmed β binding clamp sequence of C. crescentus.

problems in the bacteria (**Figure 22B**). However, the complementation strain shows a restoration of the WT phenotype, presenting a morphology similar to the WT *B. abortus* (**Figure 22C**).

1.5. ClpSA seems to be involved in DnaA degradation during the stationary phase

It has been shown in *C. crescentus* that DnaA is totally removed from the bacteria in a stationary phase (Liu *et al.*, 2016). Therefore, the investigation of the possible degradation of DnaA in *B. abortus* was one of our main objective. To assess this question, we took samples from exponential and stationary phases culture of the WT and Δ*clpSA* and performed western blot analysis to highlight DnaA protein. We used antibodies against DnaA that have been generated during the master thesis. Those antibodies were generated using a recombinant protein containing only one part of the protein (Mathilde Van der Henst & Aurelie Mayard). If the proteolysis of DnaA is indeed mediated in part by ClpSA we would expected to see an increase in DnaA abundance for the Δ*clpSA* strain. Moreover, if DnaA is degraded as in *Caulobacter crescentus,* a decrease of DnaA is expected in the stationary phase compared to the exponential phase for the WT condition. The results show that DnaA levels seem to be similar for all conditions except for the stationary phase in Δ*clpSA* where the signal seems to be lower (**Figure 23**). This is in complete contradiction with our initial hypothesis, and will be discussed in the Discussion section. PhyR was used as loading control.

2. HdaA

We also wanted to investigate the role of another protein, HdaA, which was shown to be involved in one of the major mechanism preventing the overinitation of chromosome replication in *E. coli* as well as in *C. crescentus* (Kato *et al.*, 2001; Collier *et al.*, 2009).

2.1. Tn-seq and homology analyses

Using a protein blast analysis, we found a homolog of *hdaA*$_{C.crescentus}$ in *B. abortus* (BAB1_0733) that is partially conserved. Indeed, the protein found in *B. abortus* presents a large additional segment in the N-terminal part as compared to *C. crescentus*. We performed a prediction analysis for transmembrane domains of the whole HdaA$_{B.abortus}$ (http://www.cbs.dtu.dk/cgi-bin) and we observed that the large additional part of the protein corresponds to a transmembrane domain containing 7 transmembrane segments (**Figure 24**). Looking for synteny in other micro-organisms, it was observed that this additional domain is not found in any other bacterial species, even closely related (i.e. other *Brucella* species). Interestingly, the Tn-seq analysis revealed that the conserved part of *hdaA*$_{B.abortus}$ (C-terminal) is essential for growth in rich medium whereas the part corresponding to the transmembrane domain does not seem essential at all (**Figure 25**).

HdaA$_{Caulobacter}$ was shown to bind to the β-clamp of the DNA polymerase through a consensus sequence QFKLPL localized in the N-terminal part of the protein (Fernandez-Fernandez *et al.*, 2013). In this hexapeptide, it has been shown that only Q L L are important for recognition of DnaN by HdaA (Collier *et al.*, personal communication). Therefore, we search for such a sequence and found QIPLNL, localized at the N-terminal of the conserved part of the gene (**Figure 26**). Since the three amino acids required for the binding are conserved between *B. abortus* and *C. crescentus*, and because of the N-terminal localization of the sequence, this candidate is highly relevant as a β clamp binding motif, further suggesting that HdaA of *B. abortus* may bind the β clamp through **QIPLNL**.

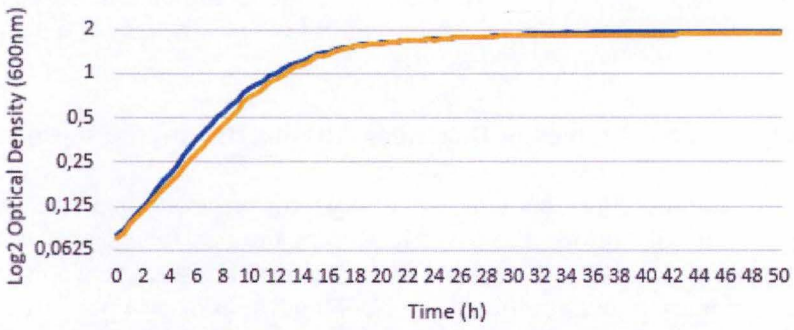

Figure 27 | Growth curve for the WT (blue) and the *hdaA-yfp* (yellow) strains for one representative experiment. For all conditions, bacteria were grown in 2YT rich medium and the bioscreen was performed for 50 hours. The OD was taken every 30 minutes for 50 h.

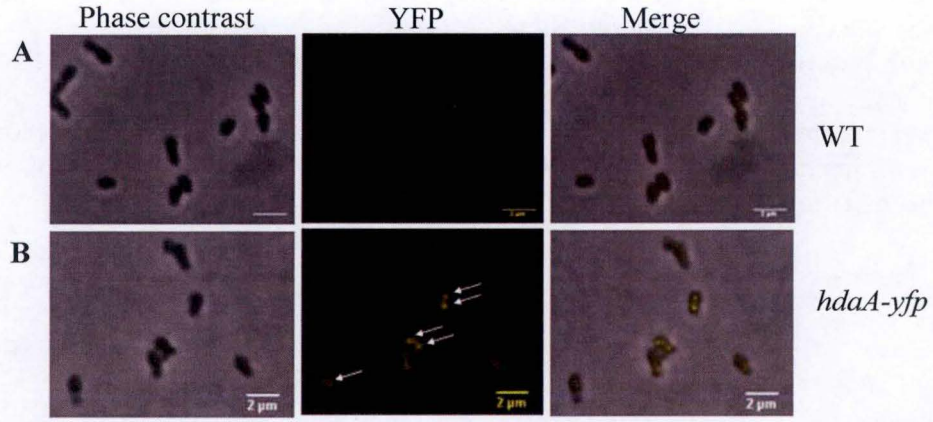

Figure 28 | Localization of HdaA-YFP in an exponential phase. Bacteria from *hdaA-yfp* (B) strain and WT (A) bacteria were observed using phase contrast and fluorescence microscopy. White arrows indicate HdaA-YFP foci. Bacteria from the *hdaA-yfp* strain show from 0 to 4 foci whereas no focus can be detected in the WT strain. The scale bar represents 2 µm.

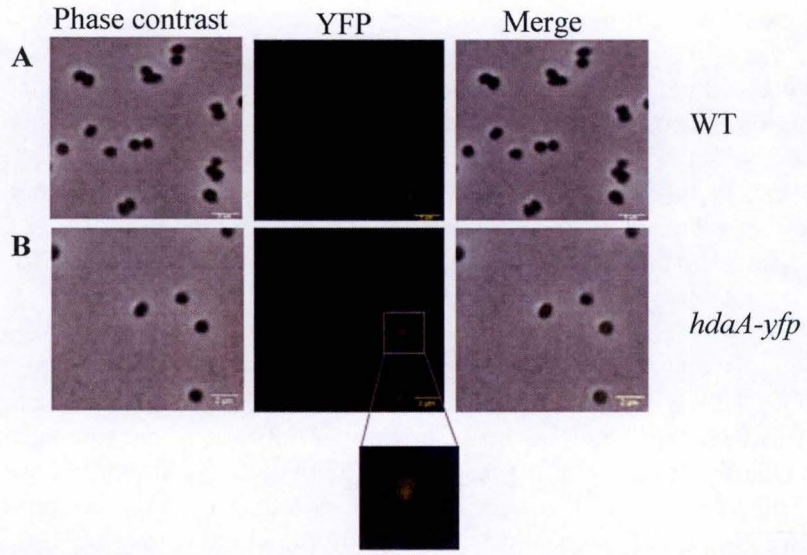

Figure 29 | Localization of HdaA-YFP in a stationary phase. Bacteria from *hdaA-yfp* (B) strain and WT (A) bacteria in stationary phase were observed using phase contrast and fluorescence microscopy. The bacterial cells from the *hdaA-yfp* strain only display one focus maximum in the stationary phase, while no focus was detected in the WT strain. The scale bar indicates 2µm.

2.2. HdaA presents a subcellular localization

In order to investigate the localization of HdaA in *B. abortus,* we constructed a strain that enables the visualization of HdaA by fluorescence microscopy. The coding sequence of the YFP (Yellow Fluorescent Protein) was fused to the C-terminal part of *hdaA*. This strain was generated by allelic replacement in *B. abortus*, allowing the expression of the fusion protein directly from its chromosomal locus, without the addition of an antibiotic resistance marker in the engineered genome. Since the fusion of a fluorochrome could impact the function of a protein, and since that *hdaA* seems essential, the growth of *hdaA-yfp* was first investigated. Therefore, we performed a bioscreen to compare the growth profile of *hdaA-yfp* with the wild type. This experiment was performed using exponential phase cultures diluted at 0.1 OD as time 0 h and the OD was measured for each strain every 30 minutes. The growth profile shows no significant difference between the WT and *hdaA-yfp*, meaning that our fusion protein does not strongly alter the growth ability of the bacteria, thus suggesting that the HdaA-YFP fusion is functional (**Figure 27**). Moreover, several clones for this construction were generated and tested for growth, and they always displayed the same results (**Figure S2**).

To investigate a potential localization of HdaA$_{B.abortus}$ as it is already published for HdaA$_{C.crescentus}$, we subsequently observed bacteria from an exponential phase of culture by fluorescence microscopy. We can see that *hdaA-yfp* strain displays from 0 to 4 fluorescent foci, with each focus representing HdaA fused to YFP (**Figure 28**). Moreover, it should be noted that a fluorescent background is observed even in the WT strain with the same settings, suggesting the HdaA-YFP expression level is rather low, close to the background. This experiment was also repeated for other clones containing this fusion protein and they all showed the same results (**Figure S3**). The number of foci is interesting because it corresponds to the range of replisome copies per cell, i.e. a maximum of 2 replisomes for each of the two chromosomes.We then decided to check the localization of HdaA-YFP when the bacteria are in the stationary phase, where we expected to observe less replisomes. Therefore, bacteria were grown until they reach a stationary phase, and they were observed by fluorescence microscopy. We found bacteria displaying from 0 to one focus maximum. Moreover, compared to an exponential phase, the foci always displayed a lower signal (**Figure 29**).

Since it has been shown that HdaA is involved in the control of replication in *C. crescentus* and it localizes in foci when replication has started (Collier *et al.*, 2009), we were interested to see how the florescent signal evolved when bacteria are inside host cells and if it could be correlated to the G1 arrest observed at the beginning of the infection. However, to study the strain in infection, the cells need to be fixed, in order to be observed by microscopy later. Therefore, we did some preliminary test using the paraformaldehyde (PFA) on *hdaA-yfp* strain to assess the resistance of the labelling after fixation. The bacteria were incubated for 20 minutes at room temperature with PFA 2%, washed and were then observed by fluorescence microscopy. Unfortunately, the fluorescent signal corresponding to HdaA-YFP is lost after the fixation (**Figure 30**), meaning that this strain cannot be used in infection to follow the localization pattern of HdaA. Another possibility would be observe living bacteria into living cells (no fixation), but this risky experiment has not been performed.

Figure 30 | Fluorescent microscopy of the strain producing HdaA-YFP fixed with PFA. The scale bar represents 2µm.

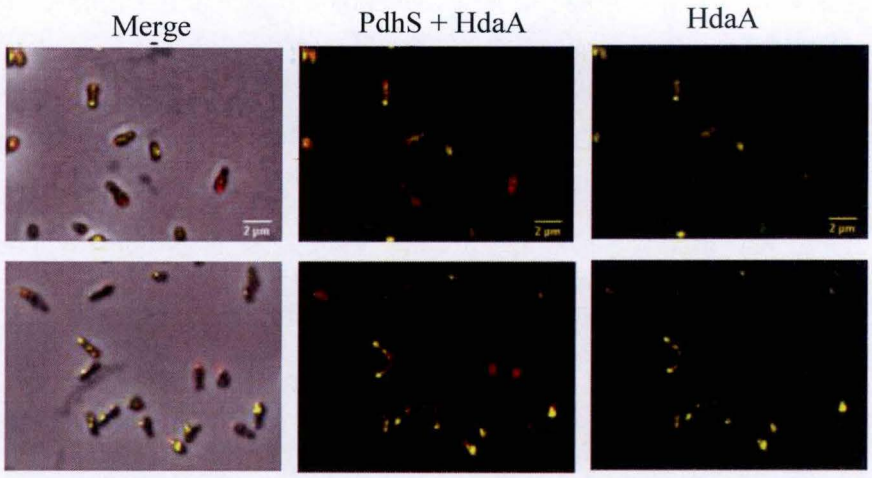

Figure 31 | Fluorescent microscopy of the *hdaA-yfp* strain highlighting the old poles with mCherry-PdhS. HdaA is highlighted in yellow and PdhS is represented in red. The scale bar represents 2µm.

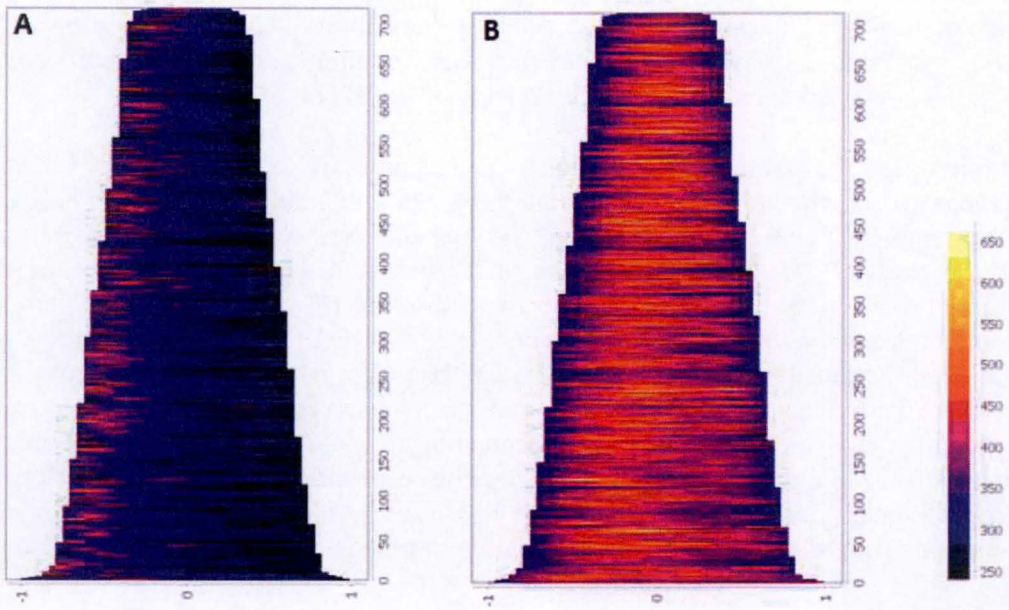

Figure 32 | Demograph analysis representing the position of PdhS, old pole marker, in bacterial cells (A) and the position of HdaA in the bacterial cells (B). The X axe represents the position of the protein in the bacteria as compared to the poles, with -1 corresponding to the old pole, 0 the mid-cell, 1 the new pole of the bacteria. The Y axe represents the number of bacteria used classified from the longer to the smaller cells. This analysis was performed on 716 bacteria on the basis of the microscopy pictures, using the software imageJ.

2.3. HdaA does not seem to be polarly localized

Since it has been shown that the origin of replication of the ChrI in *B. abortus* is fixed at the old pole (Deghelt *et al.*, 2014), and since HdaA is expected to colocalize with the replisomes that are formed in the *ori* when replication starts, we wanted to see if HdaA had a tendency to be localized at one pole or another in *B. abortus.* However, nothing is known about replisome localization in *B. abortus*. We therefore generated a strain highlighting both HdaA and the old pole of the bacteria. To do so, the coding sequence of PdhS, an already characterized old pole marker, was used fused with the one of the mCherry in order to enable the visualization of both proteins at the same time. The strain was created by conjugation of a pSKoriTcat integrative plasmid carrying PdhS-mCherry in the *hdaA-yfp* strain described above. We then observed the bacteria using fluorescence microscopy (**Figure 31**). Based on the microscopy images, we were not able to observe a tendency, and decided therefore to do a demograph analysis. This analysis allows the organization of all cells by sizes, from the longest cell to the smallest one, and using PdhS-mCherry focus, we were able to orient them according to the nature of their pole (old or new). A control of the analysis was first performed by showing the distribution of PdhS in the cell (**Figure 32A**). Since all the PdhS signal was localized to the left part of the demograph, its localization further confirmed that the cells were properly aligned based on their old pole, but this also show an example a typical polar localization. The localization of the YFP signal was then analysed. HdaA does not seem to display a polar localization, since the pole always show low signal. However, the yellow signal seems to have a slight tendency to be localized near the old pole in the largest cells (**Figure 32B**).

2.4. The transmembrane domain is not crucial for the fitness of *B. abortus* in culture

Since the domain prediction analysis revealed that HdaA$_{B.abortus}$ has an additional non-essential transmembrane domain that is not present in other species, we decided to delete this domain *(ΔTM-hdaA)* to investigate if its absence leads to any particular phenotype in *B. abortus*. For that purpose, we performed a bioscreen, and the results show that there is no difference between the WT and *ΔTM-hdaA* (**Figure 33**). We investigated by microscopy whether this deletion could lead to morphological defects and the mutant did not show any difference for the morphology compared to the WT (**Figure 34**).

2.5. Investigation of the role of the transmembrane domain in the HdaA localization

We then wondered if the localization of HdaA$_{B.abortus}$ could be impacted by the removing of its transmembrane domain. Taking advantage of our previous construction plasmids, we generated the strain *ΔTM-hdaA-yfp*. The *ΔTM-hdaA-yfp* strain presented no growth defect compared to the WT (**Figure 35**). Afterwards, to investigate the localization of the protein lacking the transmembrane domain, this strain was observed by fluorescence microscopy. Interestingly, no foci were observed, and bacteria only displayed a fluorescent background as observed in the WT (**Figure 36**).

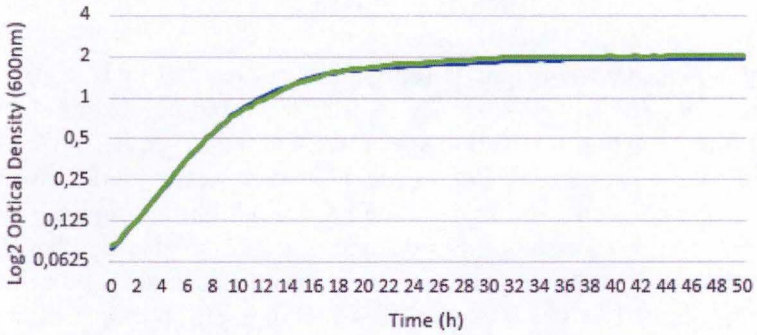

Figure 33 | Growth curve of *the* Δ*TM-hdaA* as compared to the WT. All strains were grown in 2YT rich medium and the bioscreen was performed for 50 hours. The OD of the WT (blue), the Δ*TM-hdaA* (green) strains were taken every 30 minutes for 50 hours.

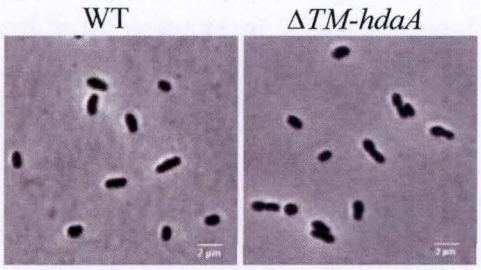

Figure 34 | Contrast phase microscopy of the WT (left) and Δ*TM-hdaA* (right). The scale bar represents 2µm.

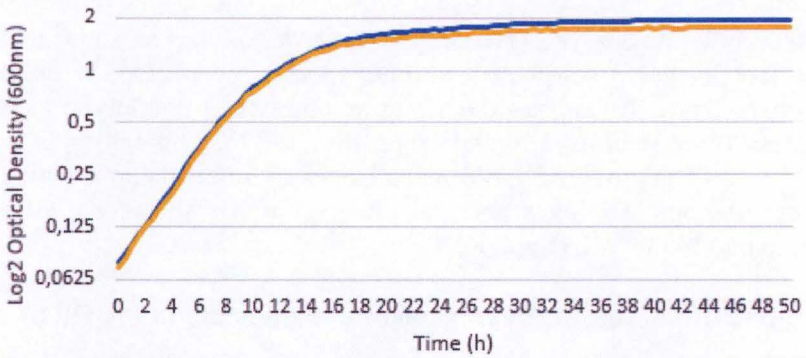

Figure 35 | Growth curve for the Δ*TM-hdaA-yfp* (yellow) strain as compared to the WT (blue).

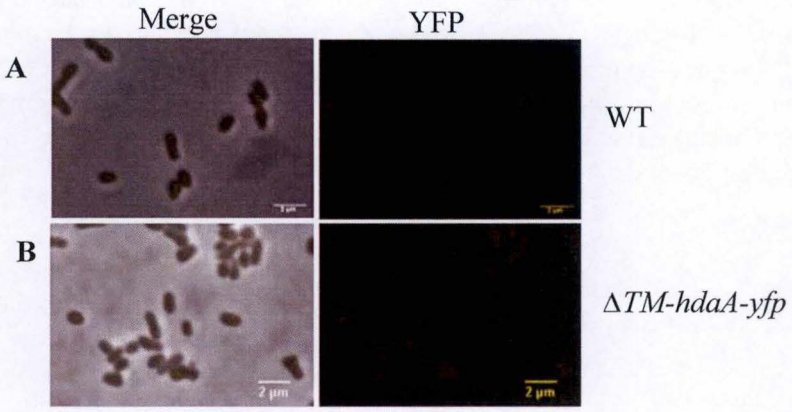

Figure 36 | Fluorescent microscopy for Δ*TM-hdaA-yfp* (B) as compared to the WT (A).

2.6. Detection of HdaA-YFP by western-blot

Because HdaA in *B. abortus* was shown to have a large additional transmembrane domain not found in other species, we wanted to investigate if the protein had the expected size. Moreover, we also wanted to investigate if the total amount of HdaA can vary in different conditions, i.e. between the exponential and the stationary phase. Since we do not have an antibody against HdaA, we needed a tagged-protein. Therefore, we took advantage of *hdaA-yfp* and *ΔTM-hdaA-yfp* strains. Both of them display the protein fused to YFP, so we can highlight HdaA-YFP and ΔTM-HdaA-YFP using an antibody against the YFP. Samples of these two strains were harvested from an exponential phase as well as from a stationary phase of liquid culture, and a western blot analysis was performed. Taking into account that the molecular weight of the YFP is around 26 kDa, we calculated the expected sizes of both fusion proteins and found an estimated size of 98.7 kDa for HdaA-YFP, and 55.15kDa for ΔTM-HdaA-YFP.

Surprisingly the HdaA-YFP protein was found with an approximative size of 55kDa in the exponential phase condition, whereas in stationary phase two sizes were observed, a first band at 55kDa and a band with a slight intensity at 100kDa (**Figure 37**). On the other hand, the western blot showed that in the ΔTM-HdaA-YFP strain, two different sizes were observed in exponential and in stationary phases: 55 and 65 kDa. The protein with a size of 65kDa seemed to be more produced in the exponential phase than in the stationary phase, whereas the opposite seemed to happen for the one with a size of 55kDa. Moreover, another band was observed at 26kDa only in the exponential phase for the *ΔTM-hdaA-yfp* strain. However, when reaching the stationary phase, both strain display a signal at 26kDa, corresponding to the molecular weight of the YFP. Moreover, in stationary phase *ΔTM-hdaA-yfp* displays an increase of signal for the three bands compared to the situation in exponential phase.

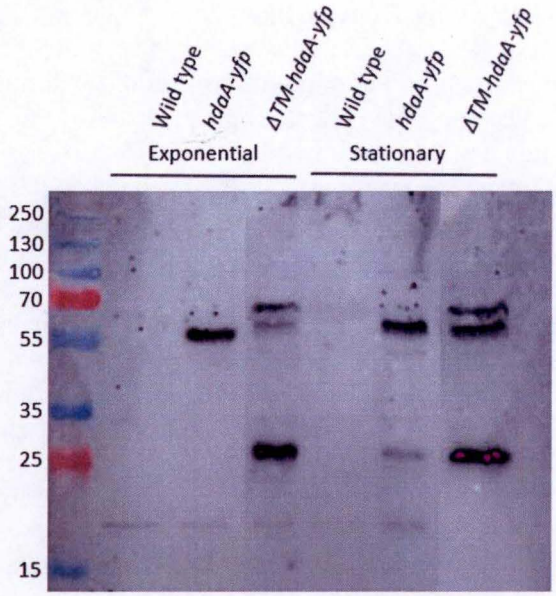

Figure 37 | Western blot anti-YFP highlighting the HdaA protein fused to YFP in exponential and in stationary phases. The strains were grown until a mid-exponential phase (OD 0.4) and until early stationary phase (OD 1.4) for the sampling. They were normalized to an optical density of 20 to perform the western blot analysis and 15 µl of each were loaded on the SDS gel. The first antibody (mouse anti-GFP) was used at a concentration of 1/1000 and incubated for two hours at RT. The secondary antibody was an anti-mouse (1/5000) for 1 h at RT. The nitrocellulose membrane was exposed to chemiluminescence for 5 minutes. The WT constitutes the negative control (absence of YFP). The complete picture can be found in the supplementary data **(Figure S1)**.

DISCUSSION & PERSPECTIVES

Chromosomal replication in *Brucella abortus*, as well as in most bacteria, is a highly-regulated process that involves many different proteins, including the crucial and highly conserved DnaA. This protein acts as the initiator of chromosomal replication, and therefore needs to be tightly regulated (Mott *et al.*, 2007). In this study, the role of three proteins potentially involved in the control of DnaA in *B. abortus* was investigated. Those three proteins, HdaA, ClpAP and Lon, were chosen since they were shown to be involved in DnaA regulation in *Caulobacter crescentus.* Indeed, even though this micro-organism harbors a different lifestyle than *Brucella* species, it is a relevant model to initiate a study of chromosomal replication in *B. abortus*.

1. Investigation of *clpSA* and *lon*

ClpAP and Lon are proteases that were shown to proteolyze DnaA in *C. crescentus* (Liu *et al.*, 2016; Jonas *et al.*, 2013), as described in the Introduction. We therefore decided to study the role of ClpA, its adaptor protein ClpS and the Lon protease in chromosomal replication of *B. abortus*. First, we searched for homologs of those genes in *B. abortus* and investigated whether they were essential or not using the Tn-seq analysis. The Tn-seq is a high throughput experiment that allows the visualization of potentially essential genes in a given condition, such as growth in a rich culture medium or in eukaryotic cells infection. In this dataset, we observed that neither the *clpSA* operon nor *lon* were essential for growth in a rich culture medium despite the fact that *lon* mutants seemed to have a slight decrease in fitness (**Figure 19A**). When infecting RAW 264.7 macrophages with transpositionnal mutants for *clpSA,* the mutants showed an attenuation at 24 h post-infection (PI). Surprisingly, when replating those transpositionnal mutants into a rich culture medium, some parts of *clpA* appeared to become essential (**Figure 19B**). This suggests that the effect observed in infection might be due to an attenuation of the intrinsic ability to grow for *clpSA* mutants, rather than an effect of the infection itself. However, since the transpositional mutants were not attenuated at 2 h PI (**Figure 19C**), as they would have been if replating itself was sufficient to score these mutants as essential, it is also predictable that Tn-seq data are not reproducible and that several biological replicates should be done to gain more robust conclusions. Regarding *lon*, the mutants infecting RAW 264.7 macrophages were found to be attenuated at 2 h PI, and this attenuation increased at 5 and 24 h PI (**Figure 19C, D, E**). This observation further suggests that Lon could be required for survival inside RAW 264.7 macrophages, and that this protease could be involved in virulence mechanisms of *Brucella.* Furthermore, when infecting macrophages, bacteria are probably facing much more stresses than in a rich culture medium, thereby making the Tn-seq results consistent with previous work performed in *C. crescentus* where Lon was shown to be important for proteins degradation in stress conditions (Jonas *et al.*, 2013). It is also worth to note that the Lon protease was shown to be important for full virulence in other bacterial species (Breidenstein *et al.*, 2012; Su *et al.*, 2006).

However, since none of these two genes were essential for growth in rich medium, we decided to generate deletion mutants for both. Unfortunately, we did not obtain the deletion mutant for *lon.* A reason for that could be that the allelic replacement used to delete *lon* has generated some polar effects that are deleterious for the bacteria, or that the deletion of *lon* is toxic when it is generated from an integrant strain, (i. e. the step before the excision of resistance cassettes). Nevertheless, the *clpSA* deletion was achieved (Δ*clpSA*), which is in contradiction with Tn-seq data on the replated library, that would have predicted that the strain could not be viable.

In order to characterize this mutant, we performed several experiments including a growth assay, a morphology investigation by microscopy, an infection of RAW 264.7 macrophages, and we finally tested the abundance of DnaA to have a fist clue on the implication of ClpSA in the proteolysis of DnaA.

The Δ*clpSA* mutant showed a statistically significant decrease in CFUs at 24 h PI when compared to the WT *B. abortus* (**Figure 21**). Although the decrease was weak, the results are consistent with the Tn-seq analysis, in which mutants with insertion of transposon in *clpSA* were shown to be slightly attenuated at 24 hours PI (**Figure 19E**). Those results first suggested that the genes are required for optimal intracellular growth in RAW 264.7 macrophages. One interesting observation is that this difference between the WT and the mutant seemed to be reduced at 48 hours PI. However, the CFUs at 48h PI needs to be repeated twice in order to be confirmed, and the experiment still needs to be performed with the complementation strain to further confirm that this phenotype is really due to the deletion of *clpSA*. Nonetheless, the observed phenotype might not be related to the infection itself but rather to the ability of the mutant to grow and proliferate. Indeed, when grown on 2YT-agar plates, the deletion mutant showed growth delay as compared to the WT *B. abortus* (i.e. the mutant needs more time to form a colony than the WT). Moreover, the bioscreen experiment performed in rich culture medium (**Figure 20**) showed a slight growth delay during exponential phase regarding the Δ*clpSA* mutant in comparison to the WT. The growth delay observed in exponential phase could explain the phenotype at 24 h PI. Although the lack of ClpA in *C. crescentus* induce growth defects mainly during stationary phase, our results are consistent with another work performed in *C. crescentus* where a slightly slower growth was reported in Δ*clpA* mutants (Liu *et al.*, 2016). Taken together, these data suggest that ClpAP is an auxiliary protease and thus its function can be substituted by the activity of other proteases, such as Lon (Liu *et al.*, 2016). Indeed, these small differences of growth in rich culture medium could be explained by the redundancy in function of ClpAP and Lon proteases, both being able to degrade protein during stress conditions.

The Δ*clpSA* strain has shown aberrant morphologies such as "Y-shape" and "donut-shape" bacteria (**Figure 22 B)**, which are probably attributable to pleiotropic effects. Those aberrant morphologies could be due to replication defects, division defects or even to toxicity inside the bacterial cells by accumulation of unfolded proteins. Indeed, since ClpA is a chaperone protein unfolding and targeting its substrate toward the ClpP protease, and since ClpS is an adaptor protein involved in the N-end rule degradation pathway, their deletion could lead to misregulation of several proteins. This could easily generate accumulation of proteins, that would lead to functional defects. Another hypothesis is that these aberrant morphologies could be related to division defects. Indeed, such branching morphologies, or other aberrations such as minicells, were shown to be typical of division defects in unipolarly growing bacteria (Brown *et al.*, 2012). This division defect has recently been reported in *Agrobacterium tumefaciens* deleted for genes involved in polar development like *podJ* or *popZ* (Anderson-Furgeson *et al.*, 2016; Grangeon *et al.*, 2017). Therefore, the misregulation of a polar development factor due to the loss of *clpSA* could be partially responsible for this phenotype. Furthermore, it has been shown in *C. crescentus* that the ClpAP protease was involved in the divisome degradation, more specifically, in FtsZ degradation (Williams *et al.*, 2014). Therefore, by deleting *clpSA*, the bacteria would not be able to provide an optimal control of FtsZ, leading to this defective morphology. Moreover, it has been reported that an overexpression of DnaA-ATP leads to a blockage of cell division because of an overinitiation of chromosomal replication (Fernandez Fernandez *et al.*, 2011). Even though the chromosome content of the Δ*clpSA* mutant has not been investigated here, one could imagine that the bacteria will not be able to regulate their

replication, leading to an abnormal chromosomal content, thereby generating a stress response that would trigger an inhibition of cell division. Taking all these data into account, the most likely explanation is that the morphology defects results from the numerous targets of the ClpAP protease. This observation further highlights that even though the ClpAP protease is not essential for growth, this protease could be involved in a lot of mechanisms, and therefore, would be important for the fitness of the bacteria. It could be interesting investigate how those Y shapes are formed using a time lapse experiment, in order to better characterize the growth mechanisms of Δ*clpSA*.

To assess whether ClpAP was involved in DnaA degradation or not, a western blot analysis against DnaA was performed using the WT and the Δ*clpSA* (**Figure 23**). When comparing the DnaA levels in the WT and in the Δ*clpSA* in an exponential phase, no difference in DnaA abundance was observed. Surprisingly, in stationary phase, a slight decrease of DnaA levels was observed in Δ*clpSA* compared to the WT. An explanation for this could be that the Δ*clpSA* mutants are not able to survive upon extended growth in stationary phase, thereby leading to a global proteolysis. This hypothesis could be tested by measuring CFU numbers at the stationary phase of culture. Another hypothesis is that since the degradation pathway depending on the ClpAP protease is thought to be impaired in Δ*clpSA*, the targets of this protease will accumulate inside the bacteria leading to proteotoxic stress that would allosterically activate other proteases, such as Lon. Indeed, this protease has been shown to be allosterically activated by proteotoxic stress in *C. crescentus* (Jonas *et al.,* 2013). To address this last hypothesis, it could be interesting to test whether Lon substrates degradation increase when deleting ClpA and ClpS. Nevertheless, one should keep in mind that the western blot has only been performed once and needs to be repeated. Intensity mean of each condition could be determined and statistical analysis could be performed afterward to test these data. However, since it was shown that *C. crescentus* remove all the DnaA upon entry in stationary phase (Wargachuck *et al.,* 2015) and since it does not seem to be the case in *B. abortus*, one could imagine the control of DnaA might be different in *B. abortus* than in *C. crescentus.* Indeed, even though *C. crescentus* represents a reliable model to study chromosomal replication in *B. abortus*, those bacteria display different lifestyles. Therefore, they have evolved with different environmental pressures and could therefore have generated different mechanisms of regulation, specifically adapted to their needs (Jonas, 2014). Here, one of the advantage of *B. abortus* not to proteolyse all its DnaA could be that it might enable the replication to start as soon as the conditions are favorable rather than waiting for DnaA *de novo* synthesis, for example. This nicely correlates with the presence of bacteria in the S phase of the cell cycle, at the stationary phase for culture in rich medium, as indicated by flow cytometry (M. Van der Henst and T.A.P. Ong, unpublished data). Moreover, a review has recently reported that, even though those regulatory have highly conserved targets such as DnaA, the underlying mechanisms can vary a lot between the bacterial species (Jonas, 2014). Other mechanisms can be involved in DnaA control, such as transcriptional regulation or post-translational modification. In *E. coli* for example, at least three mechanisms have been reported to control the chromosomal replication (Katayama *et al.*, 2010). Among those, the RIDA system was shown to be the dominant mechanism in *E. coli.* Taken together, those data highlight the importance of having other regulatory mechanisms, and further suggest the potential importance of HdaA in *B. abortus.*

One intriguing observation for the Δ*clpSA* mutant is that, when complemented, the bacteria are able to come back to a morphology similar to the WT (**Figure 22 C**) while they are not able to fully compensate the growth delay in exponential phase (**Figure 20**). On the basis of those observations, three hypotheses can be made. First, our mutant may have another mutation elsewhere in the genome that would be partially responsible for the growth delay on liquid

culture, on plate as well as on infection - since we hypothesized that the effect in infection is due to the intrinsic growth ability of the mutant rather than an infection effect. Therefore, this growth delay phenotype would only be partially due to the deletion. To assess this hypothesis, an investigation of the growth ability of other clones of Δ*clpSA* can be performed, or the entire genome of our mutant can be sequenced. The second hypothesis is that the insertion of the pMR10 in *B. abortus* might lead to some disturbances in terms of growth, thereby impeding the supplementary copy to completely alleviate the growth delay. To test this second hypothesis, a conjugation of an empty plasmid could be realized in a WT background in order to investigate if the presence of this replicative plasmid could somehow disturb the growth ability of the bacteria. Finally, a last hypothesis would be that the complementation plasmid does not allow a sufficient expression level of the genes to fully complement the phenotype, while it is sufficient to alleviate the morphology defect.

Nevertheless, among the perspectives of this work, one of the most important would be to investigate the chromosomal content of Δ*clpSA* in order to see if this deletion mutant has any impact on the chromosomal replication. Several approaches can be used to answer that question. A plasmid enabling the visualization of *oriI* could be introduced in the deletion strain in order to investigate the chromosomal pattern in this strain and count the number of foci. Flow cytometry analysis could also be performed on that strain and compared to the WT. The ratio between *ori* and *ter* could also be measured by qPCR from the extraction of genomic DNA of this mutant and compared to a WT background, as it has already been done in *C. crescentus* by Fernandez-Fernandez *et al.*, 2011.

Another interesting perspective would be to generate deletion mutants for *clpA* and *clpS* alone. The deletion of *clpA* alone (Δ*clpA*) should give a phenotype close to the one we observed in Δ*clpSA* since, to our knowledge, ClpS was never reported to act without ClpA. It would also be interesting to delete c*lpS* as well in order to investigate whether the level of DnaA are changing or not and to further assess the morphology and growth ability of those mutants. Moreover, given that there may be redundancy between the functions of ClpAP and Lon, it would also be of particular interest to create a triple deletion strain (Δ*lon,* Δ*clpSA*), in which we expect the bacteria to present much more growth defects than in each of this deletion taking separately, as previously proposed in *C. crescentus* (Liu *et al.*, 2016). Of course, one should be aware that Lon and ClpAP have a lot of targets and therefore, the observed phenotype may not be due to the effect on DnaA but rather to pleiotropic effects. However, generating such a strain would be difficult since we could not manage to obtain the deletion mutant for *lon*. Therefore, other strategies can be tried such as the generation of catalytic dead mutant for *lon* in a WT background and in Δ*clpSA*. Indeed, since one of our hypothesis is that we could not get the Δ*lon* strain is that they might be polar effect generated by the double recombination, the creation of a mutant defective for its activity could perhaps be possible. However, even though a triple deletion strain has already been done in *C. crescentus* (Liu *et al.*, 2016), the fact that this strain could lead to synthetic lethality in *B. abortus* is not unlikely.

2. Investigation of *hdaA*

Since RIDA is one of the more important mechanism preventing overinitiation in *E. coli* and in *C. crescentus,* we wanted to investigate the role of HdaA in *B. abortus.* Interestingly, we found a homolog of HdaA in *B. abortus* characterized by an additional transmembrane domain. This additional domain is not found in any other bacterial species, even closely related.

Since $HdaA_{C.crescentus}$ presents a subcellular localization when replication occurs (Collier *et al.*, 2009), we wanted to characterize the localization of HdaA in *B. abortus* as well. Therefore, we generated a mutant in which the C-terminal part of *hdaA* is fused to the coding sequence of the YFP, generating the *hdaA-yfp* strain. Interestingly, in an exponential growth phase, HdaA-YFP was seen as foci, displaying from 0 to 4 foci per bacterium (**Figure 28**). This result is highly interesting because this pattern of localization could be consistent with a replisome-associated localization of the protein. Indeed, since *B. abortus* presents two chromosomes, up to 4 replisomes can be formed within replicative cells and no replisome is formed when the cells are not replicating their chromosomes. Therefore, one could imagine that, as long as the replication has not been started, the bacteria will not display any foci and HdaA will be diffuse in the cytoplasm. However, when the replication starts, HdaA will be recruited to the replisome and, in the first time, only one focus will be observed since the two replisomes are relatively close to each other. Then the replication forks will move along the chromosome, and the foci will move away from each another, thereby allowing the detection of two foci. Subsequently, the second chromosome initiates its replication following the same pattern, therefore successively showing from 3 to 4 foci. When the replication is finished, the replisome dissociates, thereby going back to the first situation, with no detection of HdaA foci. This localization of HdaA throughout the cell cycle would be consistent with the previously demonstrated localization of HdaA in *C. crescentus* as shown in the Introduction (**Figure 15**) (Collier *et al.*, 2009). We cannot exclude that two or more replisomes could overlap in localization, especially for a small bacterium like *B. abortus,* thereby underestimating the number of replisomes formed in the cell.

To better characterize the localization of HdaA, we also observed this strain in a stationary phase of liquid culture and saw maximum one focus per bacterium (**Figure 29**), further suggesting that HdaA would not be able to form foci in stationary phase and is probably diffuse in the cytoplasm most of the time.

Nevertheless, since HdaA was shown to bind the β clamp of the DNA polymerase in *C. crescentus* through a consensus sequence localized in the N-terminal part of the protein, and since QIPLNL was proposed to be the β sliding clamp binding motif of HdaA in *B. abortus,* one could imagine that this interaction is a conserved property of the protein. To test this hypothesis, it would be of great interest to construct a strain highlighting the localization of DnaN (forming the β clamp) in order to see if HdaA and β clamp positions overlap in the cell. If the two proteins are colocalizing, it would be interesting to assess if the QIPLNL motif is the one allowing the binding. To assess this, the same experiment can be done in a strain harboring one or several point mutations in the consensus sequence to see whether the colocalization is lost or not. For that purpose, we are currently constructing a fusion protein of DnaN with the mCherry fluorescent protein in the *hdaA-yfp* strain. If HdaA-YFP can indeed highlight the replisome, the fact that up to four foci can be detectable is interesting since it means that HdaA would be able to interact with both chromosomes of *B. abortus* even though the ChrII is part of the chromid family and displays different replication characteristics.

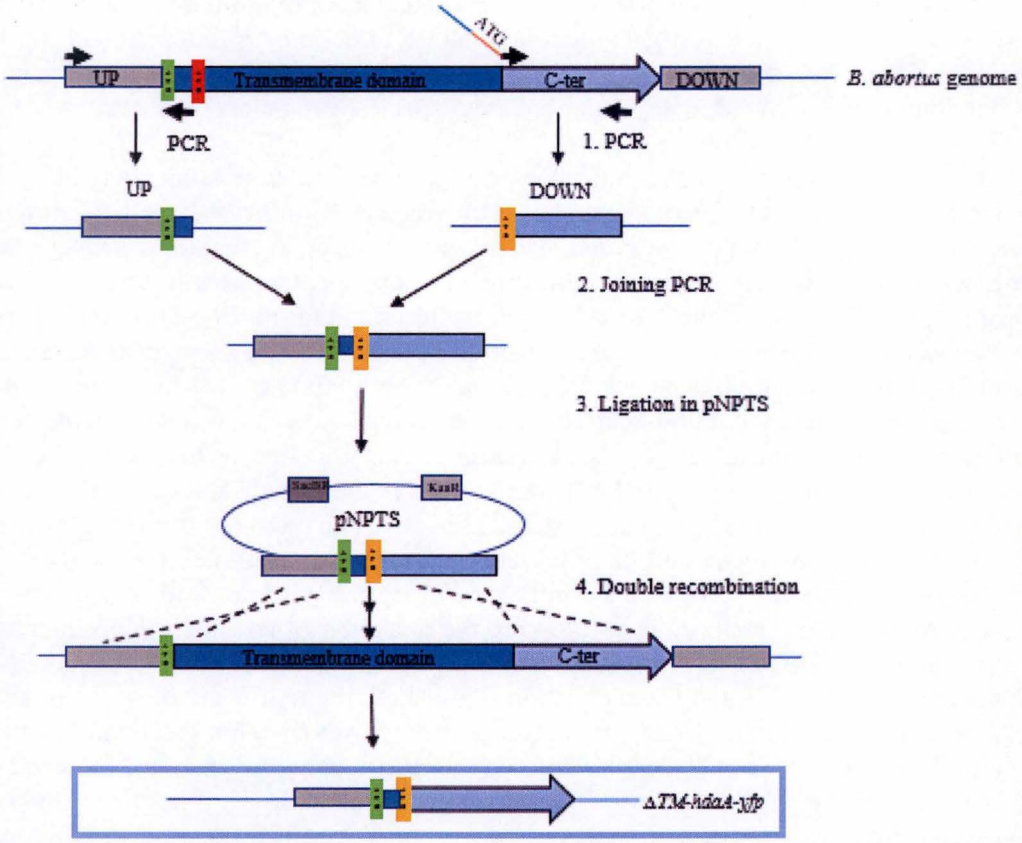

Figure 38 | Molecular strategy used to construct the *ΔTM-hdaA* strain. PCRs were performed to amplify the upstream region (UP) of the coding region of *hdaA* and the C-terminal region of *hdaA* which represents the downstream region (DOWN). The primers used for these amplifications are represented by dark arrows. Since we deleted the transmembrane domain which is in N-terminal, we also remove the start codon. Therefore, we added a new start codon (ATG) at the 5' end of the forward primer used to amplify the DOWN part. We then performed a joining PCR of both products and ligated in a pNPTS integrative plasmid which encodes resistance to kanamycin (KanR) and contains a sucrose sensitivity cassette (SacBR). This plasmid was then conjugated in Brucella were the deletion of the domain was performed by allelic replacement. The correct start codon is represented in green, the wrongly annotated start codon is represented in red, and the new start codon that we inserted is in orange.

To further characterize the localization of HdaA in the bacteria and since it has been shown that the ChrI is precisely oriented along the cell (*oriI* are either at the old pole or at both poles) we wanted to investigate whether HdaA has a tendency to be found close to one pole or another. Therefore, we performed microscopy on the *hdaA-yfp* strain in which a plasmid carrying a fusion protein of PdhS with the mCherry was integrated (**Figure 31**). The pictures were analysed with MicrobeJ and we constructed a demograph to map both signal along the cells. This graph shows that although HdaA does not seem to be localized at one pole or another in the small cells, it seems to be localized closer to the old pole in the larger cells, suggesting that HdaA may have a preferential localization in the cell, that remains to be deeply investigated (**Figure 32**). It could be interesting to perform a time lapse experiment on the *hdaA-yfp* strain in order to investigate if the foci are mobile throughout the cell cycle, as it was shown in *C. crescentus* (Collier *et al.,* 2009). However, due to the bleaching of the fluorescent signal, this experiment would be difficult to achieve.

Afterwards, we decided to further investigate the role of the additionnal transmembrane domain found in *B. abortus* HdaA by generating a mutant lacking this domain (*ΔTM-hdaA)*. Our results suggest that this deletion does not impact the fitness of the bacteria neither for the growth ability (**Figure 33**), nor for the morphology of the mutant (**Figure 34**). Since this part of the protein was indicated as non-essential by the Tn-seq analysis (**Figure 23**), those results were further raising the question of its function. Considering the hypothetical role of the protein, i.e. to prevent overinitiation by acting on DnaA, one could imagine that HdaA would present an advantage to be localized close to the membrane. Indeed, it was reported in *E. coli* that DnaA is a membrane associated protein, which strongly suggest that replication could be a membrane associated event (Newman *et al.*, 2000). Therefore, the presence of a transmembrane domain could facilitate the interaction between HdaA and DnaA for example. Nevertheless, even though our results suggest that the deletion of the transmembrane domain does not affect the bacterial fitness, one should be careful considering this interpretation. Indeed, it should be noted that because of a wrong annotation of the genome, our mutant was wrongly constructed, leaving a small portion (31 amino acids) of the transmembrane domain in the N-terminal portion of our mutant (**Figure 39**). A perspective for this part of the work would be to generate a deletion mutant of the entire transmembrane domain and to assess if the mutant still behaves the same way than ours. However, since the major part of the transmembrane domain has been removed in our mutant, it is unlikely that a difference would be observed.

We then wondered if the localization of the protein might be impacted by the deletion of the transmembrane domain. First, using the strain highlighting HdaA with the YFP and the plasmid previously used to construct a deletion of the transmembrane domain, we generated a new strain, *ΔTM-hdaA-yfp.* Interestingly, we observed that the bacteria did not display any focus anymore and presented a fluorescent signal comparable to the negative control (autofluorescence background in the WT) (**Figure 36**). Two hypotheses were first proposed. The first suggested that, deprived of its transmembrane domain, the protein was not able to localize anymore and was therefore homogeneously distributed in the cytoplasm. The second hypothesis was that the fusion protein was less stable because of post translational cleavage of the YFP for example, and therefore did not show any focused signal.

However, by performing a western blot against the YFP to highlight HdaA in *hdaA-yfp* and *ΔTM-hdaA-yfp* (**Figure 37**), other explanations emerged. Indeed, the results showed that in the *hdaA-yfp* strain, in exponential phase, HdaA-YFP is only found with a molecular weight corresponding to the protein lacking its transmembrane domain (55 kDa), while a slight band corresponding to the size of the entire protein (98 kDa) can be detected in stationary phase, in

Figure 39 | RNA-seq profile of *hdaA* in *B. abortus*. The red line displays three mains peaks representing the transcription initiation (+1 sites) within the gene.

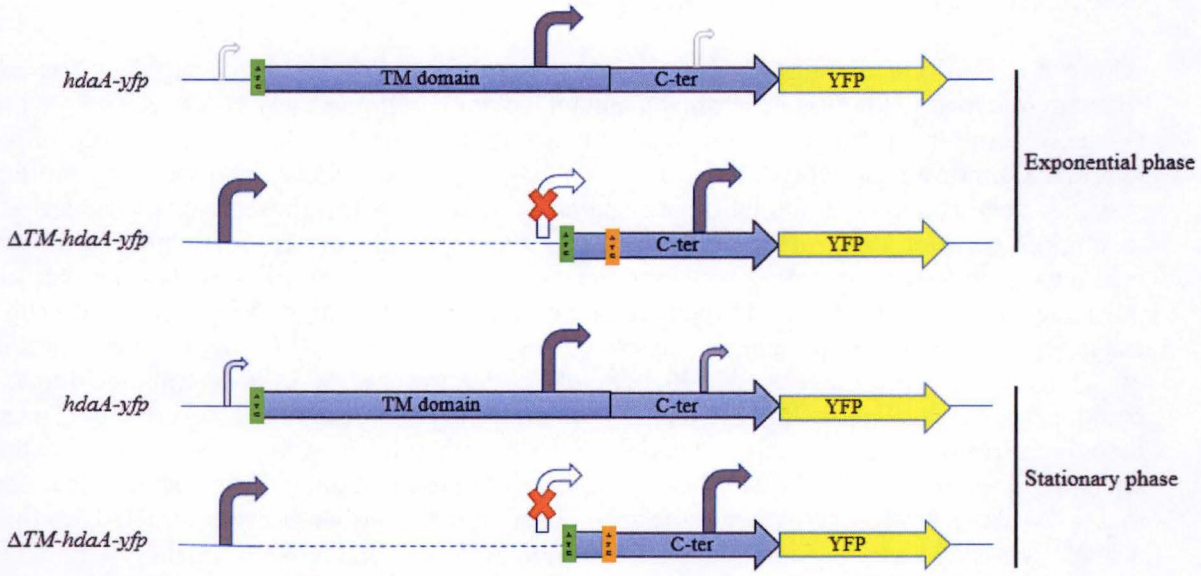

Figure 40| Schematic representation of the theoretical promoters predicted in and upstream *hdaA* and their theoretical activation in an exponential or stationary culture phases, with and without the transmembrane domain. In the *hdaA-yfp* strain, one weak promoter is thought to be localized in the upstream region, while two are supposedly localized within the gene. In an exponential phase in the WT bacteria, the first promoter is thought to be a weak promotor, the second is thought to be strong, while the third is thought to be a weak promoter as well. By creating the Δ*TM-hdaA* strain, the second promoter might have been removed, thereby impeding the transcription of the conserved part of *hdaA*. In that condition, the first promoter is thought to be turned on, allowing the expression of the essential protein. However, since the genome was wrongly annotated, Δ*TM-hdaA* include the putative start codon (green) and 31 AA constituting the N-terminal part of the transmembrane domain. Moreover, to allow the transcription of the C-terminal part, we also artificially added an ATG codon (orange). Therefore, the first promoter could potentially allow the transcription of a region with two translational start sites, one from the putative start codon (green) and from the artificially added start codon (orange). Furthermore, the deletion of the central promoter may also have led to the activation of the third promoter. Considering the promoter activity in stationary phase, the first promoter seems to be slightly activated in the WT background, while the central promoter seems to display the same activation state. However, in the Δ*TM-hdaA* strain, the situation seems to be similar to the one in exponential phase. Bent arrows represent the promoters, size and grey intensity correlate with the proposed activity of the promoter, big dark grey arrows being the strong promoter activated. The white arrow crossed in red represents the potentially deleted promoter.

addition to the band of 55 kDa. Regarding the Δ*TM-hdaA-yfp* strain, a band corresponding to the protein lacking its transmembrane domain was observed, as well as two additional bands (around 70 kDa and 25 kDa). The band of 70 kDa was at a higher size than expected and is probably due to the way we constructed the Δ*TM-hdaA-yfp* (**Figure 38**). The 25 kDa band corresponds to the expected size of the YFP alone. Consistent with the RNA-seq profile that shows three transcription peaks within the gene **(Figure 39)**, those results suggest that several promotors could be found within the gene and our data suggest that they may be activated by different conditions (**Figure 40**). One promoter could be localized upstream the transmembrane domain, allowing the transcription of the entire protein, this promotor should not be strong since the full protein seems only slightly present during the stationary phase. The second promoter could be localized in between the transmembrane domain and the conserved part of *hdaA* thereby triggering the transcription of the protein without its transmembrane domain, even in the WT background. The transcription from this promoter would be the most important according to the western blot results. Another promotor could be found in the C-terminal part of *hdaA,* allowing the expression of the gene localized downstream *hdaA.* However, since we fused the coding sequence in the C-terminal part of HdaA, the YFP may act as a reporter for this gene. Therefore, by deleting the transmembrane domain we might have remove the second promoter localized in the middle of gene. The deletion of its promoter could have led to the activation of the first one which is thought to be a very weak promotor under normal growth conditions, further allowing the transcription of the gene without its transmembrane domain. The mechanism of this activation is completely unknown, but could be linked to (a) signal(s) present inside the transmembrane coding sequence. In the Δ*TM-hdaA-yfp* strain, this first promoter would allow the transcription of two proteins with different sizes, because of the way the strain was constructed (**Figure 40**). The deletion of the second promoter could also have led to the activation of the third promotor, localized at the C-terminal part of HdaA, allowing the transcription of the downstream gene, which is here the YFP coding sequence. This activation of the transcription of the YFP would therefore generate an explanation for the absence of foci and the background signal observed in the Δ*TM-hdaA-yfp* strain. To avoid this intense background signal, another strain could be constructed with the *yfp* inserted between the transmembrane domain and the conserved part of HdaA. However, it could be interesting to further confirm the results obtained by the western blot. For example, 5'RACE experiment would be highly relevant to further confirms those hypotheses.

Other perspectives include the creation of an overexpression strain of *hdaA* to investigate the role of HdaA in the regulation of chromosomal replication. This construction was one of our initial objective, but we did not manage to express *hdaA* under the control of an inducible promoter in the pBBRi plasmid in *E. coli.* An explanation could be that since HdaA is highly conserved, expressing an extra copy of *hdaA* in *E. coli* can be deleterious for the bacteria. This is further suggested by the fact that *hdaA* overexpression is deleterious in *E. coli* (Banack *et al.*, 2005). However, this construction strain could be made in another way. For example, a strong promoter could be placed between the putative promoter of *hdaA* and the onset of the gene. By doing so, only the N-terminal part of the transmembrane domain would be amplified by PCR and expressed in *E. coli.* Since this part of the protein is not thought to be toxic, this construction should be possible. Then a homologous recombination will be performed in *B. abortus* thereby allowing a strong expression of *hdaA* directly from its chromosomal locus. Moreover, it could also be interesting to generate a depletion strain for *hdaA*. Indeed, since the gene is essential, an additional inducible copy of *hdaA* is needed to achieve the deletion of the gene.

CONCLUSION

In this work, we have shown that a deletion mutant for *clpSA* (*ΔclpSA)* leads to a slightly slower growth and a slight effect in infection, which is probably related to the growth delay rather than the infection itself. This mutant also showed aberrant morphologies that were complemented by the addition of a copy of the genes on a replicative plasmid, thereby suggesting that ClpSA are important to maintain a correct morphology. An interesting finding of this work is that, on the contrary of *C. crescentus, B. abortus* does not seem to induce DnaA proteolysis in the stationary phase of the culture. This could allow *B. abortus* to directly starts its replication when the conditions are favorable by using the pool of DnaA present in the cells. However, this observation further highlights the importance of other regulatory mechanisms to control DnaA, such as the action of HdaA. This protein is indeed commonly accepted as one of the main mechanisms controlling DNA replication in bacteria, by acting on the activation state of the initiator protein DnaA. Here, we show that, although HdaA of *B. abortus* was first proposed to exhibit an additional transmembrane domain, the deletion of this domain (*ΔTM-hdaA*) does not impact the bacterial fitness and, more surprisingly, that the protein was even produced without it most of the time. It highlights that the transmembrane protein is probably not produced (or at very low levels) and actually a promoter upstream hdaA conserved part is sufficient to drive expression of a functional HdaA protein. If this hypothesis is true, this is a good example of misleading genomic annotation. Furthermore, HdaA forms from zero to four foci in a bacterial cell and does not display any sign of polar attachment. Nevertheless, further investigations are required to gain a mechanistic understanding of the function HdaA and ClpSA in the control of chromosomal replication.

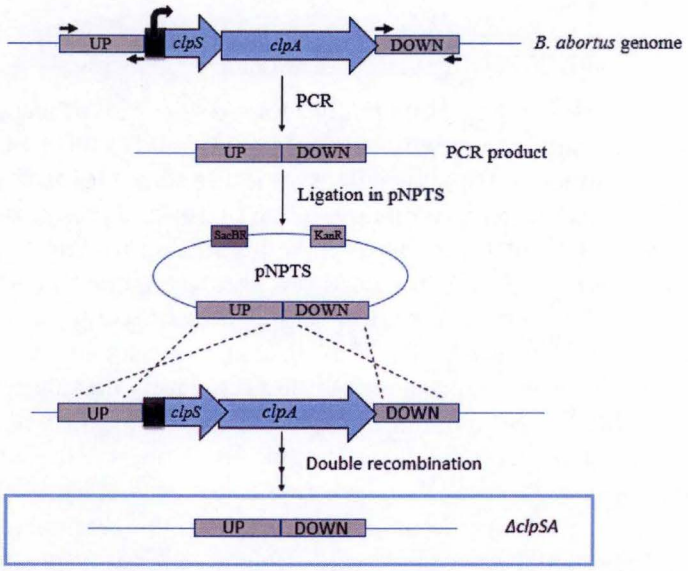

Figure 41 | Molecular strategy to construct ClpSA deletion strain. PCR were performed to amplify the upstream region (UP) of the coding region of clpS and clpA and the downstream region (DOWN) of the genes. The primers used are represented by dark arrows. Both PCR products were ligated within a pNPTS integrative plasmid which encodes resistance to kanamycin (KanR) and contains a sucrose sensitivity cassette (SacBR). This plasmid was then conjugated in Brucella were the deletion of the genes was performed by allelic replacement.

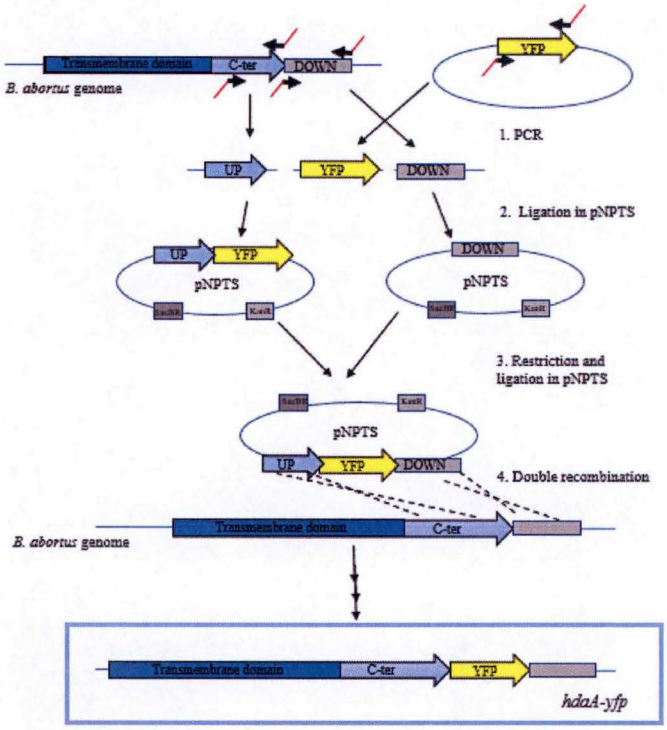

Figure 42 | Molecular strategy to construct the *hdaA-yfp* strain. PCR were performed using primers that can be found in the supplementary data. The C-terminal portion of *hdaA,* the region downstream the gene, and the YFP were amplified by PCR. The primers were constructed with restriction sites in their 5' end in order to perform ligation in pNPTS 138 in two times. In a first time, the UP part was ligated with the YFP in a pNPTS 138. Then the DOWN part was cloned in a pNPTS 138. Then a restriction was performed on those two plasmids in order to excise the insert from the plasmid. The obtained producted were then ligated in a pNPTS138. Subsequently, this plasmid was conjugated in *B. abortus* and the strain was obtained by allelic replacement. The light blue represents the transmembrane domain of hdaA, the light blue represents the C-term conserved domain, while the YFP is represented in yellow.

MATERIAL AND METHODS

Bacterial strains and growth conditions

Brucella abortus 544 strain was the WT strain used in this study. This strain has been modified to be resistant to nalidixic acid (Nal^R). All *Brucella abortus* strains were grown in solid or liquid 2YT rich medium (Yeast Extract and Tryptone; 1 % yeast extract, 1.6 % peptone, 0.5 % NaCl) at 37°C overnight.

Two different strains of *E. coli* were also used. The DH10B strain was used for plasmid constructions and the S17-1 was used for the mating in *B. abortus*. Both strains were cultivated in solid or liquid LB (Luria Bertani) medium at 37°C overnight.

For selection in *E. coli* and in *B. abortus*, the following antibiotics were added to the culture medium: kanamycin (50µg/mL for plasmid borne resistance cassettes and 10µg/mL for chromosome-encoded resistance cassettes) and chloramphenicol (20µg/mL). Nalidixic acid (25µL/mL) was also used as selection marker in *Brucella* during conjugation with S17-1 *E. coli*. The plasmids used were pNPTS138 (carrying kan^R and *sacBR*, a sucrose sensitivity cassette), pMR10 (carrying kan^R) and pSKoriTcat (carrying cm^R cassette).

Strain constructions

For the construction of the Δ*clpSA* strain, a pNPTS138 integrative plasmid in which the region before and after *clpSA* previously constructed by PCR was cloned, was used to achieve a double deletion mutant (*ΔclpS-ΔclpA*) in *B. abortus* 544. With this plasmid, a transformation of *E. coli* DH10B and then a transformation of the conjugative strain *E. coli* S17-1 were performed. The conjugation was then performed in *B. abortus* 544 and the mutant was obtained by allelic replacement (**Figure 41**).

For the construction of *hdaA-YFP* strain, a pNPTS138 integrative plasmid in which the end region of *hdaA* fused with a YFP and the beginning of the gene region following *hdaA* previously constructed by PCR was cloned, was used to achieve a fusion protein HdaA-YFP in the genome of *B. abortus*. The method used was the same as for the Δ*clpSA* strain (allelic replacement in *B.abortus*) (**Figure 42**).

For the construction of the *ΔTM-hdaA* strain, a pNPTS138 integrative plasmid, in which the region before and after the transmembrane domain of hdaA constructed by PCR was cloned, was used to achieve a deletion of *hdaA* transmembrane domain. However, since the genome was wrongly annotated in artemis, the upstream region selected included 93 nucleotides belonging to the N-terminal part of the transmembrane domain. The method used was the same as for the Δ*clpSA* strain (allelic replacement in *Brucella abortus*) (**Figure 39**).

For the construction of the *ΔTM-hdaA-YFP* strain, a pNPTS138 integrative plasmid in which the end region of *hdaA* fused with a YFP and the beginning of the gene region following *hdaA* previously constructed by PCR was cloned, was used to achieve a fusion protein ΔTM-HdaA-YFP in the genome of *ΔTM-hdaA*. The method used was the same as for the the previously cited.

Plasmidic DNA extraction

From an overnight liquid culture of *E. coli* DH10B carrying the desired plasmid, approximately 1 mL was put in Eppendorf tubes, centrifuged at 8000 RPM for 2 min and the supernatant was removed. This operation was repeated twice to increase the bacterial pellet. 300 µL of P1 buffer (RNase A 100µg/ml, TrisHCl 50 mM, EDTA 10 mM, pH 8), stored at 4°C, was added and used to resuspend the bacterial pellet. Then, 300 µL of P2 buffer (NaOH 200 mM and 1% SDS), stored at room temperature (RT), was added and the suspensions were incubated at RT for 2 min. After this incubation time, 300 µL of the P3 buffer (potassium acetate 3 M, pH 5.5), mixed by gentle inversion about 10 times, and the mix was stored at 4°C, was added. The solution was

mixed 10 times by inversion and then centrifuged at 13000 RPM for 12 min to remove the debris. The supernatant containing the plasmidic DNA was collected in new Eppendorf tubes and 600 µL of isopropanol were added to it, the solution was mixed by vigorous inversions, and centrifuged for 12 min at 13000 RPM. The supernatant was removed. Next, 500 µL of ethanol 70% were added and the solution was centrifuged one last time at 13000 RPM for 5 min. The supernatant was once again removed using the vacuum pump and the tubes were left drying in an incubator at 50°C for at least 30 min. Once they were dry, 20 µL of water were added to resuspend the pellet of each tube.

PCR

Different PCR were performed: preparative PCR, joining PCR and diagnostic PCR.

Preparative PCR. This PCR was used for the subsequent constructions. The PCR mix contains Q5 High-Fidelity DNA polymerase (2,000 U/µL, Biolabs), Q5 reaction buffer (Biolabs), forward and reverse primers (20 µM of each), dNTP (5 µM each), template DNA (about 60 ng of genomic DNA), DMSO 5% and water, for a final volume of 50 µl. The PCR programme was composed of a DNA denaturation step (at 98°C for 30 s), followed by 25 amplification cycles. These cycles were composed of a DNA denaturation step (at 98°C for 10 s), a primer hybridization step (in which the temperature must be adapted according to the primer Tm, for 30 s), and an elongation step (at 72°C, the time of elongation depends on the length of the DNA fragment to be amplified, 1 min for 2000 bp). After these 25 cycles, the last step is a final elongation (at 72°C for 2 min).

Joining PCR. This kind of PCR concatenates two PCR products together through sequence complementarity. The mix contained Q5 Highly-Fidelity DNA polymerase, Q5 reaction buffer (5X, BioLabs), dNTP (5 µM each), 1 µL of each PCR product to be joined, DMSO 5% and water. A classical PCR programme with only 5 amplification cycles was first performed to join the two products. Once this first PCR was performed, primers were added to the mix and 25 more cycles were done to amplify the entire product.

Diagnostic PCR. This PCR is used to check the presence and the size of a given DNA fragment. The PCR mix contains GoTaq polymerase (Promega®), GoTaq buffer (5X, Promega®), forward and reverse primers (20 µM of each), dNTP (5 µM of each), a fragment of a bacterial colony, DMSO 5% and water for a final volume of 30 µl. The PCR programme was composed of a DNA denaturation step (94°C for 4 min) and 25 amplification cycles. These amplification cycles were composed of the following steps: DNA denaturation (94° for 30 s), primer hybridization (54°C for 30 s) and DNA elongation (72°C for a period determined through the size of the DNA fragment to be amplified, 1 min for 1000 bp). The last step was a final elongation (72°C for 5 min).

Purification of PCR products

Each PCR product was first checked by electrophoretic migration in agarose gel containing ethidium bromide to see if the size of the given PCR product was the one expected by correspondence to a DNA ladder (Gene Ruler 0.1 µg/µL Thermo Scientific). The purification of PCR products was then achieved with the NucleoSpin, Gel and PCR Clean-up kit (Macherey-nagel), according to manufacturer instructions.

Enzymatic restriction

The purified PCR products were digested using the appropriated restriction enzyme and buffer (CutSmart) during 10 min at 37°C, and was directly put on ice afterwards to stop the enzymatic reaction. The mix for the restriction was composed of the purified PCR product or the plasmid, the appropriate enzyme and buffer (10X) for a final volume of 10 µL if one enzyme was used,

and 15 µL if two enzymes were used. The restriction products were then purified according to the previous section.

Ligation

The ligation of the PCR products into the plasmids was performed in a mix containing the T4-ligase (10X, Invitrogen), the buffer (5X, Invitrogen), the restricted plasmid and the restricted insert. The mix was then incubated overnight at 18°C.

A triple ligation was performed to ligate three PCR products together using compatible restriction sites. The DNA quantity of each product was first measured and then the quantity of each part was adapted in order to increase the likelihood of the ligation. The same enzyme and buffer were used for a final volume of 25 µL.

Transformation

E. coli DH10B and S17-1 competent strains were used for the transformations. For the DH10B transformation, 5 µL of the ligation product was added to 50 µL of competent bacteria. The mix was incubated on ice for 5 min, heat shocked for 2 min at 42°C and then put on ice again. 500 µL of liquid LB medium was then added to help bacteria recovering from the heat shock and the bacteria were incubated with agitation for 20 minutes at 37°C. After this incubation time, the bacteria were centrifuged at 5000 RPM for 3 minutes, the supernatant was removed to leave approximatively 100 µL in which the pellet was resuspended. These bacteria were then plated on LB-agar medium containing X-Gal (0.004%) and IPTG (1 mM) if a blue-white screen was performed, and the antibiotic corresponding to the plasmid used. The Petri dishes were incubated overnight at 37°C. The same protocol was used with the S17-1 strain, excepted that 15 µL of bacteria were first taken instead of 50 µL for DH10B.

Conjugation

For the conjugation, plasmids of interest were transformed into *E. coli* S17-1 conjugative strain, which were used for the mating in *B. abortus* 544. 50 µL of an overnight culture of *E. coli* S17-1 were added to 1 mL of an overnight culture of the *B. abortus* 544 (WT). The bacteria were then centrifuged for 2 min and 30 s at 7000 RPM, the supernatant was removed, and the pellet was resuspended in 100 µL of 2YT medium. The bacteria were spotted in 2YT agar without spreading and incubated at RT for 24 h. The next day, half of the drop was resuspended in 100 µL of 2YT liquid medium, plated on 2YT-agar medium supplemented with nalidixic acid (1 µL/mL) and kanamycin (10 µg/µL) and placed in the incubator at 37°C for 4 to 5 days. Colonies were then streaked on 2YT-agar containing kanamycin (10 µg/µL) but no nalidixic acid to allow them to grow better. From a streak, a bacterial culture was performed in liquid 2YT without any antibiotic to allow the second recombination (excision of the antibiotic resistance cassette and the sucrose sensitive cassette). 100 µL of this culture were plated in 2YT-agar containing sucrose (5%) and were incubated at 37°C. Approximatively 5 days after, the colonies obtained were picked and streaks were made in parallel on two squared plates, containing respectively 2YT-agar with kanamycin and 2YT-agar with sucrose. These plates were incubated for 2 to 3 days. The colonies that were grown only in the sucrose medium were picked up, placed in 100 µL of sterile PBS and then inactivated at 80°C for at least 1 h. Diagnostic PCR was then performed to check if the clone was effectively the expected mutant.

Infection of RAW 264.7 macrophages and CFU counting

RAW 264.7 macrophages were cultured in a 5% CO_2 atmosphere at 37°C in DMEM supplemented with 5% Fetal Calf Serum (Gibco). The day before infection, RAW 264.7 macrophages were diluted to have $1x10^5$ cells/mL and 500 µL was put in each well of the

24-wells plate. An overnight liquid culture of the *B. abortus* strain was also performed the day before the infection.
For the infection, we used a MOI of 50 (multiplicity of infection, meaning that there are 50 times more bacteria than cells). We assumed that the RAW 264.7 macrophages have been multiplying about 1.5 times during the night, meaning that there are about $1.5x10^5$ cells/mL in the morning. The day of the infection we first performed a wash of the bacterial culture by centrifugation (2 min and 30 s at 7000 RPM), using the appropriate amont of bacteria ($75x10^5$ bacteria/ml). Then, the pellet was resuspended in the appropriate volume of RAW 264.7 culture medium. The medium in the multiwell plate was removed and 500 µL of the bacteria in the RAW 264.7 medium were added in each condition. A centrifugation of the plate was then performed at 4°C and 1000 RPM for 10 min and the plate was incubated at 37°C, which corresponded to the beginning of the infection (T0h).
After one hour of incubation, the medium was removed and replaced by 500 µL of RAW 264.7 medium with gentamycin (50 µg/mL). Then, 2 hours post infection (PI), the medium was discarded, and replaced by the same medium but with gentamycin 10 µg/mL. For the conditions studied at 2 h PI, 2 washes of PBS were done, 500 µL of PBS-Triton X100 (0.1%) were then added in each condition and the plate was incubated for 10 min at 37°C. After this incubation time, 10 flushes were performed in each well and the bacteria were harvested in Eppendorf tubes. From these suspensions, different dilutions were performed and 20 µL of each condition were spotted in triplicate on 2YT-agar plates. The same steps were repeated for different times post infection (5, 24 and 48 h PI) and CFU were counted 3 to 4 days afterwards.

Microscopy
Before the microscopy, agarose pads were made with 350µL of agarose (1%) in PBS 1%. For observation of bacteria (*ΔclpSA*, *ΔTM-hdaA, hdaA-YFP, ΔTM-hdaA-YFP* and the WT strain), 1mL of an overnight culture were put in an Eppendorf, centrifuged at 7000RPM for 2 min 30, and washed in PBS to take off the 2YT liquid medium (which is auto-fluorescent). The pellet was then resuspended in 150 to 500µL of sterile PBS, depending on its size, in order to have an optimal amont of bacteria to visualize. Then, 2µL of the solution were dropped on the agarose pad previously made and the pads were sealed with VALAP (1/3 vaseline, 1/3 lanoline and 1/3 paraffin wax). The *Brucella* strains were observed with a Nikon 80i (objective phase contrast x100, plan Apo) connected to Hamamatsu ORCA-ER camera. The microscope which has been used is a Nikon 80i (objective 100X, plan Apo) connected to a Hamamatsu ORCA-ER camera. We also used DF type immersion oil (Nikon oil) with refraction indice of 1.5150 +/- 0.0002.

Fixation test with PFA
For the fixation test using PFA (paraformaldehyde) 1 mL of a liquid culture in an exponential phase were washed twice (at 7000RPM for 2 min 30 each time). The pellet was then resuspended in 200µL of PBS with PFA (2%) and incubated at RT for 20 minutes. 2µL of these bacteria were placed on a slide to be observed by fluorescent microscopy.

Bioscreen
Overnight pre-cultures of *B. abortus* WT and the mutant were performed two days before the bioscreen. The next day, the liquid cultures were grossly diluted in order to have an exponential phase in the evening, where the culture was again diluted to have an optical density (OD) of 0.05. The day the bioscreen was performed, the liquid cultures were diluted in fresh 2YT at an OD of 0.1 for the different conditions tested (to normalize the amount of bacteria for all of the conditions). 200 µL of each condition were put in triplicate in a multiwell plate and 2YT alone was used as a blank condition. Sterile PBS was put between the wells to avoid evaporation

problems. The bioscreen was then started for 50h. The bioscreen was repeated three times (biological triplicate).

Western Blot

Samples for the Western Blot were made according to the following steps: the optical density (OD) was first taken from an overnight culture and the sample were concentrate to an OD of 10. The samples were then centrifuged at 13000 RPM for 5 minutes and resuspended in ¾ of the optimal volume of PBS. They were left in the bath at 80°C for 1 hour in order to be inactivated. Then ¼ of the final volume of loading buffer (1M Tris-HCl pH 6.8, 10% SDS, Glycerol, β mercaptoethanol, 1% Bromophonol blue, dH2O) was added to the sample. The mix was then boiled at 95°C for 10 to 15 minutes. 15 µl of each sample was loaded on a SDS-PAGE two-parts gels, the running gel and the stacking gel (1.5M Tris-HCl pH 8.8 for running gel PH 6.6 for stacking gel, 10% SDS, 10% Ammonium Persulfate (APS), Acrylamide/ Bis acrylamide 12%, Tetramethylethylenediamine (TEMED)). The gel was run at 40 mA, 300 V, 100 W. The proteins were then transferred from the gel to the nitrocellulose membrane at 14 V, 112 mA for 30 minutes using a Transblot turbo Bio-Rad. Afterward, a blocking of the membrane was achieved with milk 5% dissolved in PBS-Tween (0.05%) overnight at 4°C. The detection of HdaA-YFP was performed via commercial antibody (Jc8) while the detection of DnaA was detected by monoclonal antibody. The incubation with the primary antibody was done for 1h ou 2h at RT, diluted at 1/300 or 1/5000 in 1% milk PBS-Tween. Then, the membrane was washed with PBS-Tween three times for 10 min each and then incubated during 1 h with the secondary antibody anti-mouse or anti-rabbit IgG (1/5000) conjugated with HRP (Horseradish peroxidase) diluted in 1% milk PBS-T. Again, the membrane was washed three times with PBS-Tween. Proteins were visualized by adding a mix of the peroxide solution and luminol/enhancer solution (1/1) to the membrane (Clarity ^{TM} ECL Western Substrate,Bio-Rad). Images were revealed with Amersham imager 6000.

SUPPLEMENTARY DATA

Supplementary table 1 – Primer table representing all the primers used in this study.

Mutant	Primer	Sequence (5'→ 3')
ΔTM-hdaA	ΔTM-hdaA-AMF	gggGTCGACcatcaatagcgatcttgagc
	ΔTM-hdaA-AMR	CATattgacatgaatgtcaccg
	ΔTM-hdaA-AVF	cggtgacattcatgtcaatATGcgttttgcattgaatagcta
	ΔTM-hdaA-AVR	gggGAATTCatctgtatcgccgatagaag
	ΔTM-hdaA-check-F	tgcacgaccagatcgttcac
hdaA-yfp	hdaA-yfp-AM-F	aaGTCGACcgggtgacaatacaggccg
	hdaA-yfp-AM-R	ttCTCGAGtccggcctgccccata
	yfp-for-hdaA-F	aaCTCGAGtcgaagggcgaag
	yfp-for-hdaA-R	ctCTGCAGtcacttatacagttcatc
	hdaA-yfp-AV-F	tttCTGCAGtgagggtggcggtcaca
	hdaA-yfp-AV-R	tttGAATTCggtcgtagagaccgcgctt
ΔclpSA	ΔclpSA-AMF	cgcGGATCCcgtatccttgttgatgcg
	ΔclpSA-AMR	gcgGAATTCggacgtcatatggggatt
	ΔclpSA-AVF	aaaGAATTCtaaacgcataaaaacggc
	ΔclpSA-AVR	aaaGCTAGCcgagataatgggcggaat
ΔclpSA+	clpSA-compl-F	aaaGGATCCgtgttcgcatcaacgacg
	clpSA-compl-R	aaaAAGCTTttatttcttgcgcggcac
dnaN-mCherry	dnaN-F	aaGGATCCgtgcgccttatcgacaaggg
	dnaN-R	ttgcggccgcGGTGGCCGACCGgacgcgcatcggcatga
	mCherry-F	aaGCGGCCGCgtgagcaagggcgaggag
	mCherry-R	ttGAATTCtcacttgtacagctcgtccatgcc

Supplementary table 2 – Strain constructed in the study

Strain	Name	Resistance/ Sensitivity
E. coli DH10B	pNPTS138 ΔTM-hdaA-AM	kanR/ sucS
	pNPTS138 ΔTM-hdaA-AV	kanR/ sucS
	pNPTS138 hdaA-AM-YFP	kanR/ sucS
	pNPTS138 hdaA-AV (for YFP)	kanR/ sucS
	pGem5-Zf(+) ΔclpSA-AM	ampR
	pGem5-Zf(+) ΔclpSA-AV	ampR
	pMR10 clpSA	kanR
E. coli S17	pNPTS138 ΔTM-hdaA	kanR/sucS
	pNPTS138 hdaA-YFP	kanR/sucS
	pNPTS138 ΔclpSA	kanR/sucS
	pMR10 ClpSA	kanR
B. abortus 544	pNPTS138 ΔTM-hdaA	/
	pNPTS138 hdaA-YFP	/
	pNPTS138 ΔclpSA	/
	pMR10 clpSA	kanR

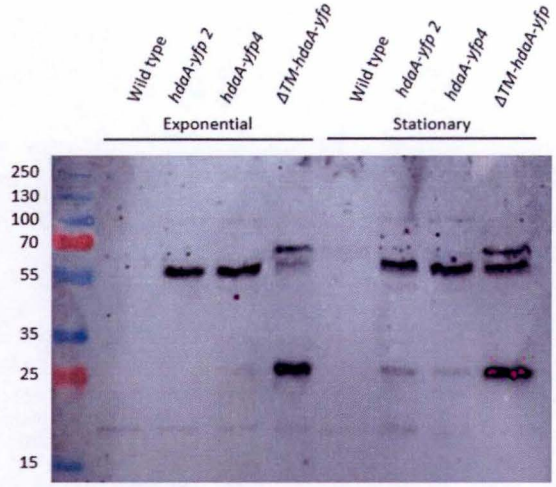

Figure S1 | Western blot anti-YFP highlighting the HdaA protein fused to YFP in exponential and in stationary phases (entire Figure). Two clones of the *hdaA-yfp* strain were tested (2 and 4) to further confirm the results. The description of the experiment is available bellow Figure 35.

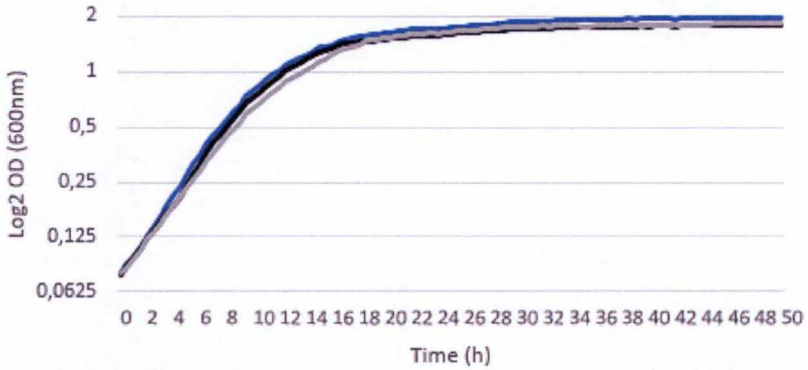

Figure S2 | Growth curve for the WT (blue) and the *hdaA-yfp* strains for one representative experiment. *hdaA-yfp1* is represented in black and *hdaA-yfp2* in grey.

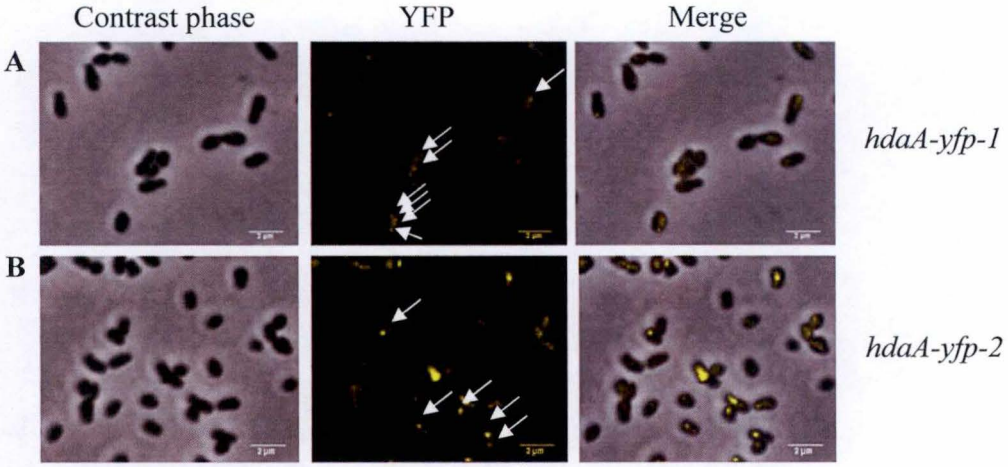

Figure S3| Localization of HdaA-YFP in an exponential phase. Bacteria from hdaA-yfp-1 (A) strain and hdaA-yfp-2 (B) strain were observed using phase contrast and fluorescence microscopy. White arrows indicate HdaA-YFP foci. The scale bar represents 2 µm.

REFERENCES

Al-Tawfiq JA and Memish ZA, 2013. "Antibiotic Susceptibility and Treatment of Brucellosis." *Recent patents on anti-infective drug discovery* 8(1):51–54.

Anderson-Furgeson JC, Zupan JR, Grangeon R, and Zambryski PC, 2016. "Loss of PodJ in Agrobacterium Tumefaciens Leads to Ectopic Polar Growth, Branching, and Reduced Cell Division." *Journal of bacteriology* 198(13):1883–91.

Archambaud C, Salcedo SP, Lelouard H, Devilard E, de Bovis B, Van Rooijen N, Gorvel JP, Malissen B, 2010. "Contrasting Roles of Macrophages and Dendritic Cells in Controlling Initial Pulmonary Brucella Infection." *European Journal of Immunology*

Atluri VL, Xavier MN, de Jong MF, den Hartigh AB and Tsolis RM, 2011. "Interactions of the Human Pathogenic *Brucella* Species with Their Hosts." *Annual Review of Microbiology*, 65(1), pp.523–541.

Baker TA and Bell SP, 1998. "Polymerases and the Replisome: Review Machines within Machines Polymerases: Template-Directed Phosphoryl Transfer Machines Synthesis of the new DNA strands occurs as a result." *Cell*, 92, pp.295–305.

Banack T, Clauson N, Ogbaa N, Villar J, Oliver D, Firshein W, 2005. "Overexpression of the Hda DnaA-Related Protein in Escherichia Coli Inhibits Multiplication, Affects Membrane Permeability, and Induces the SOS Response." *Journal of Bacteriology* 187(24):8507–10.

Barbosa AA, Figueiredo ACS, Palhao MP, Viana JHM, and Fernandes CAC. 2017. "Safety of Vaccination against Brucellosis with the Rough Strain in Pregnant Cattle." *Tropical Animal Health and Production* 49(8):1779–81.

Batut J, Andersson SGE, and O'Callaghan D, 2004. "The evolution of chronic infection strategies in the α-proteobacteria." *Nature Reviews Microbiology*, 2(12), pp.933–945.

Bloom LB, Turner J, Kelman Z, Beechem JM, O'Donnell M, and Goodman MF, 1996. "Dynamics of loading the beta sliding clamp of DNA polymerase III onto DNA." *The Journal of biological chemistry*, 271(48), pp.30699–708.

Boschiroli ML, Ouahrani-Bettache S, Foulongne V, Michaux-Charachon S, Bourg G, Allardet-Servent A, Cazevieille C, Liautard JP, Ramuz M, and O'Callaghan D, 2002. "The Brucella Suis virB Operon Is Induced Intracellularly in Macrophages." *Proceedings of the National Academy of Sciences* 99(3):1544–49.

Bossi P, Tegnell A, Baka A, van Loock F, Hendriks J, Werner A, Maidhof H, and Gouvras G, 2004. Bichat guidelines for the clinical management of brucellosis and bioterrorism-related brucellosis. *Euro surveillance : bulletin Europeen sur les maladies transmissibles = European communicable disease bulletin*, 9(12), pp.E15-6.

Bramhill D and Kornberg A, 1988. Duplex opening by dnaA protein at novel sequences in initiation of replication at the origin of the E. coli chromosome. *Cell*, 52(5), pp.743–755.

Breidenstein EB, Janot L, Strehmel J, Fernandez L, Taylor PK, Kukavica-Ibrulj, Gellatly SL, Levesque RC, Overhage J, and Hancock RE, 2012. "The Lon Protease Is Essential for Full Virulence in Pseudomonas Aeruginosa." *PloS one* 7(11): e49123.

Brown PJ, de Pedro MA, Kysela DT, Van der Henst C, Kim J, De Bolle X, Fuqua C, and Brun YV, 2012. Polar growth in the Alphaproteobacterial order Rhizobiales. *Proceedings of the National Academy of Sciences of the United States of America*, 109(5), pp.1697–701.

Bussiere DE, and Bastia D, 1999. "Termination of DNA Replication of Bacterial and Plasmid Chromosomes." *Molecular Microbiology* 31(6):1611–18.

Camara JE, Skarstad K and Crooke E, 2003. Controlled initiation of chromosomal replication in Escherichia coli requires functional Hda protein. *Journal of bacteriology*

Celli J, de Chastellier C, Franchini DM, Pizarro-Cerda J, Moreno E, and Gorvel JP, 2003. "*Brucella* Evades Macrophage Killing via VirB-Dependent Sustained Interactions with the Endoplasmic Reticulum." *The Journal of Experimental Medicine* 198(4):545–56.

Celli J, Salcedo SP, and Gorvel JP, 2005. "Brucella Coopts the Small GTPase Sar1 for Intracellular Replication." *Proceedings of the National Academy of Sciences* 102(5):1673–78.

Celli J, 2015. "The Changing Nature of the *B Rucella* -Containing Vacuole." *Cellular Microbiology* 17(7):951–58.

Collier J and Shapiro L, 2009. "Feedback control of DnaA-mediated replication initiation by replisome-associated HdaA protein in *Caulobacter*." *Journal of bacteriology*, 191(18), pp.5706–16.

Corbel MJ, 2006. "Brucellosis in Humans and Animals World Organisation for Animal Health." *WHO Library Cataloguing*.

Curtis PD & Brun YV, 2010. "Getting in the Loop: Regulation of Development in *Caulobacter crescentus*." *Microbiology and Molecular Biology Reviews*, 74(1), pp.13–41.

De Bolle X, Crosson S, Matroule JY, and Letesson JJ, 2015. "Brucella Abortus Cell Cycle and Infection Are Coordinated." *Trends in Microbiology* 23(12):812–21.

de Figueiredo P, Ficht TA, Rice-Ficht A, Rossetti CA, and Adams LG, 2015. "Pathogenesis and immunobiology of brucellosis: review of *Brucella*-host interactions." *The American journal of pathology*, 185(6), pp.1505–17.

Deghelt M, Mullier C, Sternon JF, Francis N, Laloux G, Dotreppe D, Van der Henst C, Jacobs-Wagner C, Letesson JJ, De Bolle X, 2014. "G1-arrested newborn cells are the predominant infectious form of the pathogen *Brucella abortus*." *Nature Communications*, 5, p.4366.

Dorneles EM, Sriranganathan N, and Lage AP, 2015. "Recent Advances in Brucella Abortus Vaccines." *Veterinary research* 46(1):76.

Duderstadt KE, Chuang K, and Berger JM, 2011. "DNA stretching by bacterial initiators promotes replication origin opening." *Nature*, 478(7368), pp.209–13.

Erzberger JP, Mott ML, and Berger JM, 2006. "Structural basis for ATP-dependent DnaA assembly and replication-origin remodeling." *Nature Structural & Molecular Biology*, 13(8), pp.676–683.

Fernandez-Fernandez C, Grosse K, Sourijk V, and Collier J, 2013. "The β-sliding clamp directs the localization of HdaA to the replisome in *Caulobacter crescentus*." *Microbiology*, 159(Pt_11), pp.2237–2248.

Ficht T, 2010. "*Brucella* taxonomy and evolution." *Future microbiology*, 5(6), pp.859–66.

Fiori PL, Mastrandrea S, Rappelli P, and Cappuccinelli P, 2000. "*Brucella abortus* Infection Acquired in Microbiology Laboratories." *Journal of clinical microbiology* 38(5):2005–6. R

Foster G, Osterman BS, Godfroid J, Jacques I and Cloeckaert A, 2007. "*Brucella ceti* sp. nov. and *Brucella pinnipedialis* sp. nov. for *Brucella* strains with cetaceans and seals as their preferred hosts." *International journal of systematic and evolutionary microbiology*, 57(11), pp.2688–2693.

Godfroid J, Nielsen K, and Saegerman C, 2010. "Diagnosis of Brucellosis in Livestock and Wildlife." *Croatian medical journal* 51(4):296–305.

Gorvel JP and Moreno E, 2002. "*Brucella* Intracellular Life: From Invasion to Intracellular Replication." *Veterinary microbiology* 90(1–4):281–97.

Grangeon R, Zupan J, Jeon Y, and Zambryski PC, 2017. "Loss of PopZ $_{At}$ Activity in *Agrobacterium Tumefaciens* by Deletion or Depletion Leads to Multiple Growth Poles, Minicells, and Growth Defects" edited by Bonnie Bassler. *mBio* 8(6):e01881-17.

Gur E, 2013. "The Lon AAA+ Protease." In *Sub-cellular biochemistry*. pp. 35–51.
Hallez R, Bellefontaine AF, Letesson JJ, and De Bolle X, 2004. "Morphological and functional asymmetry in α-proteobacteria." *Trends in Microbiology*, 12(8), pp.361–365.
Hallez R, Mignolet J, Van Mullem V, Wery M, Vandenhaute J, Letesson JJ, Jacobs-Wagner C, and De Bolle X, 2007. "The Asymmetric Distribution of the Essential Histidine Kinase PdhS Indicates a Differentiation Event in Brucella Abortus." *The EMBO Journal* 26(5):1444–55.
Harrison PW, Lower RP, Kim NK and Young JP. 2010. "Introducing the bacterial "chromid": not a chromosome, not a plasmid." *Trends in Microbiology*, 18(4), pp.141–148.
Scholz HC, Revilla-Fernandez S, Al Dahouk S, Hammerl JA, Zygmunt MS, Cloeckhaert A, Koylass M, Whatmore AM, Blom J, Vergnaud G, Witte A, Aitstleitner K, and Hofer E, 2016. "*Brucella vulpis* sp. nov., a novel *Brucella* species isolated from mandibular lymph nodes of red foxes (Vulpes vulpes) in Austria." *International Journal of Systematic and Evolutionary Microbiology*.
Hottes AK, Shapiro L and McAdams HH, 2005. "DnaA coordinates replication initiation and cell cycle transcription in *Caulobacter crescentus*." *Molecular Microbiology*, 58(5), pp.1340–1353.
Jonas K, Liu J, Chier P and Laub MT, 2013. "Proteotoxic stress induces a cell-cycle arrest by stimulating Lon to degrade the replication initiator DnaA." *Cell*, 154(3), pp.623–36.
Jonas K, Chen YE, and Laub MT, 2011. "Modularity of the bacterial cell cycle enables independent spatial and temporal control of DNA replication." *Current biology : CB*, 21(13), pp.1092–101.
Jonas K, 2014. "To Divide or Not to Divide: Control of the Bacterial Cell Cycle by Environmental Cues." Current Opinion in Microbiology 18:54–60.
Joshi KK and Chien P, 2016. "Regulated Proteolysis in Bacteria: *Caulobacter*." *Annual Review of Genetics*, 50(1), pp.423–445.
Jumas-Bilak E, Michaux-Charachon S, Bourg G, O'Callaghan D, and Ramuz M, 1998. "Differences in chromosome number and genome rearrangements in the genus *Brucella*." *Molecular microbiology*, 27(1), pp.99–106.
Kato J & Katayama T, 2001. "Hda, a novel DnaA-related protein, regulates the replication cycle in Escherichia coli." *The EMBO journal*, 20(15), pp.4253–62.
Katayama T, Ozaki S, Keyamura K, and Fujimitsu K. 2010. "Regulation of the Replication Cycle: Conserved and Diverse Regulatory Systems for DnaA and oriC." Nature Reviews Microbiology 8(3):163–70.
Kim PD, Banack T, Lerman DM, Tracy JC, Camara JE, Crooke E, Oliver D, and Frishein W, 2003. "Identification of a Novel Membrane-Associated Gene Product That Suppresses Toxicity of a TrfA Peptide from Plasmid RK2 and Its Relationship to the DnaA Host Initiation Protein." *Journal of bacteriology* 185(6):1817–24.
Kim JS, Nanfara MT, Chodavarapu S, Jin KS, Babu VMP, Ghazy MA, Chung S, Kaguni JM, Sutton MD, and Cho R, 2017. "Dynamic assembly of Hda and the sliding clamp in the regulation of replication licensing." *Nucleic acids research*, 45(7), pp.3888–3905.
Kornberg A & Baker TA, 2006. "*DNA replication*," University Science.
Kurz M, Dalrymphe B, Wijffels G and Kongsuwan K, 2004. "Interaction of the sliding clamp beta-subunit and Hda, a DnaA-related protein." *Journal of bacteriology*, 186(11), pp.3508–15.
Leonard AC and Grimwade JE, 2004. "Building a bacterial orisome: emergence of new regulatory features for replication origin unwinding." *Molecular Microbiology*, 55(4), pp.978–985.

Leslie DJ, Heinen C, Schramm FD, Thüring M, Aakre CD, Murray SM, Laub MT, and Jonas K, 2015. "Nutritional Control of DNA Replication Initiation through the Proteolysis and Regulated Translation of DnaA", ed. *PLOS Genetics*, 11(7), p.e1005342.

Liautard JP, Gross A, Dornand J, and Köhler S, 1996. "Interactions between Professional Phagocytes and Brucella Spp." *Microbiologia (Madrid, Spain)* 12(2):197–206.

Lui J, Francis LI, Jonas K, Laub MT, Chien P, 2016. "ClpAP is an auxiliary protease for DnaA degradation in *Caulobacter crescentus*." *Molecular Microbiology*, 102(6), pp.1075–1085.

Livny J, Yamaichi Y, and Waldor MK , 2007. "Distribution of centromere-like parS sites in bacteria: insights from comparative genomics." *Journal of bacteriology*, 189(23), pp.8693–703.

Mackiewicz P, Zakrzewska-Czerwinska J, Zawilak A, Dudek MR, and Cebrat S, 2004. "Where does bacterial replication start? Rules for predicting the oriC region." *Nucleic Acids Research*, 32(13), pp.3781–3791.

Makowska-Grzyska M and Kaguni JM, 2010. "Primase Directs the Release of DnaC from DnaB." *Molecular Cell*, 37(1), pp.90–101.

McGarry KC, Ryan VT, Grimwade JE, and Leonard AC, 2004. "Two discriminatory binding sites in the Escherichia coli replication origin are required for DNA strand opening by initiator DnaA-ATP." *Proceedings of the National Academy of Sciences of the United States of America*, 101(9), pp.2811–6.

Van Melderen L and Aertsen A, 2009. "Regulation and quality control by Lon-dependent proteolysis." *Research in Microbiology*, 160(9), pp.645–651.

Meltzer E, Sidi Y, Smolen G, Banai M, Bardenstein S, and Schwartz E, 2010. "Sexually Transmitted Brucellosis in Humans." *Clinical Infectious Diseases*, 51(2), pp.e12–e15.

Messer W, Blaesing F, Jakimowicz D, Krause M, Majka J, Nardmann J, Schaper S, Seitz H, Speck C, Weigel C, Wegrzyn G, Welzeck M, and Zakrzewska-Czerwinska J, 2001. "Bacterial replication initiator DnaA. Rules for DnaA binding and roles of DnaA in origin unwinding and helicase loading." *Biochimie*, 83(1), pp.5–12.

Messer W., 2002. "The bacterial replication initiator DnaA. DnaA and oriC, the bacterial mode to initiate DNA replication." *FEMS microbiology reviews*, 26(4), pp.355–74.

Messer W and Weigel C, 2003. "DnaA as a Transcription Regulator." In *Methods in enzymology*. pp. 338–349.

Michaux-Charachon S, Bourg G, Jumas-Bilak E, Guigue-Talet P, Allardet-Servent A, O'Callaghan D, and Ramuz M, 1997. "Genome structure and phylogeny in the genus *Brucella*." *Journal of bacteriology*, 179(10), pp.3244–9.

Moreno E, 2014. "Retrospective and prospective perspectives on zoonotic brucellosis." *Frontiers in Microbiology*, 5, p.213.

Moreno E, Cloeckaert A& Moriyón I, 2002. "*Brucella* evolution and taxonomy." *Veterinary Microbiology*, 90(1–4), pp.209–227.

Moreno E and Moriyón I, 2006. "The Genus *Brucella*." In *The Prokaryotes*. New York, NY: Springer New York, pp. 315–456.

Mott ML and Berger JM., 2007. "DNA replication initiation: mechanisms and regulation in bacteria." *Nature Reviews Microbiology*, 5(5), pp.343–354.

Nakamura K and Katayama T , 2010. "Novel essential residues of Hda for interaction with DnaA in the regulatory inactivation of DnaA: unique roles for Hda AAA $^{+}$ Box VI and VII motifs." *Molecular Microbiology*, 76(2), pp.302–317.

National Academy of Sciences (U.S.), 1980. "Biographical memoirs.", *National Academy Press.*

Neta AV, Mol JP, Xavier MN, Paixão TA, Lage AP, Santos RL, 2010. "Pathogenesis of bovine brucellosis." *The Veterinary Journal*, 184(2), pp.146–155.

Newman G and Crooke E, 2000. "DnaA, the Initiator of Escherichia Coli Chromosomal Replication, Is Located at the Cell Membrane." *Journal of bacteriology* 182(9):2604–10.
O'Donnell M, 2006. "Replisome Architecture and Dynamics in *Escherichia coli*." *Journal of Biological Chemistry*, 281(16), pp.10653–10656.
O'Donnell M, Langston L, and Stillman B, 2013. "Principles and Concepts of DNA Replication in Bacteria, Archaea, and Eukarya." *Cold Spring Harbor Perspectives in Biology*, 5(7), pp.a010108–a010108.
Pappas G, Papadimitriou P, Akritidis N, Christou L, and Tsianos EV, 2006. "The new global map of human brucellosis." *The Lancet Infectious Diseases*, 6(2), pp.91–99.
Paulsen IT, Seshadri R, Nelson KE, Eisen JA, Heidelberg JF, Read TD, Dodson RJ, Umayam L, Brinkac LM, Beanan MJ, Daugherty SC, Deboy RT, Durkin AS, Kolonay JF, Madupu R, Nelson WC, Ayodeji B, Kraul M, Shetty J, Malek J, Van Aken SE, Riedmuller S, Tettelin H, Gill SR, White O, Salzberg SL, Hoover DL, Lindler LE, Halling SM, Boyle SM and Fraser CM, 2002. "The *Brucella* suis genome reveals fundamental similarities between animal and plant pathogens and symbionts." *Proceedings of the National Academy of Sciences of the United States of America*, 99(20), pp.13148–53.
Pinto UM, Pappas KM, and Winans SC 2012. "The ABCs of plasmid replication and segregation." *Nature Reviews Microbiology*, 10(11), pp.755–765.
Pizarro-Cerda J, Meresse S, Parton RG, van der Goot G, Sola-Landa A, Lopez-Goni I, Moreno E, and Gorvel JP, 1998. "Brucella Abortus Transits through the Autophagic Pathway and Replicates in the Endoplasmic Reticulum of Nonprofessional Phagocytes." *Infection and immunity* 66(12):5711–24.
Pizarro-Cerdá J, Moreno E, and Gorvel JP, 2000. "Invasion and Intracellular Trafficking of Brucella Abortus in Nonphagocytic Cells." *Microbes and infection* 2(7):829–35.
Porte F, Liautard JP, and Köhler S, 1999. "Early Acidification of Phagosomes Containing Brucella Suis Is Essential for Intracellular Survival in Murine Macrophages." *Infection and immunity* 67(8):4041–47.
Robinson A, and van Oijen AM, 2013. "Bacterial Replication, Transcription and Translation: Mechanistic Insights from Single-Molecule Biochemical Studies." *Nature Reviews Microbiology* 11(5):303–15.
Ryan VT, Grimwade JE, Nievera CJ, and Leonard AC, 2002. "IHF and HU stimulate assembly of pre-replication complexes at Escherichia coli oriC by two different mechanisms." *Molecular microbiology*, 46(1), pp.113–24.
Sällström B and Andersson SGE, 2005. "Genome Reduction in the α-Proteobacteria." *Current Opinion in Microbiology* 8(5):579–85.
Schaper S and Messer W, 1995. "Interaction of the initiator protein DnaA of Escherichia coli with its DNA target." *The Journal of biological chemistry*, 270(29), pp.17622–6.
Schmidt R, Zahn R, Bukau B, and Mogk A, 2009. "ClpS Is the Recognition Component for *Escherichia Coli* Substrates of the N-End Rule Degradation Pathway." *Molecular Microbiology* 72(2):506–17.
Scholz HC, Nöckler K, Göllner C, Bahn P, Vergnaud G, Tomaso H, Al Dahouk S, Kämpfer P, Cloeckaert A, Maquart M, Zygmunt MS, Whatmore AM, Pfeffer M, Huber B, Busse HJ, and De BK, 2010. "*Brucella inopinata* sp. nov., isolated from a breast implant infection." *International journal of systematic and evolutionary microbiology*, 60(4), pp.801–808.
Scholz HC, Hubalek Z, Sedlácek I, Vergnaud G, Tomaso H, Al Dahouk S, Melzer F, Kämpfer P, Neubauer H, Cloeckaert A, Maquart M, Zygmunt MS, Whatmore AM, Falsen E, Bahn P, Göllner C, Pfeffer M, Huber B, Busse HJ, and Nöckler K, 2008. "*Brucella microti* sp. nov., isolated from the common vole Microtus arvalis." *International journal of systematic and evolutionary microbiology*, 58(2), pp.375–382.

Schurig GG, Roop RM 2nd, Bagchi T, Boyle S, Buhrman D, and Sriranganathan N., 1991. "Biological Properties of RB51; a Stable Rough Strain of *Brucella abortus*." *Veterinary microbiology* 28(2):171–88.

Shah IM and Wolf RE, 2006. "Sequence Requirements for Lon-dependent Degradation of the Escherichia coli Transcription Activator SoxS: Identification of the SoxS Residues Critical to Proteolysis and Specific Inhibition of in vitro Degradation by a Peptide Comprised of the N-terminal 21 Amino Acid Residues." *Journal of Molecular Biology*, 357(3), pp.718–731.

Shaheen SM, Ouimet MC and Marczynski GT, 2009. "Comparative analysis of Caulobacter chromosome replication origins." *Microbiology*, 155(4), pp.1215–1225.

Skarstad K and Katayama T, 2013. "Regulating DNA replication in bacteria." *Cold Spring Harbor perspectives in biology*, 5(4), p.a012922.

Smith JL and Grossman AD, 2015. "*In Vitro* Whole Genome DNA Binding Analysis of the Bacterial Replication Initiator and Transcription Factor DnaA C." A. Gross, ed. *PLOS Genetics*, 11(5), p.e1005258.

Snider J, Thibault G & Houry WA, 2008. "The AAA+ superfamily of functionally diverse proteins." *Genome biology*, 9(4), p.216.

Speck C, Weigel C and Messer W, 1999. "ATP- and ADP-dnaA protein, a molecular switch in gene regulation." *The EMBO journal*, 18(21), pp.6169–76.

Starr T, Ng TW, Wehrly TD, Knodler LA, and Celli J, 2008. "Brucella Intracellular Replication Requires Trafficking Through the Late Endosomal/Lysosomal Compartment." *Traffic* 9(5):678–94.

Starr T, Child R, Wehrly TD, Hansen B, Hwang S, Lopez-Otin C, Virgin HW, and Celli J, 2012. "Selective Subversion of Autophagy Complexes Facilitates Completion of the Brucella Intracellular Cycle." *Cell Host & Microbe* 11(1):33–45.

Stouf M, Meile JC, and Cornet F, 2013. "FtsK Actively Segregates Sister Chromosomes in Escherichia Coli." *Proceedings of the National Academy of Sciences* 110(27):11157–62.

Su S, Bonnie BS, Gladys A, and Stephen KF. 2006. "Lon Protease of the α-Proteobacterium Agrobacterium Tumefaciens Is Required for Normal Growth, Cellular Morphology and Full Virulence." *Microbiology* 152(4):1197–1207.

Su'etsugu M, Nakamura K, Keyamura K, Kudo Y, and Katayama T, 2008. "Hda monomerization by ADP binding promotes replicase clamp-mediated DnaA-ATP hydrolysis." *The Journal of biological chemistry*, 283(52), pp.36118–31.

Su'etsugu M, Takata M, Kubota T, Matsuda Y, and Katayama T 2004. "Molecular mechanism of DNA replication-coupled inactivation of the initiator protein in *Escherichia coli*: interaction of DnaA with the sliding clamp-loaded DNA and the sliding clamp-Hda complex." *Genes to Cells*, 9(6), pp.509–522.

Taylor JA, Ouimet MC, Wargachuk R, Marczynski GT, 2011. "The *Caulobacter crescentus* chromosome replication origin evolved two classes of weak DnaA binding sites." *Molecular Microbiology*, 82(2), pp.312–326.

Tsilibaris V, Maenhaut-Michel G and Van Melderen L, 2006. "Biological roles of the Lon ATP-dependent protease." *Research in Microbiology*, 157(8), pp.701–713.

Van der Henst C, de Barsy M, Zorreguieta A, Letesson JJ, and De Bolle X, 2013. "The *Brucella* pathogens are polarized bacteria." *Microbes and Infection*, 15(14–15), pp.998–1004.

Vass RH, Zeinert RD & Chien P, 2016. "Protease regulation and capacity during Caulobacter growth." *Current Opinion in Microbiology*, 34, pp.75–81.

Vassallo DJ, 1996. "The saga of brucellosis: controversy over credit for linking Malta fever with goats' milk." *Lancet (London, England)*, 348(9030), pp.804–8.

Wargachuk R and Marczynski GT, 2015. "The *Caulobacter crescentus* Homolog of DnaA (HdaA) Also Regulates the Proteolysis of the Replication Initiator Protein DnaA" P. de Boer, ed. *Journal of Bacteriology*, 197(22), pp.3521–3532.

Wattam AR, Williams KP, Snyder EE, Almeida NF Jr, Shukla M, Dickerman AW, Crasta OR, Kenyon R, Lu J, Shallom JM, Yoo H, Ficht TA, Tsolis RM, Munk C, Tapia R, Han CS, Detter JC, Bruce D, Brettin TS, Sobral BW, Boyle SM and Setubal JS, 2009. "Analysis of Ten Brucella Genomes Reveals Evidence for Horizontal Gene Transfer Despite a Preferred Intracellular Lifestyle." *Journal of Bacteriology*, 191(11), pp.3569–3579.

Whatmore AM, Davison N, Cloeckaert A, Al Dahouk S, Zygmunt MS, Brew SD, Perrett LL, Koylass MS, Vergnaud G, Quance C, Scholz HC, Dick EJ Jr, Hubbard G, and Schlabritz-Loutsevitch NE, 2014. "*Brucella papionis* sp. nov., isolated from baboons (Papio spp.)." *International journal of systematic and evolutionary microbiology*, 64(Pt 12), pp.4120–4128.

Wolanski M, Donczew R, Zawilak-Pawlik A, and Zakrzewska-Czerwinska J, 2015. "oriC-Encoded Instructions for the Initiation of Bacterial Chromosome Replication." *Frontiers in Microbiology* 5:735.

Wyatt HV, 2005. "How Themistocles Zammit found Malta Fever (brucellosis) to be transmitted by the milk of goats." *Journal of the Royal Society of Medicine*, 98(10), pp.451–4.

Wyatt HV, 2010. "Surgeon Captain Sheldon F. Dudley and the person to person spread of brucellosis by inhalation." *Journal of the Royal Naval Medical Service*, 96(3), pp.185–7.

Zawilak-Pawlik A, Nowaczyk M and Zakrzewska-Czerwińska J, 2017. "The Role of the N-Terminal Domains of Bacterial Initiator DnaA in the Assembly and Regulation of the Bacterial Replication Initiation Complex." *Genes*, 8(5), p.136.